

ABSTRACT

Title of Thesis: CYCLE ANALYSIS OF A NEW ENGINE DESIGN

Wiam Fadi Attar, Master of Science, 2017

Thesis Directed By: Associate Professor, Dr. Christopher P. Cadou,
Department of Aerospace Engineering

This thesis investigates a new externally heated engine design being developed by Soony Systems Inc. to serve as the prime mover in a residential-scale combined heat and power system. This is accomplished by developing a thermodynamic model for the engine and sweeping through the design parameter space in order to identify designs that maximize power output, efficiency, and brake mean effective pressure (BMEP). It was discovered that the original engine design was flawed so a new design was proposed and analyzed. The thermodynamic model was developed in four stages. The first model was quasi-static while the other three were time-dependent and used increasingly realistic models of the heat exchangers. For the range of design parameters investigated here, the peak power output is 6.8 kW, the peak efficiency is approximately 60%, and the peak BMEP is 389 kPa. These performance levels are compared to those of other closed-cycle engines. The results suggest that the Soony engine has the potential to be more efficient than Stirlings

because it more closely approximates the Carnot cycle, but this comes at the cost of significantly lower BMEP (389 kPa vs. 2,760 kPa for the SOLO Stirling engine).

CYCLE ANALYSIS OF A NEW AIR ENGINE DESIGN

by

Wiam Fadi Attar

Thesis submitted to the Faculty of the Graduate School of the
University of Maryland, College Park, in partial fulfillment
of the requirements for the degree of
Master of Science
2017

Advisory Committee:
Assoc. Professor Christopher Cadou, Chair
Assoc. Professor Ray Sedwick
Assoc. Professor Kenneth Yu

Dedication

To my family and friends who have supported me throughout my graduate career.

Acknowledgements

I would like to first thank my advisor Dr. Christopher Cadou for his guidance throughout the process. I also would like to thank Dr. Stuart Laurence, Dr. Inderjit Chopra, Dr. Allen Winkelmann, Dr. Mary Bowden, and my committee members Dr. Raymond Sedwick and Dr. Kenneth Yu for all their assistance. I also would like to thank Aileen Hentz and Tom Hurst for all their assistance during the past five years. In addition, I would like to thank my lab partners and friends Lucas Pratt, Branden Chiclana, Andrew Ceruzzi, Daanish Maqbool, Colin Adamson, Stephen Vannoy, and Stephen Cale. Finally, I want to thank my wife, my father, my sister, and the rest of my family for all their support.

Table of Contents

Dedication	ii
Acknowledgements	iii
Table of Contents	iv
Chapter 1: Introduction	1
1.1 Air Engines Overview	1
1.2 Previous Air Engines	2
1.2.1 Furnace Gas Engines	2
1.2.2 Ericsson Engines	5
1.2.3 The Stirling Engine	9
1.3 Motivation and Objective	16
Chapter 2: Soony Gen II Design	19
2.1 Soony Gen II Engine: Overview	19
2.2 Gen II Engine's Steps:	20
2.2.1 Expansion Stage	20
2.2.2 BDC	20
2.2.3 Compression Stage	21
2.2.4 Top Dead Center (TDC)	21
2.3 Soony Gen II Engine: Quasi-static Modeling	22
2.3.1 Quasi-static Assumptions	22
2.3.2 Quasi-static Steps:	23
2.3.3 Quasi-static Mathematical Formulation:	27
2.3.4 Quasi-static Model: Exploring the Parameter Space	31
2.3.5 Quasi-static Model: Disadvantages	32
2.4 Soony Gen II Engine Design: Shortcomings	32
2.5 Soony Gen II Engine: Design Improvements	33
2.6 Soony Engine's New Cycle: Similarities with Newcomen Steam Engine's Cycle	34
2.6.1 Newcomen Engine: Principle of Operation	35
2.6.2 Newcomen Engine: Efficiency and BMEP	36
Chapter 3: Thermodynamic Model	37
3.1 Overall Approach	37
3.2 Basic Formulation	37
3.3 Source Term Models	41
3.3.1 Cylinder Volume	41
3.3.2 Mass Flux Term	42
3.3.3 Enthalpy Flux Term	46
3.4 Component Models	46
3.4.1 Hot Reservoir	47
3.4.2 Cold Reservoir	47
3.4.3 Working Cylinder	47
3.5 Entropy Calculation	49
3.5.1 Entropy Calculation: Monoatomic Gas	49
3.5.2 Entropy Calculation: Diatomic Gas	50

3.6 Component Model Validation.....	50
3.6.1 Compression and expansion in an adiabatic piston-cylinder arrangement	51
3.6.2 Compression and expansion in a non-adiabatic piston-cylinder arrangement.....	52
Chapter 4: Soony Gen III Performance – Fixed Heat Rates.....	55
4.1 Overview.....	55
4.2 MATLAB Inputs and Outputs	56
4.2.1 MATLAB Inputs.....	56
4.2.2 MATLAB Outputs	56
4.3 Test Case.....	57
4.3.1 Mass Variation with Crank Angle	58
4.3.2 Pressure Variation with Crank Angle	59
4.3.3 Temperature Variation with Crank Angle	60
4.3.4 P-v Diagram.....	61
4.3.5 T-s Diagram	61
4.4 Reaching Steady-state.....	62
4.5 Current Model: Shortcomings.....	63
Chapter 5: Soony Gen III Performance – With Tubes Bank Heat Exchanger Model	64
5.1 Overview.....	64
5.2 Test Case.....	66
5.3 Cen III: Reaching Steady-state	66
5.4 Cen III: Exploring the Engine’s Parameter Space	67
5.5 Results.....	68
5.5.1 Optimum Power Output.....	68
5.5.2 Effect of Reservoirs’ Pressure on Optimal Results.....	69
5.5.3 Optimum BMEP	70
5.5.4 Optimum Efficiency.....	71
5.6 Current Model: Shortcomings.....	71
Chapter 6: Soony Gen III Performance – Another Heat Exchanger Model	72
6.1 Overview.....	72
6.2 Thermodynamic Model.....	73
6.2.1 Step 1: Specific heat at constant pressure	73
6.2.2 Step 2: Calculate the dynamic viscosity	74
6.2.3 Step 3: Calculate the thermal conductivity	74
6.2.4 Step 4: Calculate the Prandtl number.....	74
6.2.5 Step 5: Calculate the Reynolds number	74
6.2.6 Step 6: Calculate the Nusselt number	75
6.2.7 Step 7: Calculate the convective heat transfer coefficient (inside the tube)	75
6.2.8 Step 8: Compute the overall heat transfer coefficient.....	75
6.2.9 Step 9: Outside heat transfer coefficient	75
6.2.10 Step 10: Compute fluid exit temperature	76
6.2.11 Step 11: Compute the heat transfer rate	76
6.3 Exploring the Parameter Space.....	77
6.3.1 Inputs.....	77
6.4 Results.....	78

6.4.1 Power Output Peaks vs. Compression Ratio.....	78
6.4.2 Effect of source/sink mass flow rates	79
6.4.3 BMEP vs. Compression Ratio	80
6.4.4 Efficiency vs. Compression Ratio.....	81
6.4.5 Effect of changing the reservoirs volumes.....	82
Chapter 7: Conclusion.....	83
7.1 Summary of Findings.....	83
7.2 Main Contributions	83
7.3 Future Work	84
Appendices.....	86
A. Gen III a - Dynamic Model.....	86
B. Gen III b - Dynamic Model.....	105
C. Gen III c - Dynamic Model	122
Bibliography	143

Chapter 1: Introduction

1.1 Air Engines Overview

Air engines were considered a major source for mechanical power during the latter part of the nineteenth century, and thousands of these engines were produced. During that time period, numerous designs gained popularity and were used in factories and workshops. However, as time progressed, these engines were eventually replaced by high-speed internal combustion engines, whose higher power output capabilities and lower costs have proven them superior to other air engines [1]. For instance, as shown in Table 1, internal combustion engines have a clear advantage over Stirling engines in terms of power outputs and cost [2].

Table 1: IC engines and Stirling Engines Comparison

	IC Engines	Stirling Engines
Power Output (kW)	5-5,000	1-200
Cost (\$/kW)	440-830	2,000-36,000

Over the past few decades, numerous developments in the fields of material science and heat transfer applications have taken place. Such developments could be advantageous to air engines, where modernized designs with lighter and heat-resisting alloys could bring them back and put them in a new perspective.

Adolf Slaby (1878) separated air engines into three different categories, based on the cycling process of the working fluid and its interaction with the rest of the engine's components [1]:

1. Open cycle engines that allow a complete mixture between the working fluid and the products of combustion (example: furnace gas engines).

2. Open cycle engines that operate with external heating so the working fluid does not mix with the products of combustion (example: Ericsson engines).
3. Closed cycle engines: The same working fluid is used repeatedly and external heating is applied (example: Stirling engines).

A brief survey of several gas engines from each of the above categories will be presented and discussed next. Although these engines were for a time able to provide adequate mechanical work, they eventually failed to compete with modern internal combustion engines that still dominate the fields of transportation and power generation.

The Soony engine, the subject of this study, is a closed-cycle external heat engine design that shares some characteristics with many earlier air engine designs. Thus, it is first important to present a brief survey about previous work done in this field.

1.2 Previous Air Engines

1.2.1 Furnace Gas Engines

Early in the nineteenth century, steam engines were a main source of mechanical power. However, with the materials available at that time, operating these engines at high pressure led to a number of injuries and fatalities related to bursts in the boilers. Thus, for safety purposes, engineers substituted air for steam, and the combustion products were allowed to mix with the working fluid inside the cylinder [1].

According to Finkelstein, the first practical furnace gas engine ever built was designed by Sir George Cayley in 1807. While most technical details about that engine failed to survive, a sketch of that engine, shown in Figure 1, remains as a record of the first practical furnace gas engine ever built [3].

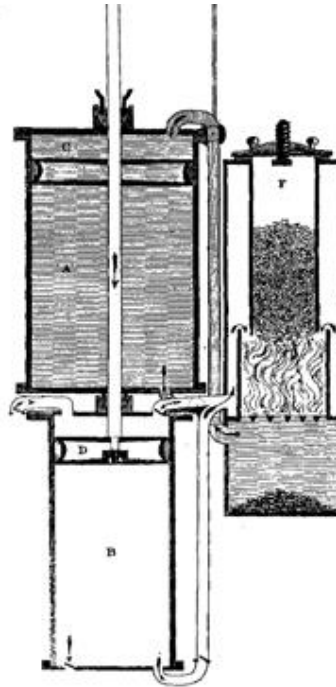


Figure 1: Sketch of the first practical gas engine (Adapted from Finkelstein [1])

Cayley continued to make improvements to his original design, and in 1837, he filed a patent for an improved design which was later manufactured by the Caloric Engine Company. The improved engine had two working cylinders. The first cylinder was a compression cylinder that admitted high-pressure air into a combustion chamber where it was used to burn fuel. Then, the hot combustion products and any remaining air were admitted into a second cylinder to expand and produce work. According to Poingdestre, the engine was able to produce 6 hp. with an approximate fuel consumption of 30 lbs. of coke per hour [4].

Afterwards, numerous furnace gas engines with varying degrees of complexity were built. For instance, Figure 2 shows a simple design of a compact engine that was known as a ‘gradual combustion engine.’ This engine was built in 1880, and had a double-acting piston with an integrated combustion chamber next to the working cylinder. The placement of the furnace in the same assembly with the working

cylinder allowed for continuous conductive heating through the walls, and forced convection when the valve opened between the cylinder and the furnace [1].

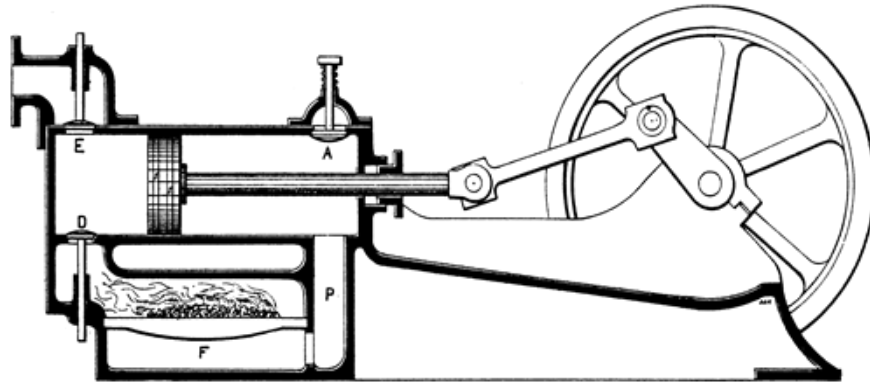


Figure 2: 'Gradual combustion engine' built in 1880 (Adapted from Finkelstein [1])

As shown in Figure 2, when the working piston moves left, it compresses the gas and it expels it through valve E, while valve D remains closed. Meanwhile, the gas to the right of the working piston expands and its pressure drops below atmospheric pressure, so new atmospheric air enters through valve A. Towards the end of the stroke, valve E closes and valve D opens, which allows the gas on the left side of the piston to be heated, and that increases its pressure, which allows the gas to expand on the left side, and the piston starts its return stroke.

During that same time period, more complex furnace gas furnace engines were built. For example, Figure 3 is a drawing of a very intricate design for a furnace gas engine, which included an expansion cylinder, a compression cylinder, a preheater, a furnace, and a hopper that allows for continuous fuel addition. This engine was known as the 'Buckett engine', and it was an improvement to Cayley's engine that was discussed earlier. The Buckett engine was also built around 1880 by the Caloric Engine Company [1].

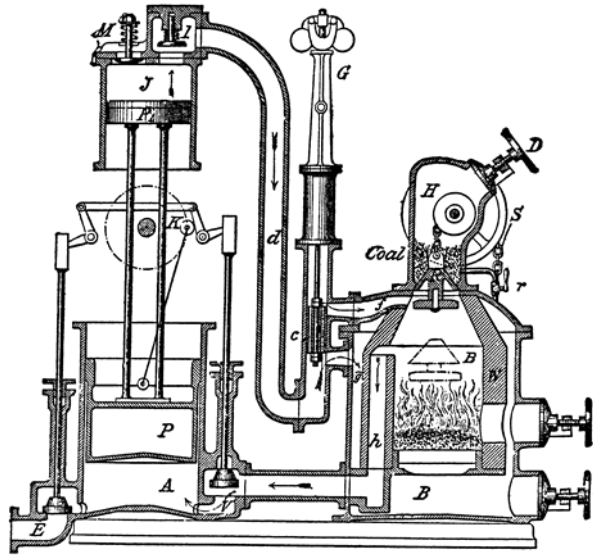


Figure 3: The Buckett engine (Adapted from Finkelstein [1])

Unfortunately, these furnace gas engines had short lifespans. The dust and ashes mixing with the working fluid and then carried into the working cylinder, along with deficiency in lubrication, had led to damaging the working cylinder fairly quickly [1].

1.2.2 Ericsson Engines

Numerous original designs of open cycle engines with external heating were developed during the early part of the nineteenth century. However, most of the successful ones were designed and perfected by one man alone, John Ericsson, whose innovations also extended to other fields like locomotives, ships, torpedoes, screw propellers, and others [1].

After moving to America, Ericsson continued his work on open cycle engines, and he built eight experimental models between 1840 and 1850, each with certain improvements over its predecessor. The eighth model, shown in Figure 4 with Ericsson's own annotations, was built in New York in 1851 and was able to generate 5 hp. It ended up being used at the Delameter iron foundry in New York [1].

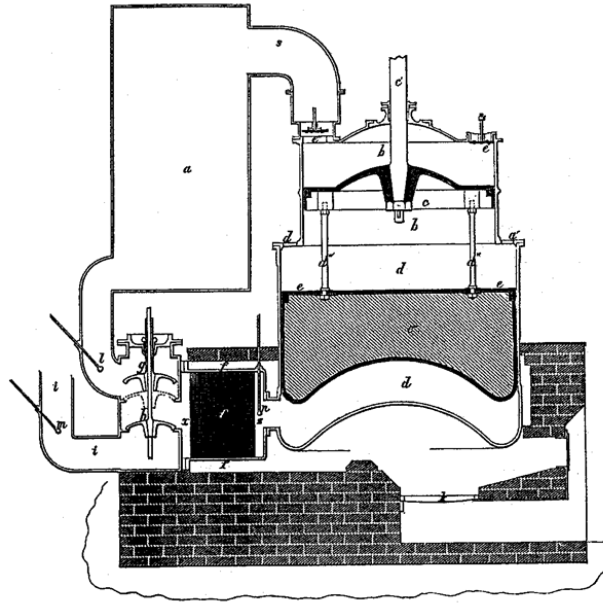


Figure 4: Experimental engine built by Ericsson in 1851 (Adapted from Finkelstein [1])

The operating principle of Ericsson's engine shared some similarities with the Buckett engine in that it had coupled pistons that operated both the compression and expansion cylinders. However, Ericsson's engine used external heating that separated the working fluid from the combustion products. More than that, the engine's employment of a regenerator had a crucial role in its success. The placement of the regenerator between the air receiver and the expansion cylinder helped to heat up the regenerator and retain much of the heat in the system after the air was expelled [1]. The cycle steps of the Ericsson's engine are explained next, with reference to the letters in Figure 4.

As the pressure of the gas inside the compression cylinder 'b' increases, air flows into reservoir 'a' whose pressure starts to rise. When both pistons reach bottom dead-center, air flows from reservoir 'a' through the regenerator (shown as a black box in Figure 4), and the air heats up. Afterwards, air flows into the expansion cylinder 'd' where it continues to heat up (because cylinder 'd' is built into the furnace). As the air

pressure starts to increase inside cylinder 'd', the expansion cylinder starts moving up until halfway through the upstroke. During the second half of the upstroke, no more air is allowed to flow into the expansion cylinder from reservoir 'a' (valve 'g' closes), and the rest of the expansion in cylinder 'd' is isothermal. During the downstroke, valve 'b' opens while valve 'g' remains closed, and the air is expelled through the regenerator, while most of the heat is retained by the regenerator [1].

It is important to note that the regenerator that was employed in Ericsson's engine was the invention of Robert Stirling, the inventor of the Stirling engine, who will be discussed in the next section [1].

Afterwards, a company headed by John Kitching started building a 2200-ton ship that was powered by four much larger versions of Ericsson's engines. The cylinders' diameters were approximately 14 ft. and the stroke was 6 ft. This posed a manufacturing challenge to make close-fitting pistons, and frictional losses were large. Furthermore, the wires that formed the regenerators added significant weight and size penalties: the wires' length was about 50 miles and their weight was about 33,000 lbs. [1].

Ericsson had very optimistic expectations for his engine. He predicted a power output of 600 hp. and a coal consumption of 8 tons per 24 hours. Unfortunately, these expectations were much higher than the engine's actual capabilities. The engine generated 300 hp. and had double the fuel consumption expected. Eventually, the vessel's engines were replaced by steam engines due to their poor performance [1].

After this setback, Ericsson was determined to perfect his engine design, and he continued to build improved versions. After building 15 different improved models,

he finally was able to create a very successful model that had a very similar cycle process to the previous models, but with various mechanical differences. For instance, the two working cylinders were replaced by only one that served as both a compression and power cylinder. This new engine model, shown in Figure 5, gained a lot of popularity during that time, and it was the first air engine that was ever mass-produced. By 1860, over 3000 engines were already sold in England, United States, Sweden, France, and Germany [1].

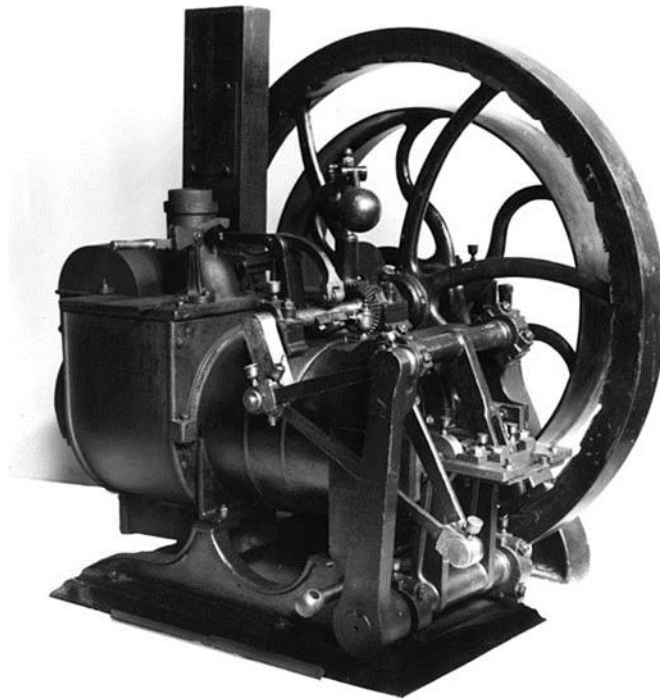


Figure 5: First hot air engine ever mass produced (Adapted from Finkelstein [1])

Eventually, these engines lost popularity due to their massive size and weight. Also, starting these engines and getting them warmed up and ready was a lengthy process that initially took about two hours. Later improvements helped to shorten the warm-up time of these engines to about 20 minutes. With all the improvement attempts, these engines produced about $\frac{1}{2}$ hp. and their average fuel consumption was about 15

lbs. per brake horsepower-hour, which was very high [1].

1.2.3 The Stirling Engine

As previously discussed, all air engines belonging to the first and second categories had numerous problems that varied from one design to another. Eventually, all those designs lost their popularity and were replaced by other designs like Stirlings. The Stirling engine belongs to the third and last air engine category described by Adolf Slaby.

This type of closed-cycle engine employed a critical component called a regenerator, which served as a thermal store and means by which heat is transferred to and from the working fluid during different phases of the engine's cycle. Additionally, all open-cycle engines previously discussed followed a series of successive operations such as air intake, compression, expansion, convection, and exhaust. However, in the case of a closed-cycle engine, many of these operations happen simultaneously. For example, when a portion of the working fluid is being heated, another portion is being cooled. The expansion and compression processes also happen simultaneously.

The invention of closed-cycle external combustion engine was made in 1816 by Reverend Robert Stirling. At the time, he was 26 years old and had just been ordained to his first parish. His original patent had the lengthy title *'Improvements for Diminishing the Consumption of Fuel, and in particular an Engine capable of being applied to the Moving (of) Machinery on a Principle Entirely New'*. In that patent, Stirling explained the construction details of his engine and the implementation of a regenerator for the first time in history [1]. Figure 6 shows a drawing of the first Stirling engine.

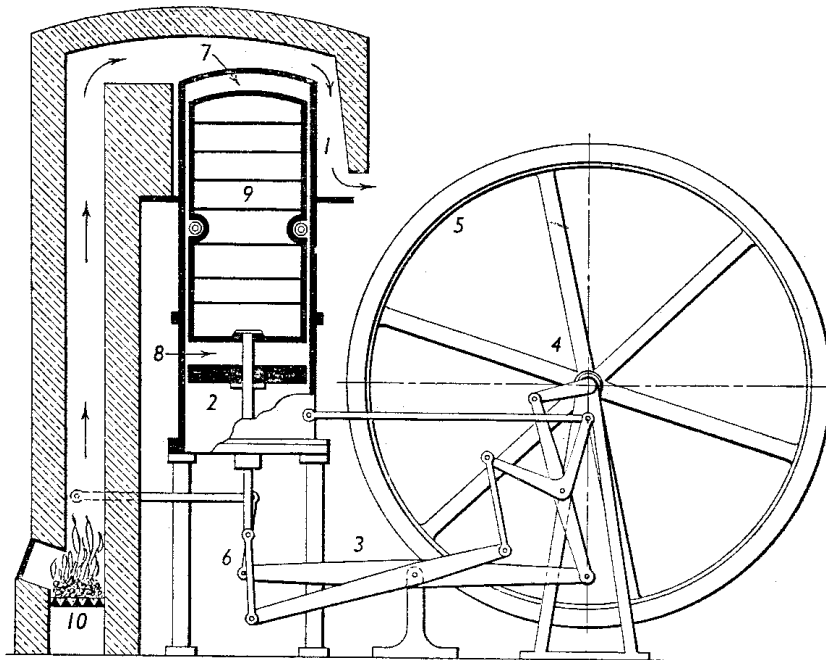


Figure 6: Drawing of the first Stirling engine (adapted from Finkelstein [1])

The drawing above had each of the engines' components numbered as follows:

1. Vertical working cylinder.
2. Working piston.
3. Rocking beam.
4. Crankshaft.
5. Flywheel.
6. Link motion.
7. Hot working fluid.
8. Cold working fluid.
9. Hollow displacer that separates the hot and cold working fluids. It also has the regenerator installed in the annular space located halfway on its cylindrical surface.
10. Combustion chamber.

The working fluid inside the working cylinder is divided by the displacer into a hot space and a cold space, where the hot space is located above the displacer and the cold space is located below it. The temperature of the hot space is maintained by the heat transfer from the hot flue gases that are generated in the combustion chamber, and the temperature of the cold space is maintained by water cooling. The cycling process of the working fluid is divided into four steps.

At the beginning of the cycle, the cold space is at maximum volume. During the first step, the working piston compresses the cold fluid isothermally requiring that heat be rejected. Afterward, the power piston remains in place while the motion of the displacer piston forces the working fluid past the regenerator transferring stored heat to the fluid which increases its pressure. In the third step, the expansion process occurs isothermally at an elevated temperature requiring heat to be transferred to the working fluid during the expansion. Finally, the power piston stays motionless while the displacer forces the air through the regenerator and back to the hot side of the engine [1].

The working cylinder was about 10 ft. high and 2 ft. in diameter. The displacer was made of thin iron sheets and had a diameter slightly smaller than the cylinder's. The displacer had small wheels on its surface to keep it centered as it moved inside the cylinder. The annular space on the surface of the displacer was about 0.5 in thick. In that space, a thin wire was wound, and it served as a regenerator. According to some accounts, the first Stirling engine shown in Figure 6 was able to produce about 2 hp. [1].

Between 1824 and 1840, Robert Stirling continued making improvements to his

engine, in collaboration with his brother James. In 1840, they registered a joint patent for an improved model, shown in Figure 7. A key modification was that the regenerator became stationary instead of moving with the displacer. The improved model had the cylinder bottom directly exposed to the flames. This made natural convection inadequate for cooling, so water cooling was used instead. The working cylinder also was made much longer to keep its upper end cool [1].

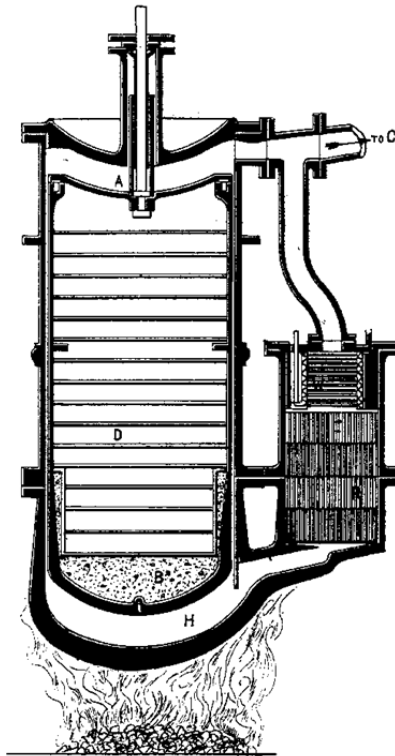


Figure 7: Improved Stirling engine designed by Stirling brothers (Adapted from Finkelstein [1])

However, these models failed to gain commercial popularity because the cylinder's bottom tended to overheat from the direct exposure to the flames; heat-resisting metals were not available at the time. For instance, in March 1843, Stirling's engine had an industrial application when it was installed in a foundry in Dundee.

Unfortunately, the cylinder's bottom was badly damaged by the fire, and it was replaced in December 1845. The second cylinder only lasted until May 1846, and the

third cylinder lasted until January 1847. At that point the foundry's owner decided to replace Stirling's engine with a steam engine [1].

However, in recent decades, extensive developments in the field of material science have taken place, and modern materials such as light-weight alloys and heat-resisting steels have become available. Also, more in-depth understanding of thermodynamics and heat transfer has enabled the revival of Stirling and other air engines as well.

The net result is that and after years of research and development, today's Stirling engines could become potential competitors to other mature power generation technologies, such as internal combustion engines.

Current Stirling models follow the same (Stirling) cycle that was patented by Robert Stirling in 1816. The ideal cycle consists of four thermodynamic processes:

1. Isothermal Expansion: The working fluid is isothermally expanded by external heating.
2. Isochoric Heat Removal: Heat is transferred from the working fluid to the regenerator where it is stored for use later in the cycle.
3. Isothermal Compression: The working fluid is compressed while being cooled by an external sink.
4. Isochoric Heat Addition: Heat stored in the regenerator is transferred back to the working fluid.

Modern Stirling engine technologies target several applications such as vehicle propulsion, air propulsion, and auxiliary and submarine power generation. However, the main Stirling application that has been under ongoing development is combined heat and power generation for residential and commercial uses. A key advantage of

this technology is fuel-flexibility and the ability to exploit inexpensive heat sources like biomass and industrial waste heat.

Developers of modern Stirling engines continue to improve their designs and models by addressing important factors that impact the engine's performance like [2]:

1. Temperature Range: Most Stirling developers are targeting an operating temperature of around 1000 K. Others are trying to work with higher temperatures (around 1400 K) to increase efficiency, or lower operating temperatures to reduce material-related problems [2].
2. Engine's Speed: While most Stirling engines operate at high rpm (1200-1800 rpm), developers are also investigating running the engine at low speed to reduce viscous losses and extend the engine's life [2].
3. Leakage: The most common working fluids currently in use are hydrogen and helium because their high gas constants improve performance. However, leak problems offset much of this advantage, so developers have been investigating the use of other working fluids like nitrogen or air that are easier to seal.

Furthermore, while current Stirling engines provide higher thermodynamic efficiency than IC engines, the latter are still the dominant technology in the fields of transportation and power generation due to their compactness, lighter weights, higher power outputs, and lower costs. Table 2 lists the power output and BMEP for a number of Stirling engines. It also includes a common internal combustion engine, for comparison [2]. As shown in the table, the IC engine (Waukesha F18GL) produces higher power output than all the Stirling engines presented. In addition, The SOLO

Stirling engine is the only engine with higher BMEP than the Waukesha engine, but its price is significantly higher than Waukesha [2].

Table 2: BMEP and power output for various Stirling engines (and the Waukesha IC engine) [2]

Engine	Rated Shaft Output (bhp)	BMEP (psi)
Uwe Moch (Stirling)	0.7	19
STM (Stirling)	37.3	69
Sigma (Stirling)	4.5	136
SOLO (Stirling)	14.9	400
Waukesha –Single Cylinder (F18GL IC Engine)	73	176

Another obstacle that still faces the commercialization of Stirling engines is related to unproven long-term durability and reliability. There are also challenges associated with the seals that separate the high-pressure fluid from the lubricant used for the mechanical drive train as well as other issues related to corrosion in high temperature and pressure operating regimes. Some of the challenges described can be addressed by incorporating special materials, but their high cost impedes the development of this technology [2].

For example, Figure 8 presents a logarithmic plot that compares prices of various beta demonstration models to the ‘Target Wholesale Price’ [2]. Thus, Stirling technology still has many obstacles to overcome in order to become competitive with IC engines.

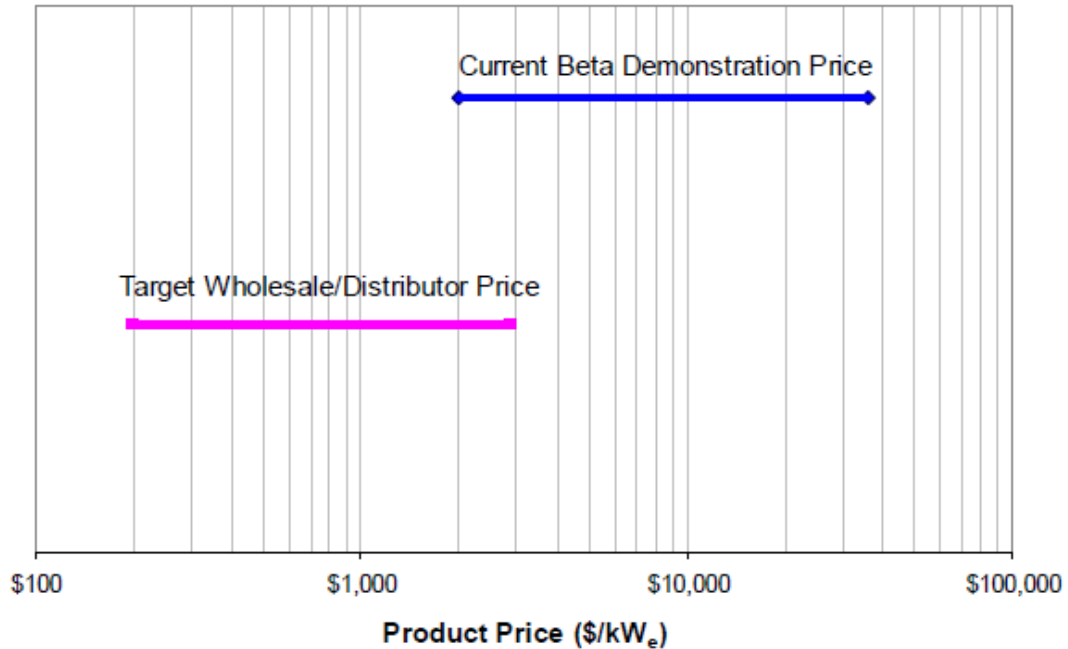


Figure 8: Stirling engines prices [2]

1.3 Motivation and Objective

Soony Systems Inc. has developed its own version of an air engine that it claims can outperform and be constructed more economically than existing Stirling engines [5]. One intended application is an affordable combined heat and power system for private residences. The original version of this engine (Gen I, Figure 9) used a patented mechanism to move fluid between the hot and cold sides of the engine. It was soon discovered that the Gen I ‘engine’ was not capable of producing power so some design changes were proposed. The main objectives of this thesis are to evaluate the performance of this revised (Gen II) engine and to suggest further improvements to it. This is accomplished by constructing a thermodynamic model of the engine’s cycle and using it to identify optimum designs and operating conditions.

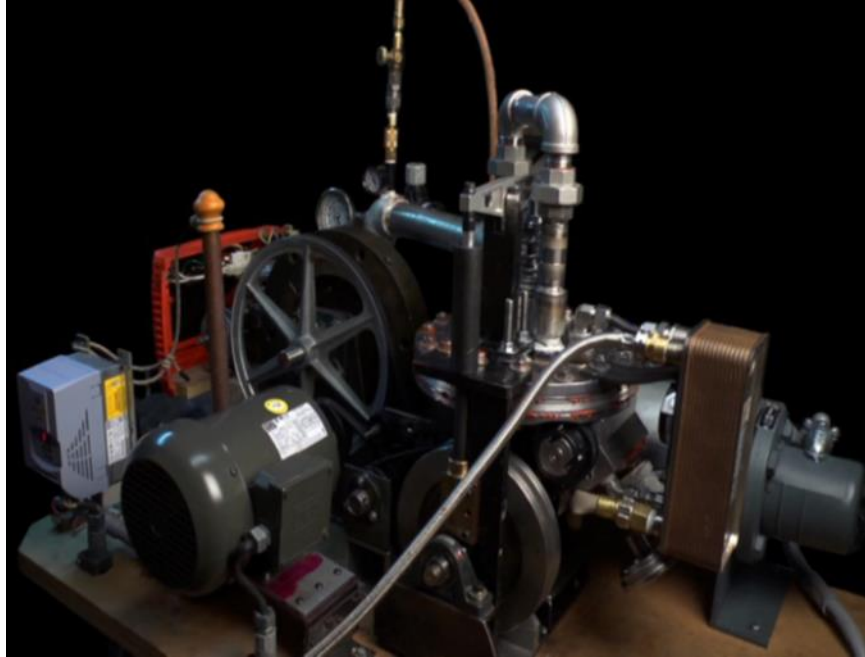


Figure 9: Bench-scale model of the Soony system (Gen I)

The specific steps in the model development process are listed below:

1. Develop a quasi-static thermodynamic model of the Soony Gen II engine based on steady-state versions of the mass and energy conservation equations:
 - a. Develop physics- based models for heat and mass change in each of the engine's volumes (cylinder volume, pump volume, heat exchangers volumes, tubes volumes, etc.).
 - b. Connect the quasi-static models to create a quasi-static thermodynamic model of the engine.
 - c. Run the quasi-static model at different engine speeds and with different values of key design parameters to predict the engine's performance.
2. Build a more realistic dynamic model of the engine cycle using unsteady versions of the conservation equations.

3. Use the dynamic model to refine the design of the engine by exploring how changes in design and operating parameters influence the engine's performance.
 - a. Study the effect of changing the volumes of the hot/cold reservoirs.
 - b. Study the effect of changing the volume ratio of the reservoirs.
 - c. Study the effect of changing the expansion ratio.
 - d. Study the effect of changing the temperatures and pressures of the hot/cold reservoirs.
 - e. Add time-dependent heat transfer models in the hot and cold reservoirs.
 - f. Incorporate discharge coefficients to more realistically estimate pressure losses.
4. Develop a realistic thermodynamic model of the hot and cold reservoir heat exchangers and investigate the effect of their performance on the Soony engine's ability to extract useful work from various flows of hot air.
5. Identify engine designs that maximize:
 - a. Efficiency
 - b. Power Output
 - c. Brake Mean Effective Pressure (BMEP)

Chapter 2: Soony Gen II Design

2.1 Soony Gen II Engine: Overview

A CAD model of Soony's Gen II engine is shown in Figure 10. The Gen II engine consists of five interconnected volumes (as shown in Figure 11):

1. Hot Reservoir
2. Cold Reservoir
3. Working Cylinder
4. Expansion/Compression Chamber
5. Pump Chamber

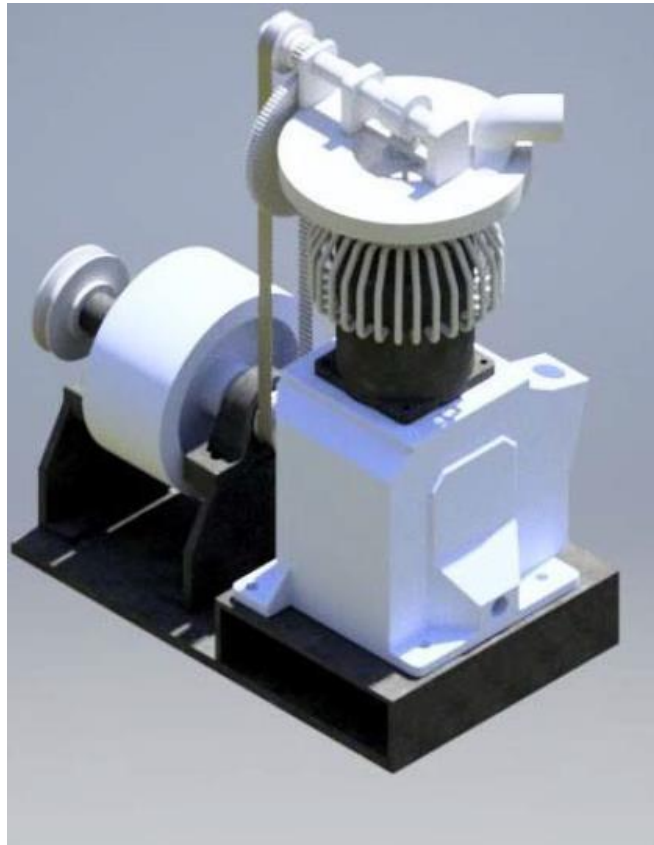


Figure 10: Soony Gen II CAD assembly (Barry Johnston)

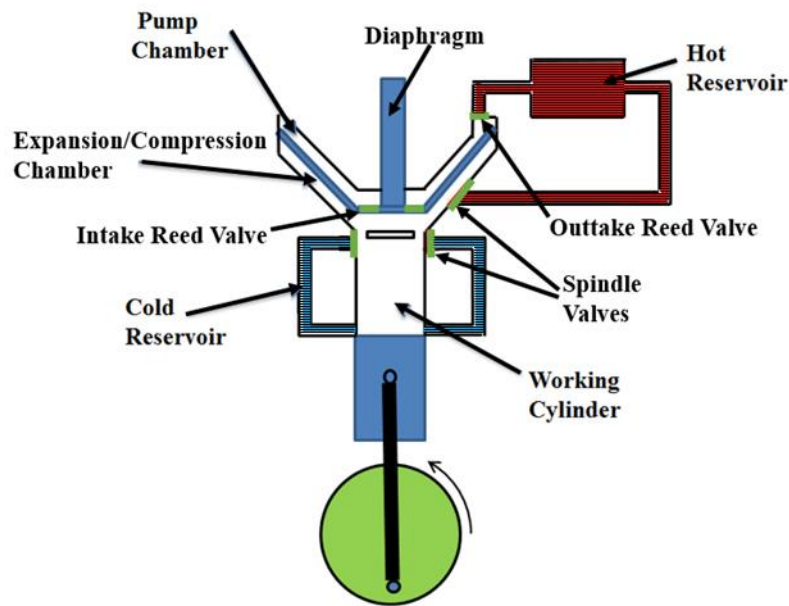


Figure 11: Soony Gen II components

2.2 Gen II Engine's Steps:

The following steps explain the operating principle of the Soony Gen II engine, as described by the inventor of the Soony system:

2.2.1 Expansion Stage

During this phase, the diaphragm is at its highest point of travel and the working fluid in both the expansion chamber and working chambers is isolated from the hot and cold reservoirs. The working fluid expands, driving the power piston downward to BDC (bottom dead center). The spindle valves and reed valves, shown in Figure 11, remain closed during this stage.

2.2.2 BDC

When the power piston reaches BDC, the spindle valves open, and the fluids inside the working cylinder and cold reservoir become able to interact. At this point, a cam

starts driving the diaphragm downward, and the expansion chamber becomes a compression chamber. Soony claims that the downward motion of the diaphragm occurs in a “balanced pressure environment.” In other words, the pressure above and below the diaphragm will be almost equal during the diaphragm’s downward motion so that little work must be performed to move it.

2.2.3 Compression Stage

During this stage, the diaphragm continues its downward motion while the power piston continues its upward motion. This drives the fully expanded working fluid out of the piston chamber, and into the cold reservoir and the volume above the diaphragm (i.e. pump volume). Again, Soony claims that the pressures above and below the diaphragm remain approximately equal during this stage. Additionally, the volume above the diaphragm (pump volume) will continue to fill up.

2.2.4 Top Dead Center (TDC)

As the piston reaches TDC, the diaphragm is at its lowest point of travel, but the pressure in the pump (the volume above the diaphragm) is still less than that in the heat exchanger. At this point, there is no more fluid below the diaphragm, and a loaded spring (the spring was loaded during the downstroke) starts pushing the diaphragm upward in order to increase the pressure in the pump volume. As the spring pushes the diaphragm upward, the diaphragm reaches a distance at which the pressure inside the pump volume becomes equal to the pressure inside the heat reservoir, which is higher than in the working cylinder.

As the diaphragm continues its upward travel, the pressure in the pump volume becomes higher than the hot reservoir’s pressure, so the unidirectional reed valve

between the pump and the hot reservoir opens. This allows the working fluid in the pump to flow into the hot reservoir, and the diaphragm eventually reaches its highest point of travel.

At this point, the spindle valves in the hot reservoir open, and hot fluid flows from the heat exchanger into the region below the diaphragm. It is important to note that the expansion of the hot gas into a larger volume will ensure a lower pressure below the diaphragm. This slight pressure difference will prohibit any fluid to flow from the expansion chamber into the pump volume. So, during the upward travel of the diaphragm, the pump chamber will always have a higher pressure than the expansion chamber. At this point, the cycle is ready to repeat.

2.3 Soony Gen II Engine: Quasi-static Modeling

2.3.1 Quasi-static Assumptions

A quasi-static model assumes a very slow thermodynamic process. This ensures that the system being studied remain in internal equilibrium. Thus, the power piston is assumed to be moving slowly enough to allow uniform pressure throughout the volume.

Additionally, this idealized analysis has broken the engine's cycle into a series of compression, expansion, and fluid transfer steps with the following assumptions:

1. Isentropic compressions and expansions
2. Uniform temperature and pressure in all volumes:
 - a. Perfect and instantaneous mixing
 - b. Thermal equilibration upon valve opening
3. No flow losses

4. No heat addition/loss in the working cylinder, except via mass transfer
5. Instantaneous re-heat in the hot reservoir
6. Instantaneous cool-down in the cold reservoir

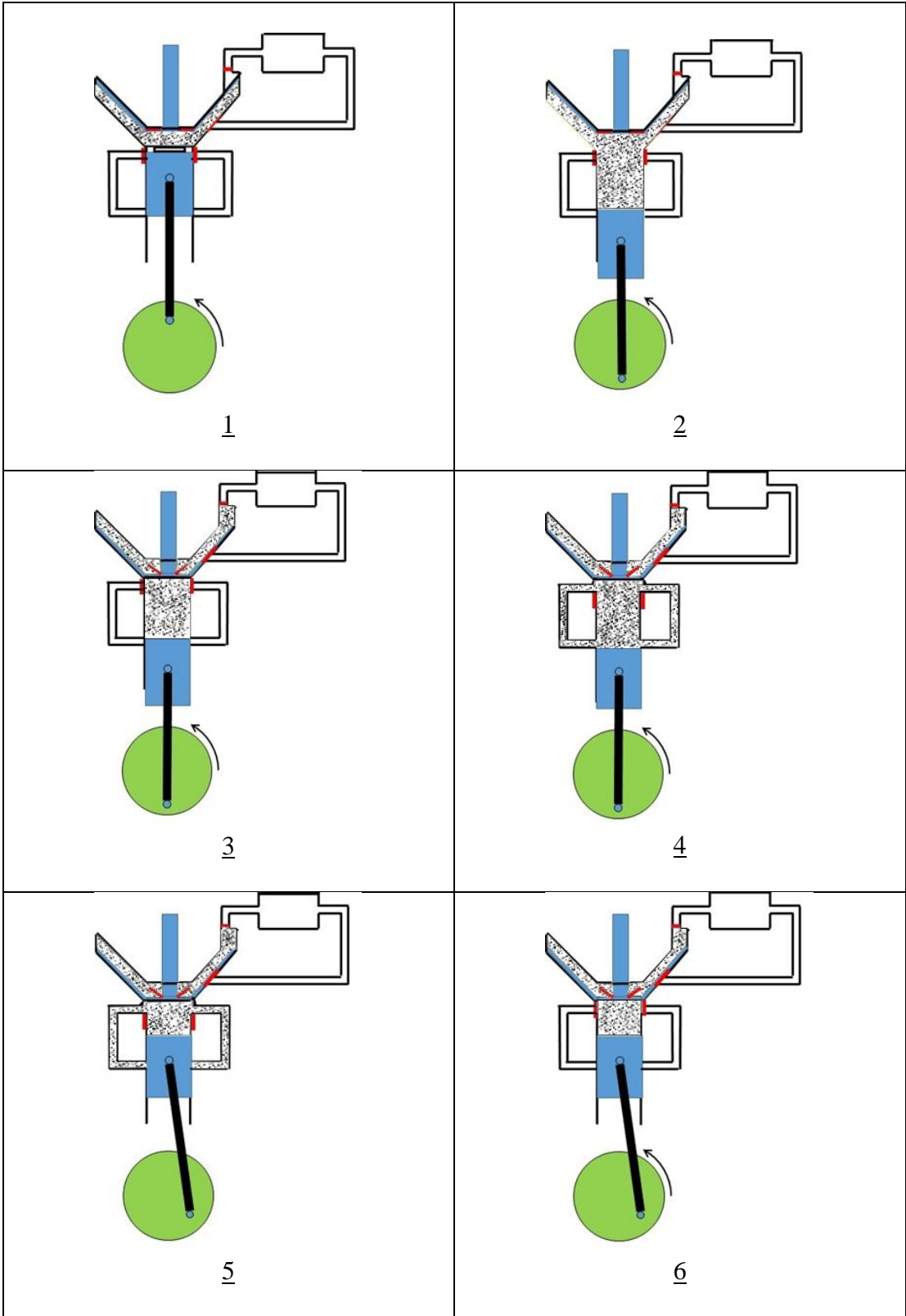
2.3.2 Quasi-static Steps:

In order to solve the quasi-static model, the engine's cycle has been divided into 12 discrete steps illustrated below. The working fluid in every step (shown in Figure 12) is represented using randomly spaced dots:

1. Step 1: The power piston is at TDC, and the diaphragm is at its highest point of travel.
2. Step 2: The power piston is at BDC. At this point, the diaphragm hasn't moved down yet, and the cooling reservoir is still not open to the working cylinder/expansion chamber.
3. Step 3: The power piston is still at BDC. At this point, the diaphragm has moved down, but the cooling reservoir is still not open to the working cylinder.
4. Step 4: The power piston is still at BDC, and the valves in the cold reservoir open. At this point, the working fluid in both the cold reservoir and working cylinder are able to mix.
5. Step 5: During the upstroke, the pressure will increase inside the working cylinder. As a result, the working fluid will flow into the cold reservoir and into the pump chamber. At some point during the upstroke, the cold reservoir recovers the mass it had during step 3, and this is when the cold reservoir's valves close.

6. Step 6: At this point, the cold reservoir's valves have closed, and the working fluid being analyzed is located inside the working cylinder and the pump chamber. It is also important to note that the diaphragm is still at the bottom.
7. Step 7: At this point, the working piston has reached TDC, and all the working fluid (from step 6) is now located inside the pump chamber. The diaphragm is still at the bottom.
8. Step 8: During this stage, the cold reservoir is being cooled down to its original temperature. This process is assumed to happen instantaneously.
9. Step 9: During the stage, the diaphragm has started compressing the working fluid inside the pump volume, and the pressure inside the pump volume has reached a pressure value equal to the pressure inside the hot reservoir.
10. Step 10: At this point, the fluid that was in the pump is nearly completely emptied into the heat reservoir.
11. Step 11: During this stage, the hot reservoir is heated up to its original temperature. This process is assumed to happen instantaneously.
12. Step 12: At this point, the spindle valve in the hot reservoir opens, and a certain amount of hot fluid is transferred from the hot reservoir into the expansion chamber. The cycle is ready to repeat.

The quasi-static steps described above are presented in Figure 12 next.



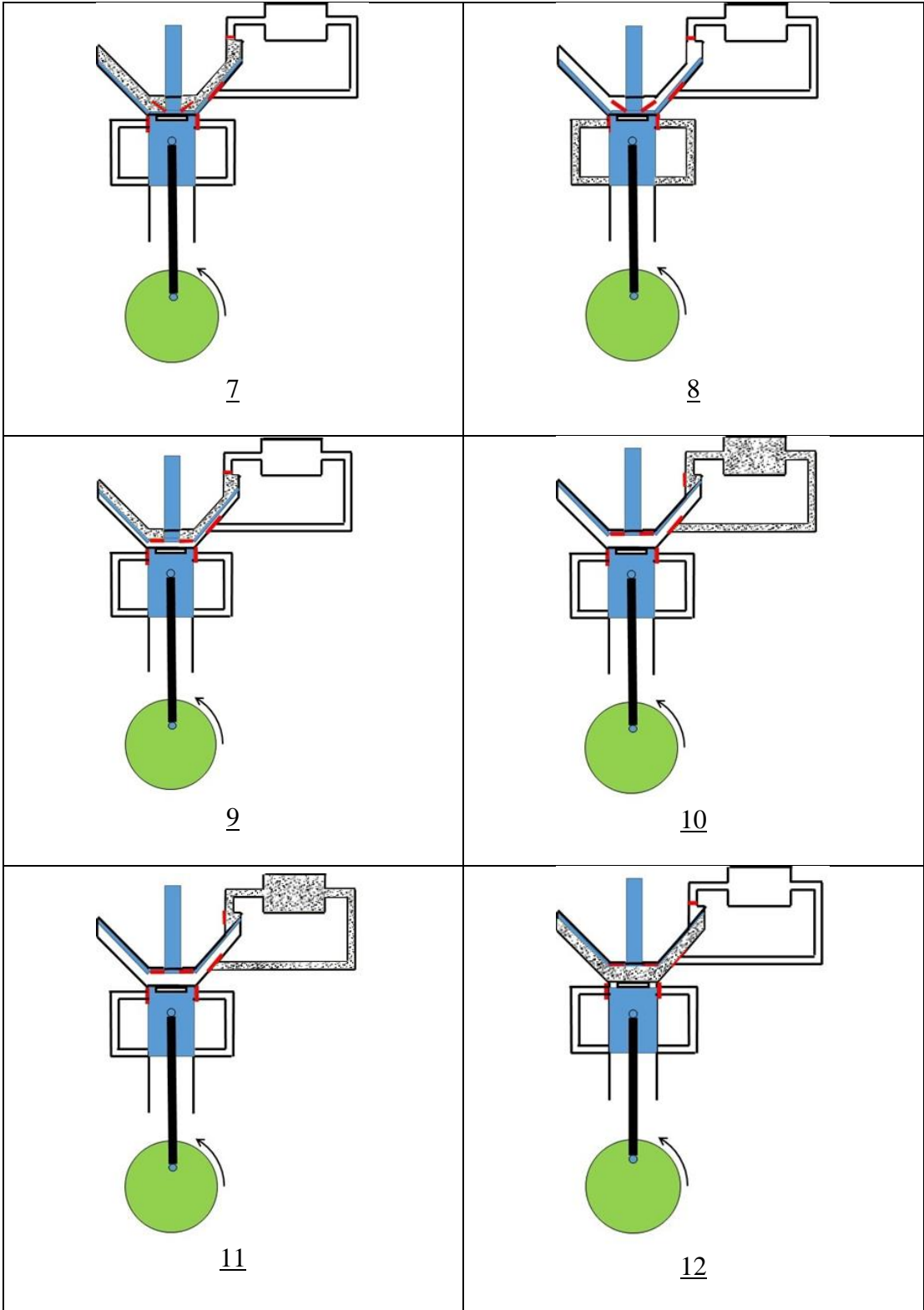


Figure 12: Quasi-static steps

2.3.3 Quasi-static Mathematical Formulation:

In order to calculate the pressure, volume, temperature, mass, internal energy, heat gain/loss, and work in each chamber, the following equations were used:

1. Conservation of Energy (First Law of Thermodynamics):

$$W = Q - \Delta U \quad (1)$$

2. Isentropic Compression/Expansion:

$$PV^\gamma = \text{Constant} \quad (2)$$

3. Equation of State:

$$PV = mRT \quad (3)$$

4. Internal Energy of an Ideal Gas:

$$U = mc_v T \quad (4)$$

5. Mass conservation (inside control volume)

$$m_{cv} = \text{constant} \quad (5)$$

The above equations were first solved using Microsoft Excel in order to get a general understanding of the engine's performance. Figure 13, Figure 14, and Figure 15 show an example of a quasi-static trial, where Microsoft Excel was given initial conditions in each chamber in order to calculate the work output and efficiency.

Working Cylinder + Pump/Expansion Chamber							
P (Mpa)	V (cm ³)	T (K)	m (kg)	U (kJ)	ΔU (kJ)	Q (kJ)	W (kJ)
TDC							
12	114	1200	0.003972125	3.415233449			
between steps 1 and 2					-2.191059723	0	2.191059723
BDC. At this point, the diaphragm hasn't moved down yet, and the cooling reservoir is still not open to the working cylinder/expansion chamber							
0.330872409	1482	430.1341311	0.003972125	1.224173727			
between steps 2 and 3					0	0	0
BDC. At this point, the diaphragm has moved down, but the cooling reservoir is still not open to the working cylinder							
0.330872409	1482	430.1341311	0.003972125	1.224173727			
between steps 3 and 4					0.061634694	0.061634694	0
BDC. The cold reservoir opens to the working cylinder							
0.347531171	11482	311.5840877	0.044622532	9.961978605	:==> Working Cylinder + Pump Chamber + Cold Reservoir		
0.347531171	1482	311.5840877	0.005759501	1.285808421	:==> Working Cylinder + Pump Chamber		
between steps 4 and 5					-0.382937552	-0.563736369	-0.180798817
At some point during the upstroke stage, immediately before the valve to the cold reservoir closes (in order to recover the original mass in the cold reservoir)							
0.370112098	10977.14286	317.238941	0.044622532	10.14277742	:==> Working Cylinder + Pump Chamber + Cold Reservoir		
0.370112098	977.1428571	317.238941	0.003972125	0.902870869	:==> Working Cylinder + Pump Chamber		
between steps 5 and 6.					0	0	0
Immediately after the valve to the cold reservoir closes							
0.370112098	977.1428571	317.238941	0.003972125	0.902870869			
between steps 6 and 7					1.229422346	0	-1.229422346
Continuing the upstroke until we reach TDC							
7.49217263	114	749.217263	0.003972125	2.132293215			
between steps 7 and 8					0	0	0
Cooling the cold reservoir to its original temperature							
7.49217263	114	749.217263	0.003972125	2.132293215			
between steps 8 and 9					0.307182438	0	-0.307182438
Start the compression of Diaphragm in order for the pressure in the pump to be equal to the pressure in the heat reservoir							
12	81.42934545	857.1510048	0.003972125	2.439475652			
between steps 9 and 10					-2.439475652	-2.439475652	-2.66454E-14
The fluid that is in the pump is nearly completely emptied into the heat reservoir							
N/A	0	N/A	0	0			
between steps 10 and 11					0	0	0
We add heat to the hot reservoir to recover the original temperature							
N/A	0	N/A	0	0			
between steps 11 and 12					3.415233449	3.415233449	1.73195E-14
The Original fluid the we started with is now emptied back into the expansion chamber							
12	114	1200	0.003972125	3.415233449			

Figure 13: Quasi-static analysis (working cylinder)

Cold Reservoir						
P (Mpa)	V (cm ³)	T (K)	m (kg)	U (kJ)	ΔU (kJ)	Q (kJ)
TDC						
0.35	10000	300	0.040650407	8.737804878		
between steps 1 and 2					0	0
BDC. At this point, the diaphragm hasn't moved down yet, and the cooling reservoir is still not open to the working cylinder/expansion chamber						
0.35	10000	300	0.040650407	8.737804878		
between steps 2 and 3					0	0
BDC. At this point, the diaphragm has moved down, but the cooling reservoir is still not open to the working cylinder						
0.35	10000	300	0.040650407	8.737804878		
between steps 3 and 4					-0.061634694	-0.061634694
=====						
BDC. The cold reservoir opens to the working cylinder.						
0.347531171	10000	311.5840377	0.038863031	8.676170184		
between step 4 and 5					0.563736369	0.563736369
At some point during the upstroke stage, immediately before the valve to the cold reservoir closes (in order to recover the original mass in the cold reservoir)						
0.370112098	10000	317.238941	0.040650407	9.239906553		
between steps 5 and 6					0	0
=====						
Immediately after the valve to the cold reservoir closes						
0.370112098	10000	317.238941	0.040650407	9.239906553		
between steps 6 and 7					0	0
Continuing the upstroke until we reach TDC						
0.370112098	10000	317.238941	0.040650407	9.239906553		
between steps 7 and 8					-0.502101675	-0.502101675
Cooling the cold reservoir to its original temperature						
0.35	10000	300	0.040650407	8.737804878		
between steps 8 and 9					0	0
Start the compression of Diaphragm in order for the pressure in the pump to be equal to the pressure in the heat reservoir						
0.35	10000	300	0.040650407	8.737804878		
between steps 9 and 10					0	0
The fluid that is in the pump is nearly completely emptied into the heat reservoir						
0.35	10000	300	0.040650407	8.737804878		
between steps 10 and 11					0	0
We add heat to the hot reservoir to recover the original temperature						
0.35	10000	300	0.040650407	8.737804878		
between steps 11 and 12					0	0
The Original fluid the we started with is now emptied back into the expansion chamber						
0.35	10000	300	0.040650407	8.737804878		

Figure 14: Quasi-static analysis (cold reservoir)

Hot Reservoir						
P (Mpa)	V (cm ³)	T (K)	m (kg)	U (kJ)	ΔU (kJ)	Q (kJ)
TDC						
12	5000	1200	0.174216028	149.7909408		
between steps 1 and 2					0	0
BDC. At this point, the diaphragm hasn't moved down yet, and the cooling reservoir is still not open to the working cylinder/expansion chamber						
12	5000	1200	0.174216028	149.7909408		
between steps 2 and 3					0	0
BDC. At this point, the diaphragm has moved down, but the cooling reservoir is still not open to the working cylinder						
12	5000	1200	0.174216028	149.7909408		
between steps 3 and 4					0	0
BDC. The cold reservoir opens to the working cylinder.						
12	5000	1200	0.174216028	149.7909408		
between steps 4 and 5					0	0
At some point during the upstroke stage, immediately before the valve to the cold reservoir closes (in order to recover the original mass in the cold reservoir)						
12	5000	1200	0.174216028	149.7909408		
between steps 5 and 6					0	0
Immediately after the valve to the cold reservoir closes						
12	5000	1200	0.174216028	149.7909408		
between steps 6 and 7					0	0
Continuing the upstroke until we reach TDC						
12	5000	1200	0.174216028	149.7909408		
between steps 7 and 8					0	0
Cooling the cold reservoir to its original temperature						
12	5000	1200	0.174216028	149.7909408		
between steps 8 and 9					0	0
Start the compression of Diaphragm in order for the pressure in the pump to be equal to the pressure in the heat reservoir						
12	5000	1200	0.174216028	149.7909408		
between steps 9 and 10					2.439475652	2.439475652
The fluid that is in the pump is nearly completely emptied into the heat reservoir						
12.19543043	5000	1192.357297	0.178188153	152.2304164		
between steps 10 and 11					0.975757797	0.975757797
We add heat to the hot reservoir to recover the original temperature						
12.2736	5000	1200	0.178188153	153.2061742		
between steps 11 and 12					-3.415233449	-3.415233449
The Original fluid that we started with is now emptied back into the expansion chamber						
12	5000	1200	0.174216028	149.7909408		

Figure 15: Quasi-static analysis (hot reservoir)

2.3.4 Quasi-static Model: Exploring the Parameter Space

A MATLAB script was created to explore the parameter space of the quasi-static model by running the engine's cycle through a number of cases. Each case corresponds to a set of initial conditions. The goal of the MATLAB script was to find the engine's optimal work output and efficiency, and the design/operating conditions associated with these optima.

The following ranges of initial conditions were examined:

1. Hot Reservoir Pressure: 8 -12 MPa (0.1 MPa increments)
2. Hot Reservoir Temperature: 800 - 1200 K. (20 K. increments)
3. Expansion Ratio: 3 – 19
4. Cold Reservoir Pressure: 0.1 – 3 MPa (0.1 MPa increments)
6. Initial Volume of Working Fluid: 50 – 300 cm³ (10 cm³ increments)

A total of 55,371,722 combinations were investigated. The initial working cylinder pressure and temperature were assumed to be equal to the initial hot reservoir pressure and temperature, respectively in these calculations. The optima identified by the investigation are presented the following table:

Table 3: Peak work output and efficiency

	Work (KJ/cycle)	Eff. (%)	P_{hot} (MPa)	T_{hot} (K)	ER	P_{cold} (MPa)	V_{init} (cm³)
Peak Work	1.24	37.58	12	1200	8	0.7	290
Peak Efficiency	0.003	56.93	10.5	980	19	0.17	50

2.3.5 Quasi-static Model: Disadvantages

While the quasi-static model provided a useful general summary of the cycle's performance, it had a number of important shortcomings:

1. **Time Dependency:** The quasi-static model does not incorporate the time-dependence of realistic transport processes. For example, the rates of heat and mass transport between components are set by the temperature and pressure differences between components. Thus, the engine's performance depends on its operating speed.
2. **Thermal Equilibrium Assumption:** The quasi-static model assumes that thermal equilibrium between two reservoirs occurs instantaneously upon valve opening. This is not realistic and can significantly impact the engine's performance.
3. **Pressure Losses:** The quasi-static model neglects flow losses, but in reality, there are pressure losses associated with the mass flow rate through each constriction (i.e. valves). A time-dependent dynamic model is necessary to incorporate the effects of these losses.

2.4 Soony Gen II Engine Design: Shortcomings

The quasi-static model also provided some additional useful insights into the Gen II design:

1. "Pressureless Environment" Claim: The diaphragm does not move in a 'balanced pressure environment'
 - a. Diaphragm downward motion: The pressure below the diaphragm has to be higher than the pressure above the diaphragm in order for the

working fluid in the working cylinder to flow into the pump volume through the inlet reed valves.

- b. Diaphragm upward motion: During the diaphragm upward motion, the pressure inside the pump becomes larger than the pressure below the diaphragm. Numerous factors could lead to a significant pressure differences including the spring's stiffness, the diaphragm's upward acceleration, and the area of the hot reservoir's valves.
2. Redundancy: The implementation of the diaphragm is redundant. The diaphragm's main purpose is to force the cooled working fluid into the hot reservoir to be re-heated. This job can be accomplished just as easily (and far more simply) using the cylinder's power piston and a few adjustments to the valve timing.

2.5 Soony Gen II Engine: Design Improvements

After discussing the above observations with Soony Systems Inc., it was decided to abandon the Gen II design in favor of an improved (Gen III) design that does not have a diaphragm (shown in Figure 16). The new operating cycle breaks into 4 steps:

1. From BDC to halfway through the upstroke: During this stage, the valves between the working chamber and the cold reservoir are open allowing fluid in both reservoirs to mix and interact.
2. Halfway through the upstroke to TDC: The valve between the working cylinder and cold reservoir is closed while the valve between the working cylinder and hot reservoir is open. The piston moves up driving the expanded and cooled working fluid into the hot reservoir to be re-heated.

3. TDC to BDC part 1: Gas flows from the hot reservoir into the working cylinder depending on the pressure difference between the two chambers. At this stage, gas will continue to flow from the hot reservoir until the working cylinder recovers the mass it lost during the upstroke.
4. TDC to BDC part 2: All valves are closed and the hot working fluid continues to expand in the working cylinder pushing the piston down.

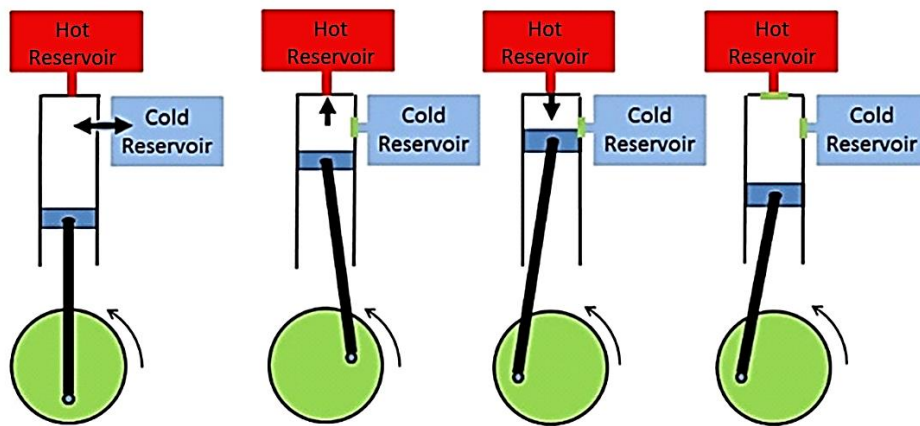


Figure 16: Soony Gen III cycle steps

2.6 Soony Engine's New Cycle: Similarities with Newcomen Steam Engine's Cycle

The cycle of the Soony Gen III model has some similarities to a steam engine, named the Newcomen engine. The Newcomen engine was built in 1712 by Thomas Newcomen. During the 18th century, over 1400 of these steam engines were built for the purpose of pumping water from coal mines. This engine is considered an “atmospheric” engine, where the atmospheric pressure is the force that drives the piston downward into the vacuum that forms under the piston. This vacuum is created when steam is condensed into water [6]. Figure 17 shows a schematic of the engine.

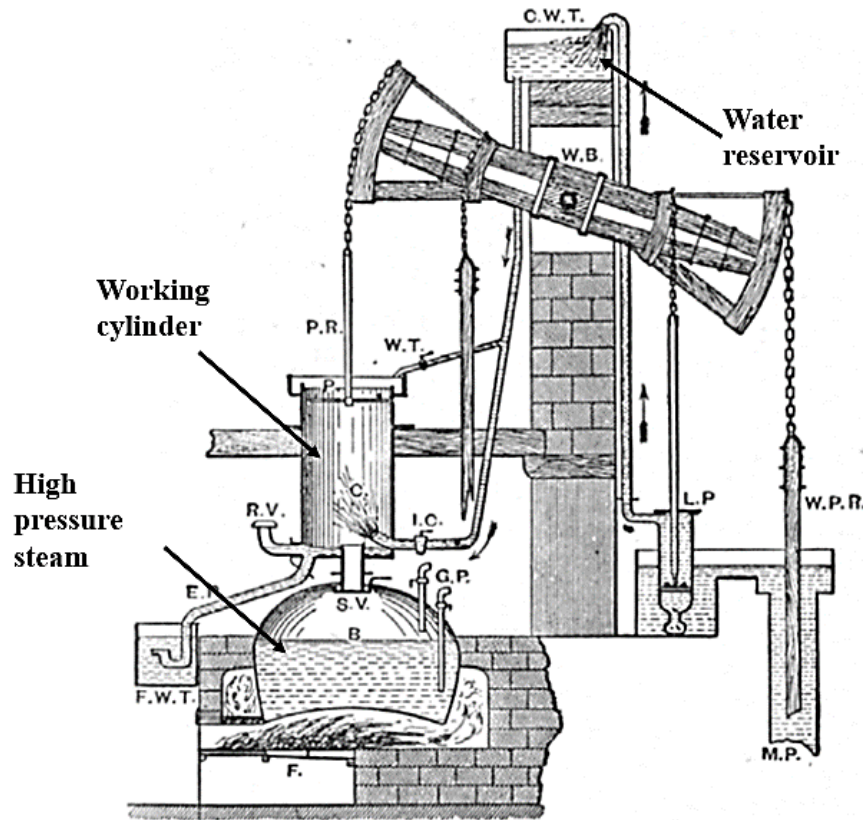


Figure 17: Newcomen engine schematic [6]

2.6.1 Newcomen Engine: Principle of Operation

The Newcomen engine uses a different working fluid than the Soony model. However, its cycle's steps and interaction with the hot and cold reservoirs share similarities with the Soony engine's cycle. The Newcomen steam engine's working cylinder sits directly above a boiler. At bottom dead center, steam is admitted into the working cylinder from the boiler. The weight of the pump, which is attached to the piston, will raise the piston to top dead center. When the piston reaches top dead center, cold water is sprayed into the working cylinder in order to condense the steam into water, causing the pressure in the cylinder to drop below atmospheric pressure

and forces the piston down. At BDC more steam is admitted, causing the pressure to rise, and the cycle is repeated at a rate of approximately 10 strokes per minute [6].

2.6.2 Newcomen Engine: Efficiency and BMEP

The Newcomen engine's overall efficiency is 1.3%. Its efficiency is very low due to its high fuel consumption. Also, the water sprayed into the working cylinder, which is intended to condense the steam in the working cylinder, also cools the cylinder itself which has a negative impact on the engine's overall performance. Additionally, the Newcomen engine's brake mean effective pressure (BMEP) is 165 kPa [6]. This low BMEP means that the engine's power output, relative to its displaced volume, is low.

Chapter 3: Thermodynamic Model

3.1 Overall Approach

Thermodynamic models for each fluid volume in the engine are derived by applying conservation of mass, the first law of thermodynamics (conservation of energy), the second law of thermodynamics, and the equation of state to the generic fluid ‘system’ illustrated in Figure 18. Fluid properties are assumed to be spatially uniform within the control volume but are allowed to vary with time as a result of heat addition, work extraction, mass addition/loss and compression/expansion due to a moving boundary. Mass and enthalpy may also enter or exit the control volume as a result of the difference in pressure between the control volume and the connected reservoir. While the illustration shows all possible interactions between the control volume and its surroundings, not all components will experience all interactions.

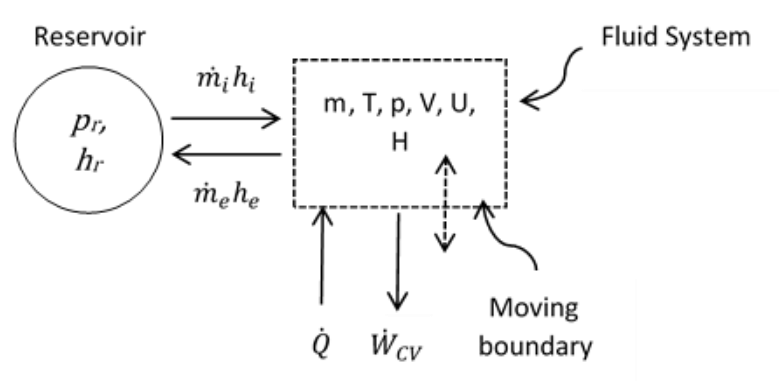


Figure 18: Schematic illustration of the generic control volume with moving boundary used to develop the physical model for each volume of the engine.

3.2 Basic Formulation

Conservation of mass in the control volume is given by:

$$\frac{dm}{dt} = \dot{m}_i - \dot{m}_e \quad (6)$$

where m is the mass of the gas contained within the control volume, \dot{m}_i is the rate of mass flow into the control volume and \dot{m}_e is the rate of mass flow rate exiting the control volume. How \dot{m}_i and \dot{m}_e depend on the difference in pressure between the control volume and the upstream or downstream reservoirs will be explained in following section.

The first law of thermodynamics is given by:

$$\frac{dU}{dt} = \dot{m}_i h_i - \dot{m}_e h_e + \dot{Q} - \dot{W}_{CV} \quad (7)$$

where U is the internal energy inside the control volume, h_i is the enthalpy per unit mass of the fluid entering the control volume, h_e is the enthalpy per unit mass of the fluid exiting the control volume, \dot{Q} is the rate of heat addition to the control volume from the surroundings and \dot{W}_{CV} is the rate of work being done by the control volume on the surroundings through $p dV$ work:

$$\dot{W}_{CV} = p \frac{dV}{dt} \quad (8)$$

The equation of state is given by:

$$pV = mRT \quad (9)$$

Where p is the pressure, V is the volume, R is the gas constant, and T is the temperature. Rearranging and differentiating (9) with respect to time gives:

$$V \frac{dp}{dt} + p \frac{dV}{dt} - mR \frac{dT}{dt} - RT \frac{dm}{dt} = 0 \quad (10)$$

It is also assumed that the working fluid is thermally and calorically perfect leading to the following expressions for the changes in thermal energy/mass (u) and

enthalpy/mass (h) in terms of specific heat at constant volume (c_v) and the specific heat at constant pressure (c_p).

The equations of internal energy and enthalpy can be written:

$$U = mc_v T \quad (11)$$

$$H = mc_p T \quad (12)$$

where,

$$H = U + pV \quad (13)$$

Note also that

$$R = c_p - c_v \quad (14)$$

The second law of thermodynamics is given by:

$$ds = c_p \frac{dT}{T} - R \frac{dp}{p} \quad (15)$$

where s is the specific entropy.

Solving these equations over the course of the engine's cycle is simplified by using a state space formulation where A is an $N \times N$ matrix of sensitivity coefficients, X is a vector of N state variables associated with the fluid system, and B is a vector representing sources/sinks for each state variable:

$$[A] \frac{d\vec{X}}{dt} = \vec{B}$$

Eight state variables are considered here: the pressure (p), mass (m), volume (V), temperature (T), internal energy (U), and entropy (S) of the fluid in the control volume along with the heat transfer (Q) and work done (W_{cv}). The time variations of properties inside the control volume as a function of time are determined by integrating the following system of equations:

$$\begin{bmatrix} V & -RT & 0 & 0 & p & -mR & 0 \\ 0 & 1 & 0 & 0 & 0 & 0 & 0 \\ 0 & 0 & 1 & 0 & -p & 0 & 0 \\ 0 & 0 & 0 & 1 & 0 & 0 & 0 \\ 0 & 0 & 0 & 0 & 1 & 0 & 0 \\ 0 & 0 & 1 & -1 & 0 & mc_v & 0 \\ 0 & 0 & 0 & -1/T & 0 & 0 & 1 \end{bmatrix} \frac{d}{dt} \begin{bmatrix} P \\ m \\ W_{cv} \\ Q \\ V \\ T \\ S \end{bmatrix} = \begin{bmatrix} 0 \\ \dot{m}_i - \dot{m}_e \\ 0 \\ \dot{Q} \\ \dot{V}(t) \\ \dot{m}_i h_i - \dot{m}_e h_e \\ 0 \end{bmatrix} \quad (16)$$

The first row of the matrix equation corresponds to the equation of state (10), the second row corresponds to mass conservation (6), the third row corresponds to the definition of work (8), the fourth row corresponds to heat addition, the fifth row corresponds to volume forcing function (to be discussed next), the sixth row corresponds to temperature, and the seventh row corresponds to the second law of thermodynamics. The vector of source terms on the right hand side of Eq. 16 has three non-zero elements. In most cases, they depend on conditions in adjacent components. These source terms will be discussed individually in the next section. Often, it is more convenient to replace

time with crank angle. Since $\omega = \frac{d\theta}{dt}$, $\frac{d}{dt} = \omega \frac{d}{d\theta}$ and Eq. 16 becomes:

$$\begin{bmatrix} V & -RT & 0 & 0 & p & -mR & 0 \\ 0 & 1 & 0 & 0 & 0 & 0 & 0 \\ 0 & 0 & 1 & 0 & -p & 0 & 0 \\ 0 & 0 & 0 & 1 & 0 & 0 & 0 \\ 0 & 0 & 0 & 0 & 1 & 0 & 0 \\ 0 & 0 & 1 & -1 & 0 & mc_v & 0 \\ 0 & 0 & 0 & -1/T & 0 & 0 & 1 \end{bmatrix} \frac{d}{d\theta} \begin{bmatrix} P \\ m \\ W_{cv} \\ Q \\ V \\ T \\ S \end{bmatrix} = \frac{1}{\omega} \begin{bmatrix} 0 \\ \dot{m}_i - \dot{m}_e \\ 0 \\ \dot{Q} \\ \dot{V}(t) \\ \dot{m}_i h_i - \dot{m}_e h_e \\ 0 \end{bmatrix} \quad (17)$$

Each component of the engine is modeled using its own version of Eq. 16 or 17. The model of the entire engine is created by assembling the models for each component and solving then simultaneously. However, since not all processes represented in Eq. 16 occur in every component, some components can be represented using smaller models. The models used to represent each component will be described in greater detail in a following section.

3.3 Source Term Models

3.3.1 Cylinder Volume

The generic system illustrated in Figure 18 and represented mathematically by Eq. 16/17 is ‘driven’ by changing the volume of the cylinder as a function of time. The rate of change of cylinder volume is found from the expression for the working cylinder volume as a function of crank angle θ [7]:

$$V(\theta) = V_{min} \left[1 + \frac{1}{2}(rc - 1) \left(1 - \cos\theta + \frac{2l}{S} \left\{ 1 - \sqrt{1 - \left(\frac{S}{2l}\right)^2 \sin^2\theta} \right\} \right) \right] \quad (18)$$

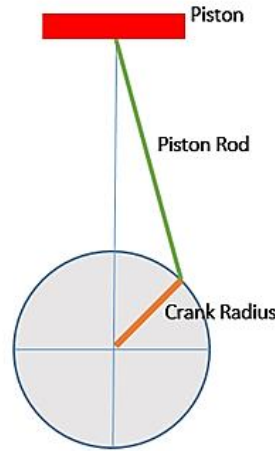


Figure 19: Sketch of an engine's crank radius and piston rod

In the above expression, V_{min} corresponds to the minimum volume in the working cylinder, rc is the compression ratio, l is the rod length, and S is the stroke. Also, the ratio of connecting rod length to crank radius (R_{crank}) can be written as:

$$R_{crank} = \frac{2l}{S}$$

Thus, the volume of working cylinder can be written as:

$$V(\theta) = V_{min} \left[1 + \frac{1}{2}(rc - 1) \left(R_{crank} + 1 - \cos\theta - \sqrt{(R_{crank}^2 - \sin^2\theta)} \right) \right] \quad (19)$$

In order to differentiate the above equation with respect to time, the crank angle needs to be converted to time. This is accomplished using the definition of the angular velocity ω , where ω is in rad/sec.

$$\omega = \frac{d\theta}{dt} \quad (20)$$

Integrating the above equation gives θ as a function of time:

$$\theta(t) = \omega t + \theta_0 \quad (21)$$

With an initial condition, θ_0 to be defined. For instance, at $t = 0$, the piston is at BDC. Thus:

$$\theta(t) = \omega t + \pi \quad (22)$$

Thus, the cylinder volume can be expressed as a function of time:

$$V(t) = V_{min} \left[\left(\frac{rc - 1}{2} \right) \left(R_{crank} + 1 - \cos(\omega t + \pi) + 1 - \sqrt{(R_{crank}^2 - \sin^2(\omega t + \pi))} \right) \right] \quad (23)$$

Differentiating the volume equation with respect to time gives:

$$\frac{dV}{dt} = \frac{V_{min}}{2} (rc - 1) \left[\omega \sin(\omega t + \pi) + \frac{\omega \sin(\omega t + \pi) * \cos(\omega t + \pi)}{\sqrt{R_{crank}^2 - \sin^2(\omega t + \pi)}} \right] \quad (24)$$

3.3.2 Mass Flux Term

Flow enters and leaves the various volumes of the engine through passages that open and close at different points in the cycle. Flow through these passages is modeled as pressure-driven flow through an orifice. Two cases are considered: Cases when the

pressure difference across the orifice is large enough to induce sonic flow at the minimum area point (choked flow), and cases where the pressure difference is not that large.

1. Choked Flow

During a blow-down process, if the pressure difference across the orifice is less than the critical pressure, then the Mach number of the flow exiting the control volume will be sonic, and the flow is considered choked. Under these conditions, the mass flow rate only depends upon the upstream conditions and can be expressed as [8]:

$$\dot{m} = C_D A^* \frac{P_r}{\sqrt{T_r}} \sqrt{\frac{\gamma}{R} \left(\frac{2}{\gamma + 1} \right)^{\frac{\gamma+1}{\gamma-1}}} \quad (25)$$

In the equation above, A^* is the orifice area, γ is the ratio of specific heats, C_D is the discharge coefficient, and R is the gas constant.

2. Unchoked Flow

When the outside pressure is larger than the critical pressure, then the Mach number of the flow exiting the control volume is not sonic, and the flow is considered unchoked. Thus, the mass flow rate can be expressed as [9]:

$$\dot{m} = C_D A \sqrt{2P_r \rho_r \left(\frac{\gamma}{\gamma - 1} \right) \left[\left(\frac{P}{P_r} \right)^{\frac{2}{\gamma}} - \left(\frac{P}{P_r} \right)^{\frac{\gamma+1}{\gamma}} \right]} \quad (26)$$

Where A is the orifice area, C_D is the discharge coefficient, P_r and ρ_r are the total conditions inside the reservoir, and P inside the moving boundary, in Figure 18.

3. Critical Pressure Ratio

Calculating the critical pressure ratio can be obtained using the isentropic relation:

$$\frac{P_r}{P^*} = \left[1 + \frac{\gamma - 1}{2} \right]^{\frac{\gamma}{\gamma - 1}} \Rightarrow \frac{P_r}{P^*} = \left[\frac{\gamma + 1}{2} \right]^{\frac{\gamma}{\gamma - 1}} \quad (27)$$

Thus, for air:

$$P^* = 0.528 * P_r \quad (28)$$

4. Pressure Losses Through Valves

The discharge coefficient is a dimensionless number that accounts for the reduction in effective flow area due to viscous and other geometric effects in flows through ‘real’ orifices. Its value ranges from zero to one to reflect the fact that reducing the flow area for a particular pressure difference reduces the mass flow rate. According to the International Organization for Standardization (ISO 5167), the discharge coefficient for various orifice plates is calculated based on Reynolds number (for $Re_D > 30,000$) [10], which in turn is a function of pressure, temperature, and viscosity.

As shown in Figure 20, the orifice’s diameter ratio (β) is defined as the ratio of bore diameter over the pipe diameter, and the aspect ratio (t/d) is defined as the ratio of orifice thickness over bore diameter [11].

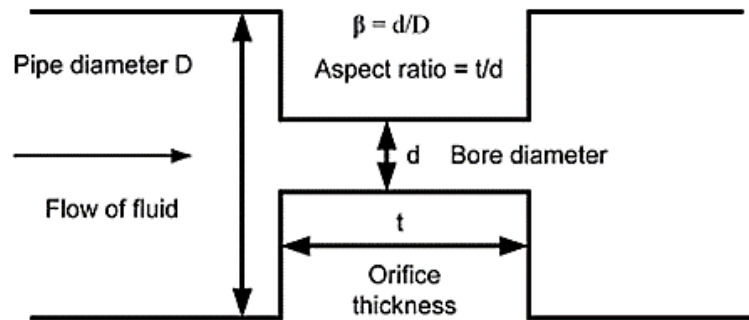


Figure 20: Schematic of an orifice plate [11]

Furthermore, for small values of β , the pressure variation away from the orifice’s axis

becomes small, and the discharge coefficient can now be expressed as a function of the orifice's geometry only [12]. Thus, if β is less than 0.1, the coefficient of discharge can be expressed as:

1. If $t/d < 0.8$:

$$C_D = 0.608 \left(1 + \left(\frac{t}{d} \right)^{3.5} \right) \quad (29)$$

2. If $t/d > 0.8$:

$$C_D = 0.872 - 0.0149 \frac{t}{d} - 0.08 \frac{d}{t} \quad (30)$$

The variation of discharge coefficient with passage aspect ratio (t/d) is compared to experimental results for $\beta < 0.063$ in Figure 21 and Figure 22.

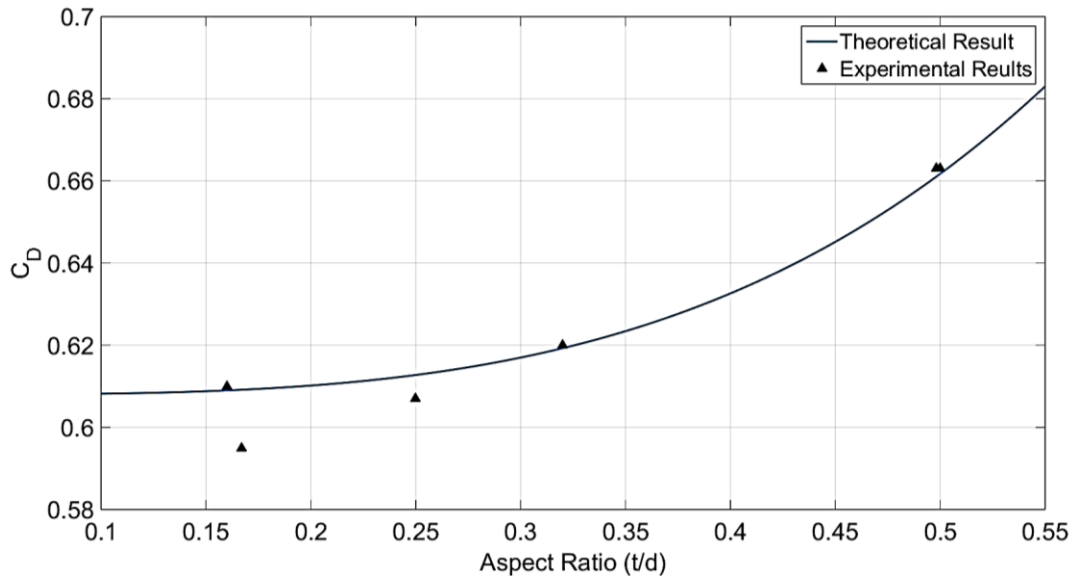


Figure 21: Coefficient of discharge vs. aspect ratio for $t/d < 0.8$

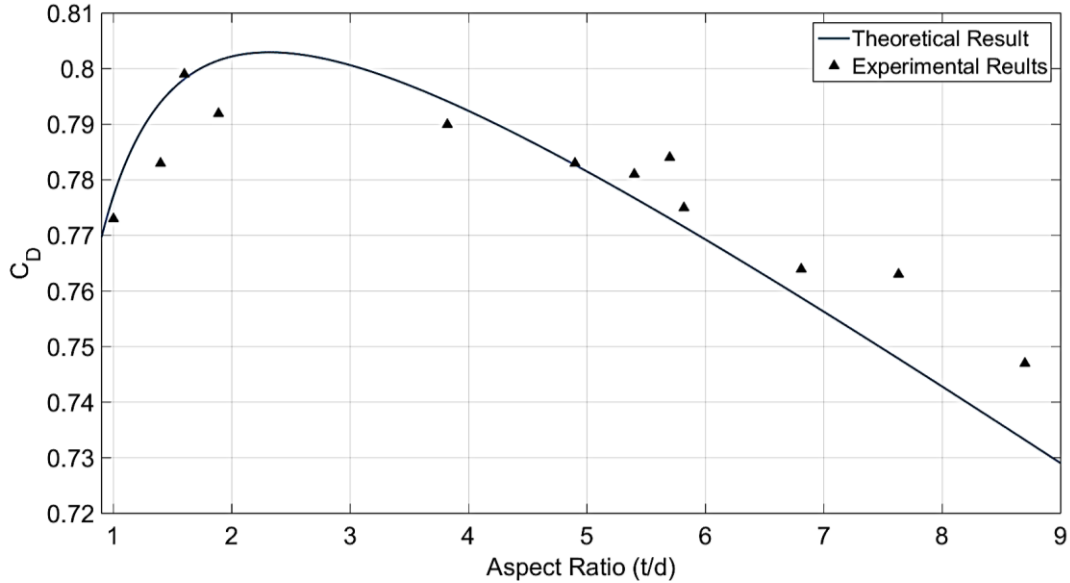


Figure 22: Coefficient of discharge vs. aspect ratio for $t/d > 0.8$

All of the flow orifices in the engine model are assumed to have the basic geometry illustrated in Figure 20. Also, the opening and closing processes of the valves are assumed to happen instantaneously. Furthermore, there is no current physical design of the Soony engine’s flow orifices, so it is assumed that their aspect ratio is around 0.2, which corresponds to a coefficient of discharge equal to 0.61.

3.3.3 Enthalpy Flux Term

The enthalpy of the flow entering the control volume (from a reservoir into the control volume) is equal to the reservoir’s enthalpy. Similarly, the enthalpy of the flow exiting the control volume (from the control volume into a reservoir) is equal to the control volume’s enthalpy.

3.4 Component Models

The state space formulation (Eq. 16 or 17) will be applied to all 3 components of the Soony engine. These components are: hot reservoir, cold reservoir, and working cylinder.

3.4.1 Hot Reservoir

Applying Eq. 16 to the hot reservoir:

$$\begin{bmatrix} V & -RT & 0 & 0 & p & -mR & 0 \\ 0 & 1 & 0 & 0 & 0 & 0 & 0 \\ 0 & 0 & 1 & 0 & -p & 0 & 0 \\ 0 & 0 & 0 & 1 & 0 & 0 & 0 \\ 0 & 0 & 1 & -1 & 0 & mc_v & 0 \\ 0 & 0 & 0 & -1/T & 0 & 0 & 1 \end{bmatrix} \frac{d}{d\theta} \begin{bmatrix} P \\ m \\ W_{CV} \\ Q \\ T \\ S \end{bmatrix} = \frac{1}{\omega} \begin{bmatrix} 0 \\ \dot{m}_i - \dot{m}_e \\ 0 \\ \dot{Q} \\ \dot{m}_i h_{cyl} - \dot{m}_e h_{hr} \\ 0 \end{bmatrix} \quad (31)$$

In the above equation, h_{cyl} represents the cylinder's enthalpy and h_{hr} is the hot reservoir's enthalpy, \dot{m}_i is the mass flow rate entering the hot reservoir, and \dot{m}_e is the mass flow rate exiting the hot reservoir.

3.4.2 Cold Reservoir

Applying Eq. 16 to the cold reservoir:

$$\begin{bmatrix} V & -RT & 0 & 0 & p & -mR & 0 \\ 0 & 1 & 0 & 0 & 0 & 0 & 0 \\ 0 & 0 & 1 & 0 & -p & 0 & 0 \\ 0 & 0 & 0 & 1 & 0 & 0 & 0 \\ 0 & 0 & 1 & -1 & 0 & mc_v & 0 \\ 0 & 0 & 0 & -1/T & 0 & 0 & 1 \end{bmatrix} \frac{d}{d\theta} \begin{bmatrix} P \\ m \\ W_{CV} \\ Q \\ T \\ S \end{bmatrix} = \frac{1}{\omega} \begin{bmatrix} 0 \\ \dot{m}_i - \dot{m}_e \\ 0 \\ \dot{Q} \\ \dot{m}_i h_{cyl} - \dot{m}_e h_{cr} \\ 0 \end{bmatrix} \quad (32)$$

In the above equation, h_{cyl} represents the cylinder's enthalpy and h_{cr} is the cold reservoir's enthalpy, \dot{m}_i is the mass flow rate entering the cold reservoir, and \dot{m}_e is the mass flow rate exiting the cold reservoir.

3.4.3 Working Cylinder

Similarly, Eq. 16 is applied to the working cylinder. The only difference is that the working cylinder will interact with both reservoirs during the cycle. However, these reservoirs are never open to the working cylinder at the same time.

$$\begin{bmatrix} V & -RT & 0 & 0 & p & -mR & 0 \\ 0 & 1 & 0 & 0 & 0 & 0 & 0 \\ 0 & 0 & 1 & 0 & -p & 0 & 0 \\ 0 & 0 & 0 & 1 & 0 & 0 & 0 \\ 0 & 0 & 0 & 0 & 1 & 0 & 0 \\ 0 & 0 & 1 & -1 & 0 & mc_v & 0 \\ 0 & 0 & 0 & -1/T & 0 & 0 & 1 \end{bmatrix} \frac{d}{d\theta} \begin{bmatrix} P \\ m \\ W_{CV} \\ Q \\ V \\ T \\ S \end{bmatrix} = \frac{1}{\omega} \begin{bmatrix} 0 \\ \dot{m}_i - \dot{m}_e \\ 0 \\ \dot{Q} \\ \dot{V}(t) \\ \dot{m}_i h_i - \dot{m}_e h_{cyl} \\ 0 \end{bmatrix} \quad (33)$$

In the above equation, h_{cyl} is the working cylinder's enthalpy, \dot{m}_i is the mass flow rate entering the working cylinder, and \dot{m}_e is the mass flow rate exiting the working cylinder. However, h_i represents the cold reservoir's enthalpy during the upstroke, and it represents the hot reservoir's enthalpy during the downstroke.

Eq. 31, 32, and 33 are analytically solved to find the differential equations for each step of the engine's cycle. The equations are presented in Figure 23 and Figure 24.

Step 1 ($P_{cold} > P_{cyl}$)	Step 1 ($P_{cold} < P_{cyl}$)
$\dot{m}_{cyl} = \dot{m}_i$	$\dot{m}_{cyl} = -\dot{m}_e$
$\dot{W}_{cyl} = P_{cyl} \frac{dV_{cyl}}{dt}$	$\dot{W}_{cyl} = P_{cyl} \frac{dV_{cyl}}{dt}$
$\frac{dT_{cyl}}{dt} = \frac{-\dot{W}_{cyl} + \dot{m}_{cyl}(h_{cold} - h_{cyl} + RT_{cyl})}{m_{cyl}(c_p - R)}$	$\frac{dT_{cyl}}{dt} = \frac{-\dot{W}_{cyl} + \dot{m}_{cyl}RT_{cyl}}{m_{cyl}(c_p - R)}$
$\frac{dP_{cyl}}{dt} = \frac{\dot{m}_{cyl}RT_{cyl} + m_{cyl}R \frac{dT_{cyl}}{dt} - P_{cyl} \frac{dV_{cyl}}{dt}}{V_{cyl}}$	$\frac{dP_{cyl}}{dt} = \frac{\dot{m}_{cyl}RT_{cyl} + m_{cyl}R \frac{dT_{cyl}}{dt} - P_{cyl} \frac{dV_{cyl}}{dt}}{V_{cyl}}$
$\dot{m}_{cold} = -\dot{m}_e$	$\dot{m}_{cold} = \dot{m}_i$
$\frac{dT_{cold}}{dt} = \frac{\dot{m}_{cold} RT_{cold} - \dot{Q}_{cold}}{m_{cold}(C_p - R)}$	$\frac{dT_{cold}}{dt} = \frac{\dot{m}_{cold} (h_{cyl} - h_{cold} + RT_{cold}) - \dot{Q}_{cold}}{m_{cold}(C_p - R)}$
$\frac{dP_{cold}}{dt} = P_{cold} \left[\frac{\dot{m}_{cold}}{m_{cold}} + \frac{1}{T_{cold}} \frac{dT_{cold}}{dt} \right]$	$\frac{dP_{cold}}{dt} = P_{cold} \left[\frac{\dot{m}_{cold}}{m_{cold}} + \frac{1}{T_{cold}} \frac{dT_{cold}}{dt} \right]$
$\dot{m}_{hot} = 0$	$\dot{m}_{hot} = 0$
$\frac{dT_{hot}}{dt} = \frac{\dot{Q}_{hot}}{m_{hot}(C_p - R)}$	$\frac{dT_{hot}}{dt} = \frac{\dot{Q}_{hot}}{m_{hot}(C_p - R)}$
$\frac{dP_{hot}}{dt} = P_{hot} \left[\frac{1}{T_{hot}} \frac{dT_{hot}}{dt} \right]$	$\frac{dP_{hot}}{dt} = P_{hot} \left[\frac{1}{T_{hot}} \frac{dT_{hot}}{dt} \right]$

Figure 23: List of differential equations (step 1)

Step 2	Step 3 & 4
$\dot{m}_{cyl} = -\dot{m}_e$	$\dot{m}_{cyl} = \dot{m}_i$
$\dot{W}_{cyl} = P_{cyl} \frac{dV_{cyl}}{dt}$	$\dot{W}_{cyl} = P_{cyl} \frac{dV_{cyl}}{dt}$
$\frac{dT_{cyl}}{dt} = \frac{-\dot{W}_{cyl} + \dot{m}_{cyl}RT_{cyl}}{m_{cyl}(c_p - R)}$	$\frac{dT_{cyl}}{dt} = \frac{-\dot{W}_{cyl} + \dot{m}_{cyl}(h_{hot} - h_{cyl} + RT_{cyl})}{m_{cyl}(c_p - R)}$
$\frac{dP_{cyl}}{dt} = \frac{\dot{m}_{cyl}RT_{cyl} + m_{cyl}R \frac{dT_{cyl}}{dt} - P_{cyl} \frac{dV_{cyl}}{dt}}{V_{cyl}}$	$\frac{dP_{cyl}}{dt} = \frac{\dot{m}_{cyl}RT_{cyl} + m_{cyl}R \frac{dT_{cyl}}{dt} - P_{cyl} \frac{dV_{cyl}}{dt}}{V_{cyl}}$
$\dot{m}_{cold} = 0$	$\dot{m}_{cold} = 0$
$\frac{dT_{cold}}{dt} = \frac{-\dot{Q}_{cold}}{m_{cold}(C_p - R)}$	$\frac{dT_{cold}}{dt} = \frac{-\dot{Q}_{cold}}{m_{cold}(C_p - R)}$
$\frac{dP_{cold}}{dt} = P_{cold} \left[\frac{1}{T_{cold}} \frac{dT_{cold}}{dt} \right]$	$\frac{dP_{cold}}{dt} = P_{cold} \left[\frac{1}{T_{cold}} \frac{dT_{cold}}{dt} \right]$
$\dot{m}_{hot} = \dot{m}_i$	$\dot{m}_{hot} = -\dot{m}_e$
$\frac{dT_{hot}}{dt} = \frac{\dot{Q}_{hot} + \dot{m}_{hot}(h_{cyl} - h_{hot} + RT_{hot})}{m_{hot}(c_p - R)}$	$\frac{dT_{hot}}{dt} = \frac{\dot{Q}_{hot} + \dot{m}_{hot}(RT_{hot})}{m_{hot}(c_p - R)}$
$\frac{dP_{hot}}{dt} = P_{hot} \left[\frac{\dot{m}_{hot}}{m_{hot}} + \frac{1}{T_{hot}} \frac{dT_{hot}}{dt} \right]$	$\frac{dP_{hot}}{dt} = P_{hot} \left[\frac{\dot{m}_{hot}}{m_{hot}} + \frac{1}{T_{hot}} \frac{dT_{hot}}{dt} \right]$

Figure 24: List of differential equations (step 2, 3, and 4)

3.5 Entropy Calculation

Entropy calculation depends on the type of gas. In other words, calculating the entropy of a monatomic gas is different than a diatomic gas.

3.5.1 Entropy Calculation: Monoatomic Gas

For a monatomic gas such as helium or argon, the entropy can be calculated using Sackur-Tetrode equation [13].

$$S = K_B N \ln \left[\left(\frac{4\pi m}{3h^2} \right)^{\frac{3}{2}} e^{\frac{5}{2}} \left(\frac{U}{N} \right)^{\frac{3}{2}} \left(\frac{V}{N} \right) \right] \quad (34)$$

where h is the Planck constant, m is the mass of the particle, K_B is the Boltzmann constant, and N is the number of particles.

3.5.2 Entropy Calculation: Diatomic Gas

In the case of a diatomic gas, calculating the entropy is more complex than a monatomic gas. For a diatomic gas such as nitrogen, entropy is a function of rotational temperature θ_r , vibrational temperature θ_v , dissociation energy D_0 , ground state electronic degeneracy $\omega_{elect,1}$, symmetry number σ , electronic partition function q_{elect} , vibrational partition function q_{vib} , rotational partition function q_{rot} , and translational partition function q_{trans} [14]. Also, many of these variables are tabulated for each diatomic gas. Furthermore, the partition function is [14]:

$$q = q_{trans} q_{rot} q_{vib} q_{elect}$$

$$\Rightarrow q = \left[\left(\frac{2\pi m k T}{h^2} \right)^{\frac{3}{2}} V \right] * \left[\frac{T}{\sigma \theta_r} \right] * \left[\omega_{elect,1} \frac{e^{\frac{D_0}{kT}}}{1 - e^{-\frac{\theta_v}{T}}} \right] \quad (35)$$

The entropy of a diatomic gas is [14]:

$$\frac{S}{Nk} = \frac{7}{2} + \ln \left[\left(\frac{2\pi(m_1 + m_2)kT}{h^2} \right)^{\frac{3}{2}} \frac{V}{N} \right] + \ln \left(\frac{T}{\sigma \theta_r} \right) + \frac{\theta_v}{T} \frac{e^{-\frac{\theta_v}{T}}}{1 - e^{-\frac{\theta_v}{T}}} - \ln \left(1 - e^{-\frac{\theta_v}{T}} \right) + \ln \omega_{elect,1} \quad (36)$$

3.6 Component Model Validation

In order to validate the modeling of the engine, two unit problems will be tested.

3.6.1 Compression and expansion in an adiabatic piston-cylinder arrangement

The piston-cylinder arrangement is illustrated in Figure 25, where the dashed box shows the boundaries of the fluid system to which the conservation laws are applied.

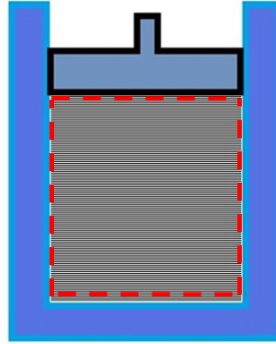


Figure 25: Schematic illustration of adiabatic closed piston-cylinder assembly

Since the cylinder is closed, the mass flow rates into and out of the control volume are zero and the statement of energy conservation (7) reduces to:

$$\frac{dU}{dt} = \dot{Q} - \dot{W}_{cv} \quad (37)$$

In terms of enthalpy:

$$\frac{dH}{dt} = \dot{Q} + V \frac{dP}{dt} \quad (38)$$

Dividing Eq. 38 by 37, inserting the definitions of U and H (Eq. 11 and 12) gives:

$$\frac{mc_p dT/dt}{mc_v dT/dt} = \frac{dQ/dt + V dp/dt}{dQ/dt - p dV/dt} \quad (39)$$

Noting that $\dot{Q} = 0$, cancelling terms, make use of Eq. 14, and performing some algebra yields the following expression for the rate of change of cylinder pressure as a function of the rate of change of cylinder volume:

$$\frac{dp}{dt} = -\left(1 + \frac{R}{C_v}\right) \frac{p}{V} \frac{dV}{dt} \quad (40)$$

The expression for the rate of change in temperature as a function of the rate of change of cylinder volume is derived by inserting the definitions of work (Eq. 8) and internal energy (Eq. 11) into the closed system energy equation (37), with \dot{Q} set equal to zero, this yields:

$$\frac{dT}{dt} = -\frac{p}{mC_v} \frac{dV}{dt} \quad (41)$$

Note that the same expression results by inserting equation 40 into the time-dependent equation of state (Eq. 10) with $\frac{dm}{dt}=0$. Re-writing Eq. 8 explicitly in terms of time gives:

$$\frac{dW_{CV}}{dt} = p \frac{dV}{dt} \quad (42)$$

The entropy change is zero because the compression process is assumed to be adiabatic and reversible. Thus:

$$\frac{dS}{dt} = 0 \quad (43)$$

Eq. 40-43 together give the rates of change of pressure, temperature, work, and entropy as functions of the rate of change of the closed cylinder's volume when no heat transfer is occurring.

3.6.2 Compression and expansion in a non-adiabatic piston-cylinder arrangement.

A similar derivation process will be applied, as in the previous section, in order to find expressions for the rate of change of cylinder pressure, temperature, work, and entropy as a function of rate of change of cylinder volume when heat transfer is occurring (Figure 26). These expressions are shown in Eq. 44-47.

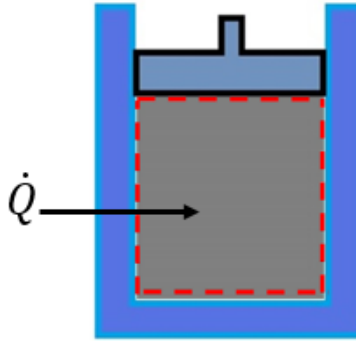


Figure 26: Schematic illustration of non-adiabatic closed piston-cylinder assembly

$$\frac{dp}{dt} = \frac{R}{c_v} \frac{1}{V} \frac{dQ}{dt} - \left(1 + \frac{R}{c_v}\right) \frac{p}{V} \frac{dV}{dt} \quad (44)$$

$$\frac{dT}{dt} = \frac{1}{mc_v} \left[\frac{dQ}{dt} - p \frac{dV}{dt} \right] \quad (45)$$

$$\frac{dW_{CV}}{dt} = p \frac{dV}{dt} \quad (46)$$

$$\frac{dS}{dt} = \frac{1}{T} \frac{dQ}{dt} \quad (47)$$

These differential equations, obtained above, can be integrated in MATLAB using *ODE45*. Below are example plots of pressure and temperature variations as functions of crank angle at 1800 RPM (Figure 27 and Figure 28). The solid lines are for an adiabatic compression and expansion process while the dashed lines are for a process with a uniform heat addition rate of 10 kW. As expected, adding heat increases the pressure and temperature in the cylinder.

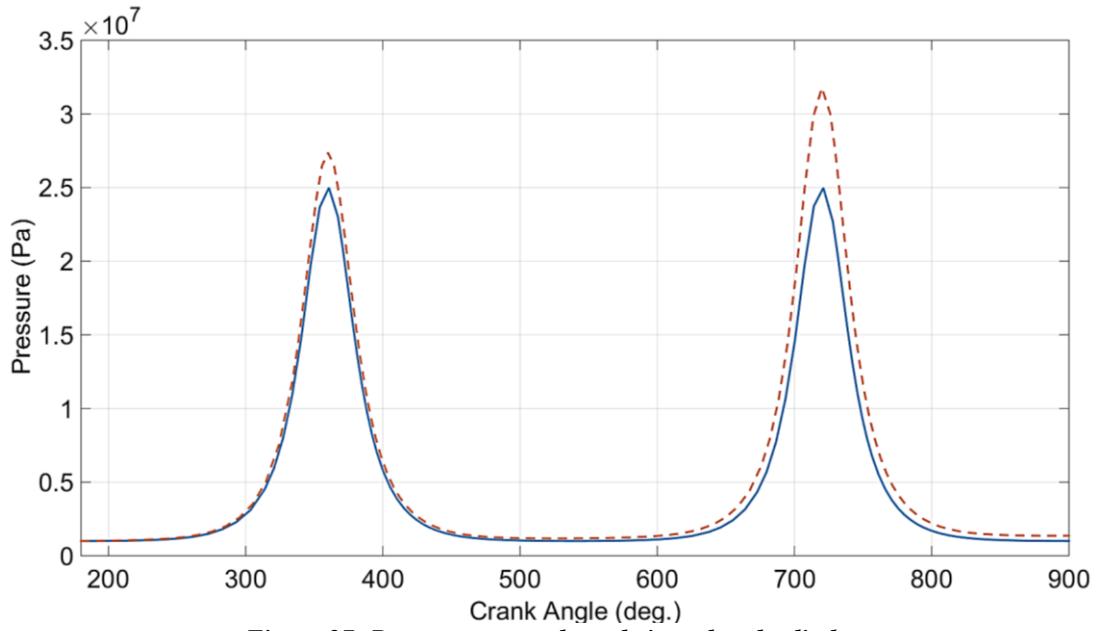


Figure 27: Pressure vs. crank angle in a closed cylinder

9

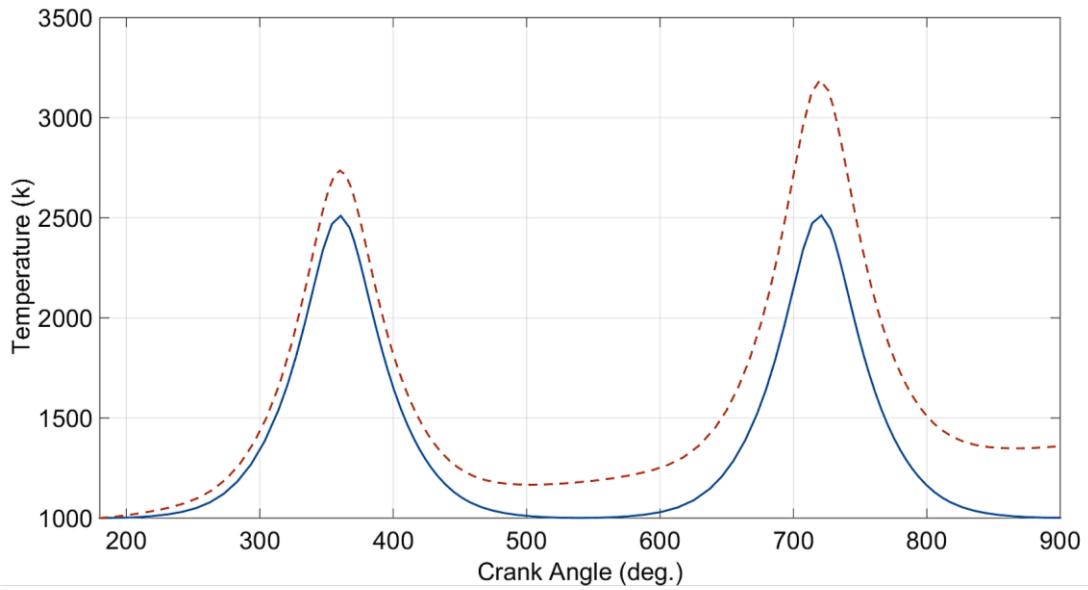


Figure 28: Temperature vs. crank angle in a closed cylinder

Chapter 4: Soony Gen III Performance – Fixed Heat Rates

4.1 Overview

The rates of heat transfer to the hot reservoir (\dot{Q}_H) and from the cold reservoir (\dot{Q}_C) were treated as known parameters in the thermodynamic model of the engine developed in the previous section. While expedient, in practice they are determined by the performance of the hot and cold side heat exchangers and temperatures and flow rates of the high and low temperature streams they communicate with. This also means that the performance of the GEN III engine is limited by the performance of the hot and cold side heat exchangers.

So, a three-step approach is taken to evaluate the performance of the GEN III engine. The first step (presented in this chapter) is simply to report engine performance as functions of constant \dot{Q}_H and \dot{Q}_C , shown in Figure 29. The second step (presented in the following chapter) is to develop simple isothermal tube models for the hot and cold side heat exchangers and report engine performance as functions of the temperatures and flow rates of the hot and cold external flows used to supply the heat exchangers. The third step (presented in Chapter 6) is to do the same thing with more realistic non-isothermal tube heat exchanger models.

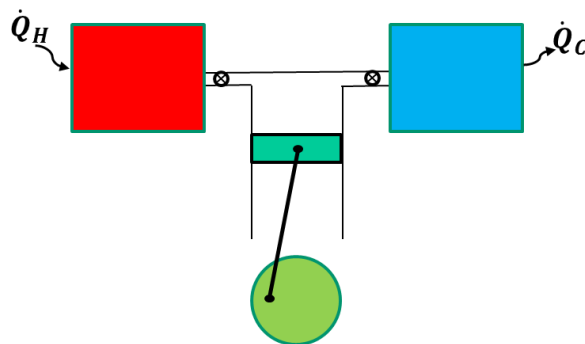


Figure 29: Schematic of the first dynamic model (constant heat rates)

4.2 MATLAB Inputs and Outputs

4.2.1 MATLAB Inputs

The MATLAB script has the following inputs:

1. Coefficient of discharge: In order to take the pressure losses through valves into account, the coefficient of discharge is set equal to 0.61, assuming an aspect ratio $t/d \approx 0.2$ and $\beta < 0.1$ (as discussed in chapter 3).
2. Heat rate values (constant): \dot{Q}_{hot} and \dot{Q}_{cold}
3. Engine's speed (*rpm*)
4. Engine's dead volume (V_{min}) and compression ratio (rc)
5. Working fluid properties (air): $R, \gamma, C_p, C_v, \theta_v, D_0, \theta_r, q_{vib}, q_{rot}, q_{trans}, \sigma$.
6. Hot and cold reservoir volumes: V_{hot} and V_{cold}
7. Initial conditions: initial pressure and temperature in every chamber

4.2.2 MATLAB Outputs

Based on the inputs given, MATLAB *ODE45* will run the thermodynamic model through a number of cycles in order to reach steady-state, and then it will output the following:

1. Piston chamber's volume, as a function of crank angle
2. Mass inside every volume, as a function of crank angle
3. Pressure inside every volume, as a function of crank angle
4. Temperature inside every volume, as a function of crank angle
5. P-v diagram
6. T-s diagram
7. Power output

8. Efficiency

4.3 Test Case

In order to test the new computational model, a test case is presented next. The engine model presented here is running at 1800 rpm, the working fluid is air, and the compression ratio is 7. The dead volume is 70 cm^3 , $\dot{Q}_{hot} = 7 \text{ kW}$, and $\dot{Q}_{cold} = 4.1 \text{ kW}$.

The initial conditions/inputs are presented in the table below:

Table 4: Initial conditions at BDC

	Piston Chamber	Hot Reservoir	Cold Reservoir
$P_{initial}$ (Pa)	0.2 e+06	9 e+06	1.5 e+06
$T_{initial}$ (K.)	273.15	1200	300
Volume (m³)	4.9 e-04 (V_{max})	1 e-03	1 e-03

Based on the given inputs/ initial conditions above, this particular engine is able to produce 2.9 kW, with 41% efficiency and BMEP equal to 230 kPa. The main plots are presented next to show the thermodynamic cycle.

In order to check that the model is working correctly, the power output and efficiency can be calculated based on the heat rates:

1. Efficiency Verification:

$$Eff = \frac{\dot{Q}_{hot} - \dot{Q}_{cold}}{\dot{Q}_{hot}} = 41.4 \%$$

2. Power Output Verification:

$$Power = \dot{Q}_{hot} - \dot{Q}_{cold} = 2.9 \text{ kW}$$

4.3.1 Mass Variation with Crank Angle

As shown in Figure 30, during the first half of the upstroke, the interaction occurs between the cold reservoir and the piston chamber. At BDC, the cold reservoir's pressure is larger than the piston chamber's. Thus, the cold fluid flows into the piston chamber. As the pressure of the piston chamber increases, the flow reverses direction, and it flows back into the cold reservoir. A similar fluid interaction occurs afterwards between the piston chamber and the hot reservoir.

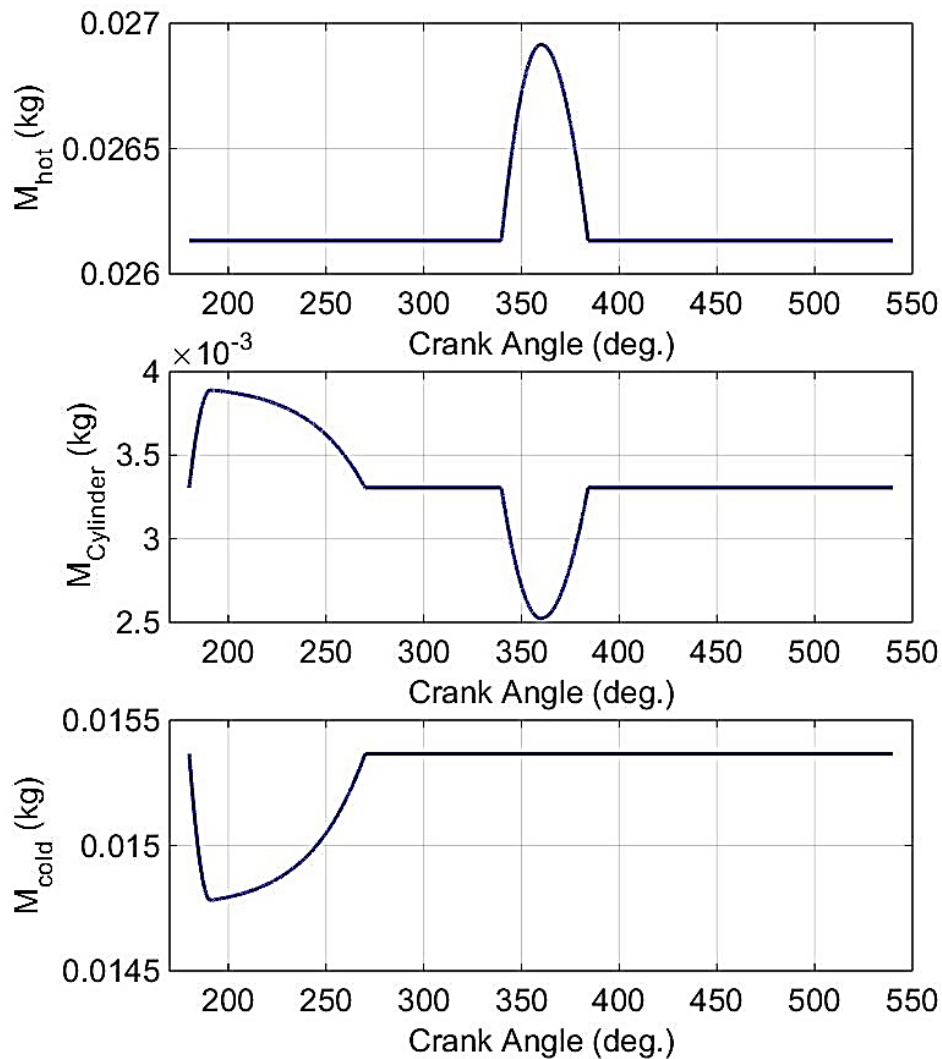


Figure 30: Mass variation with crank angle inside each volume

4.3.2 Pressure Variation with Crank Angle

Figure 31 shows the pressure variation inside each volume, as a function of crank angle. It is important to note that the pressure inside the hot/cold reservoir will change due to the fluid interaction with the piston chamber, and due to the constant rates of heat addition and removal inside the hot and cold reservoirs, respectively.

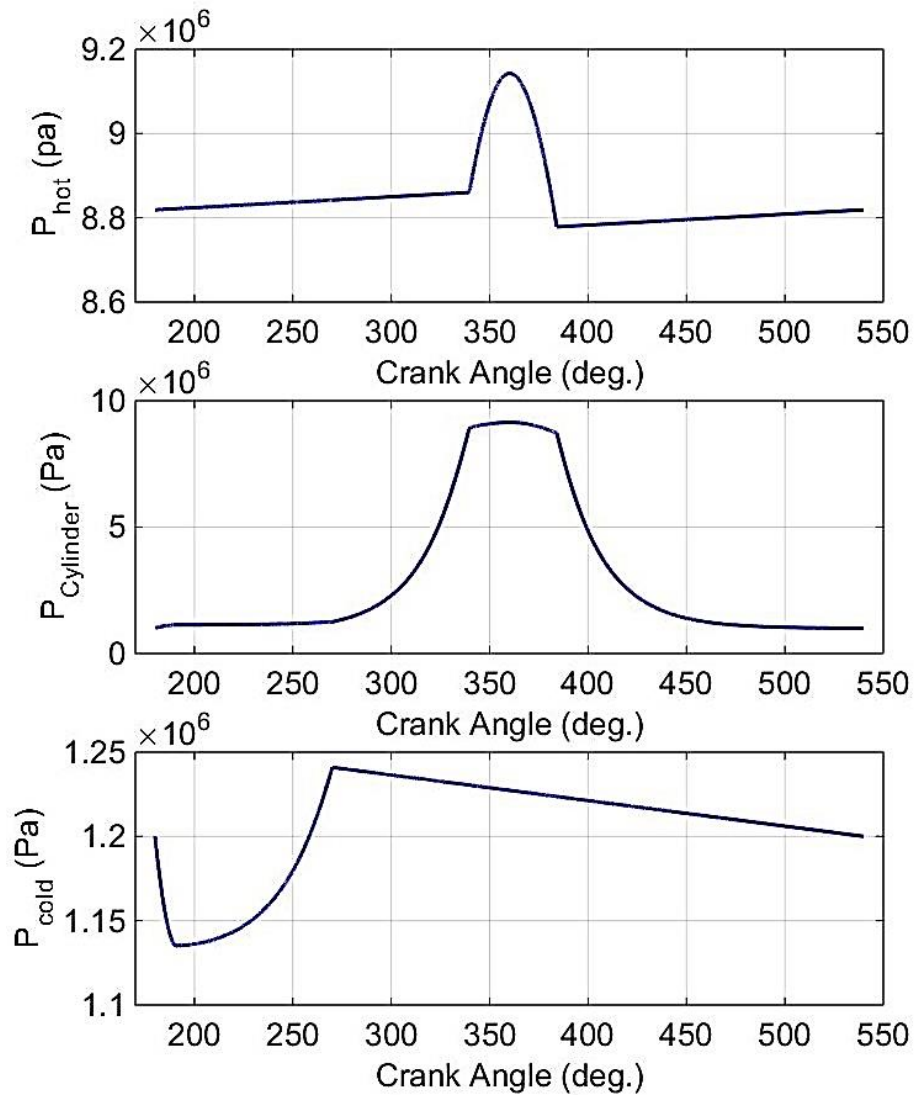


Figure 31: Pressure variation with crank angle inside each volume

4.3.3 Temperature Variation with Crank Angle

Figure 32 shows that the temperature will change inside each of the reservoirs, even when there is no fluid interaction with the piston chamber. This is because of the constant heat rate addition to the hot reservoir, and the constant heat removal from the cold reservoir.

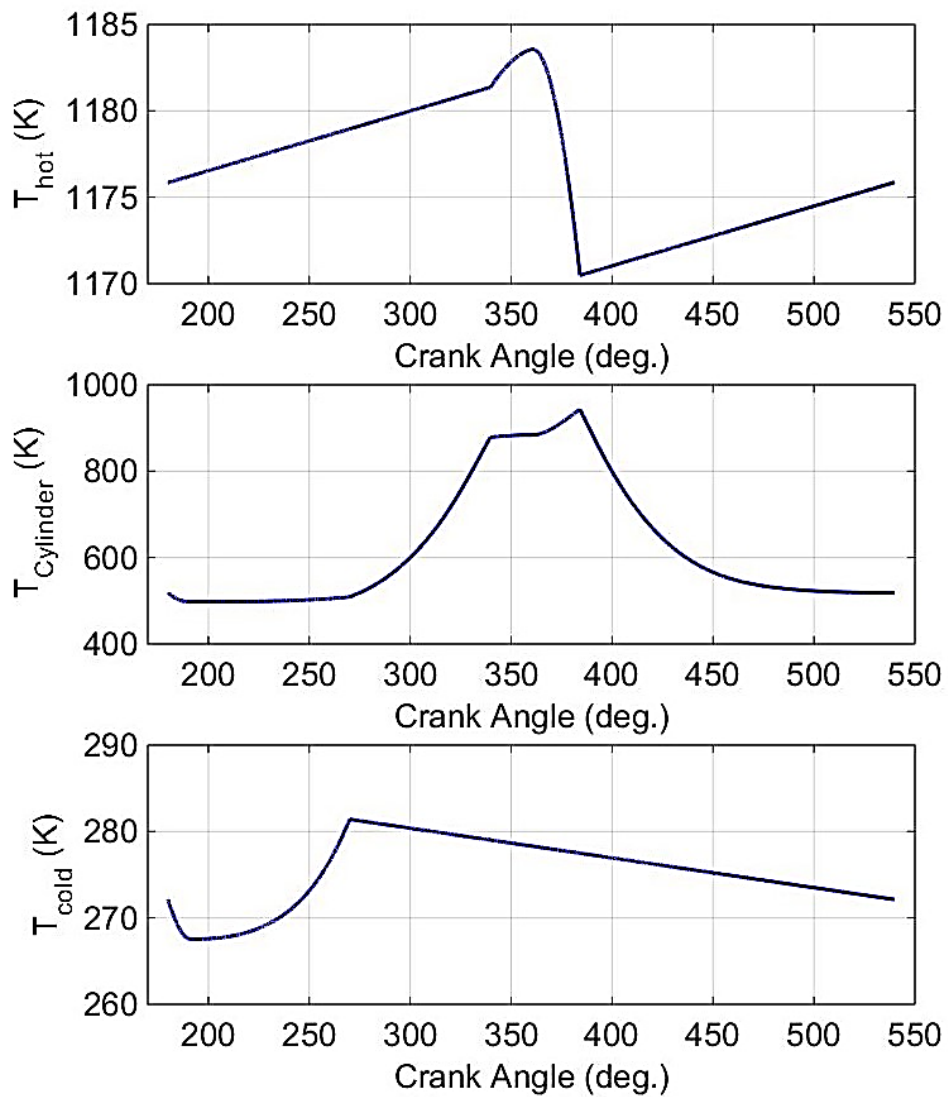


Figure 32: Temperature variation with crank angle inside each volume

4.3.4 P-v Diagram

The “skinny” Pv diagram shown in Figure 33 represents the 4 steps of the engine’s cycle. Also, it is customary to describe a heat engine’s performance based on its Pv diagram, where the net work done by a heat engine is indicated by the area enclosed by its $P-v$ diagram. Based on the shape of the diagram for this test case, it shows that while the engine is very efficient (41%), it doesn’t do a lot of work per unit mass of working fluid.

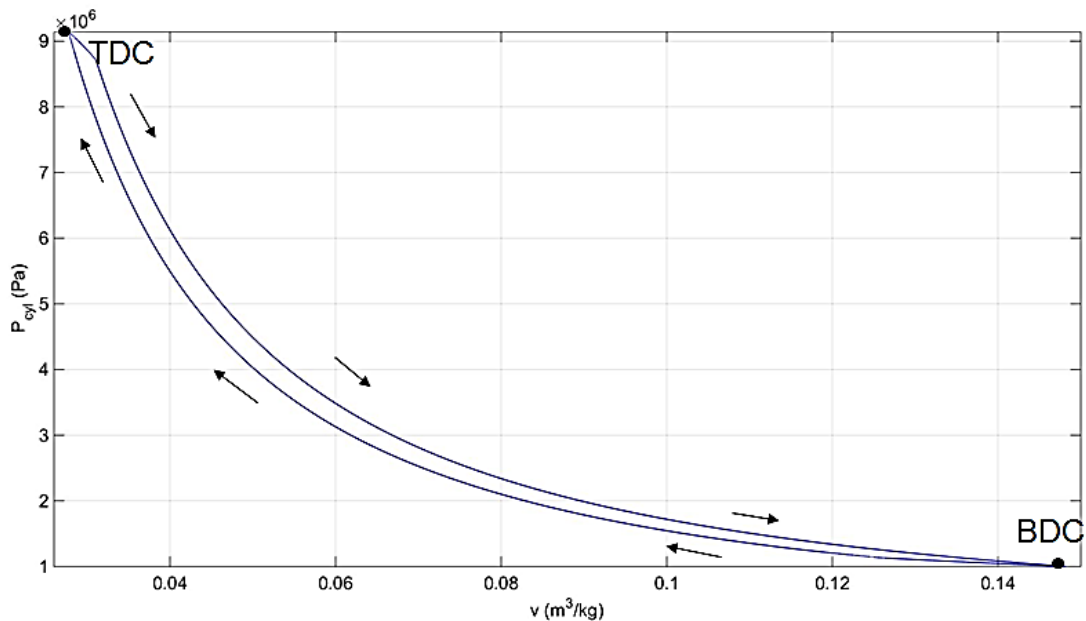


Figure 33: P-v diagram

4.3.5 T-s Diagram

Figure 34 shows the $T-s$ diagram for the engine. The fact that the cycle approximates a rectangle (Carnot cycle) is an indicator of the cycle’s relatively high efficiency.

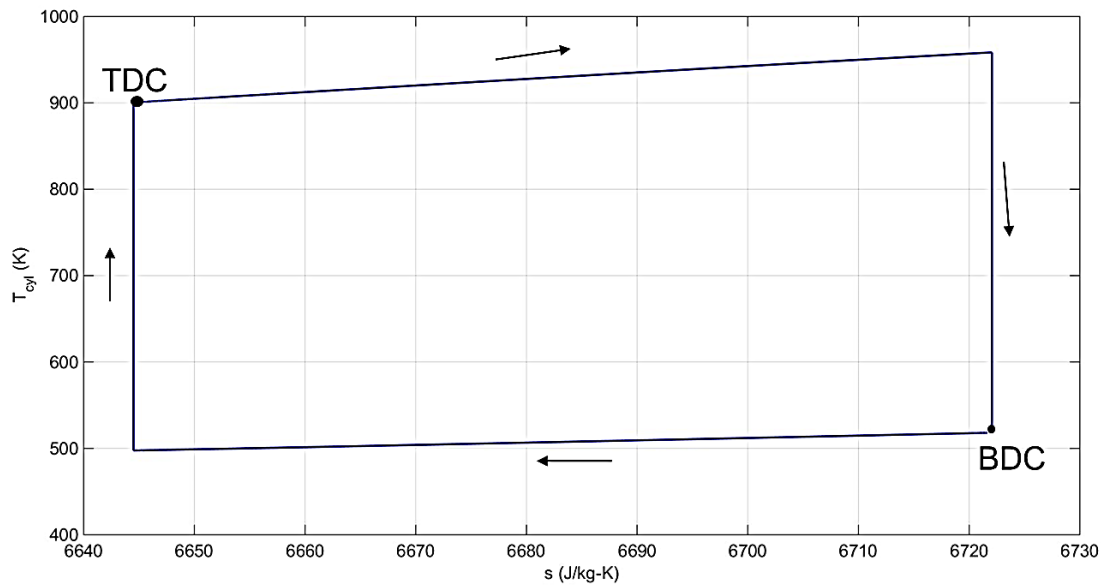


Figure 34: T-s diagram

4.4 Reaching Steady-state

As shown in Figure 35, it takes the model only nine cycle to reach steady-state. This is related to the simplified assumption about the constant rates of heat transfer inside the hot and cold reservoirs.

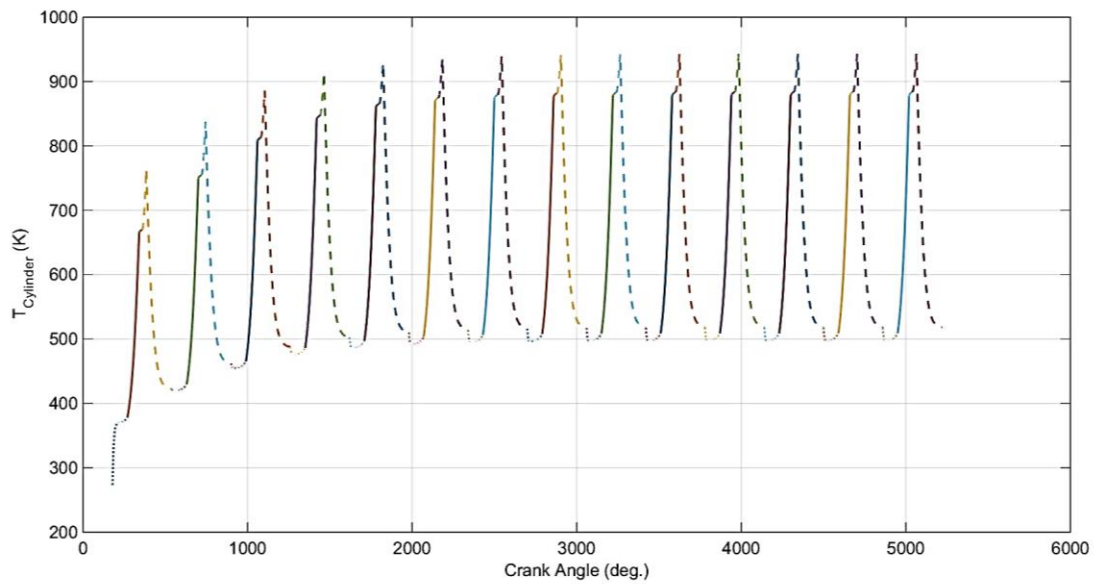


Figure 35: Reaching steady-state variations (Gen III a)

4.5 Current Model: Shortcomings

The current computational model is successfully capable of modeling the variation of pressure, temperature, mass, and other properties as a function of time, which is then converted to crank angle. However, the current heat transfer model is not realistic, where it is assuming constant heat addition and removal rates. Thus, a more realistic, time-dependent, heat transfer model needs to be implemented. In the next chapter, the computational model will investigate another engine model (Gen III b), where the heat transfer is from an isothermal tubes bank inside each reservoir.

Chapter 5: Soony Gen III Performance – With Tubes Bank Heat Exchanger Model

5.1 Overview

This chapter will investigate the engine's performance with a more realistic means of determining \dot{Q}_H and \dot{Q}_C . Figure 37 shows a schematic of the new Gen III model (Gen III b). The hot and cold side heat exchangers consist of a tubes bank, where the external flow passes across the tubes, and the tubes are assumed to maintain their wall at a uniform temperature. Heat is transferred from the outer surface of the tubes to the reservoir volume.

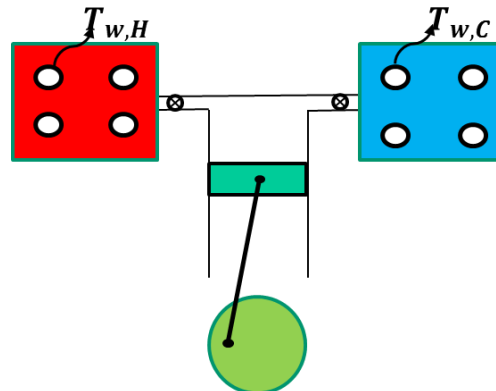


Figure 36: Schematic of Gen III b engine model

Additionally, Figure 37 shows a schematic of the tubes arrangement inside each of the reservoirs, where S_D is the diagonal pitch, S_L is the longitudinal distance between the tubes, S_T is the transverse distance between the tubes, and D is the tube diameter. Also, \mathcal{L}_T and \mathcal{L}_L are the non-dimensional transverse and longitudinal pitches, respectively (where longitudinal distance and transverse distance are divided by the tube diameter).

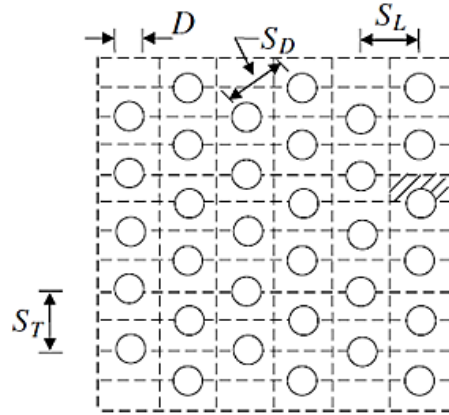


Figure 37: Schematic for staggered arrangement (Adapted from Khan [15])

The rate of convective heat transfer can be approximated using the following equation [16]:

$$\dot{Q} = h A \Delta T \quad (48)$$

where h is the convective heat transfer coefficient, A is the surface area of the tubes, and ΔT is the temperature difference between the tubes surface temperature and the fluid temperature.

The value of the convective heat transfer coefficient can vary significantly based on the compactness of the tube bank. According to Khan, if both the dimensional transverse and longitudinal pitches are less than 1.25, then the tube bank is considered ‘compact’ and the heat transfer convection coefficient is larger than if the tubes were widely spaced [15]. According to Khan, for an isothermal tubes bank, the heat transfer convection coefficient varies with longitudinal and transverse pitches, Reynolds number, and Prandtl number [15].

Furthermore, it is important to note that the current Soony model is still a conceptual design, and it doesn’t have a physical geometry for the hot and cold reservoirs. Also, in the case of an isothermal tubes bank, the convection heat transfer coefficient can

vary significantly based on the geometry [16]. Thus, average values for the convection heat transfer coefficients were approximated for the Soony Gen III engine model based on the literature.

Moreover, whenever the flow orifice between the working cylinder and the reservoir (hot or cold) is open, the heat transfer between the tubes bank and the working fluid is considered a forced convection, and an average value for the heat transfer convection coefficient is approximated to be around $230 \text{ W/m}^2 \text{ K}$ [15]. When the reservoir is not interacting with the working cylinder, the heat transfer is assumed a free convection, and an average heat transfer coefficient is approximated to be $30 \text{ W/m}^2 \text{ K}$ [17].

5.2 Test Case

In order to test the new computational model, a test case is presented. The initial conditions/inputs given to the MATLAB code are the same as those given in the previous test case (in chapter 4).

The results of the current model (Gen III b) are shown in Table 5, which also includes the results of the Gen III a model, for comparison. The table shows that the current model has a lower performance because it is more realistic than the previous one.

Table 5: Results of Gen III b and Gen III a models

	Gen III a	Gen III b
Power (kW)	2.9	2.2
Efficiency (%)	41	31
BMEP (kPa)	230	174.6

5.3 Cen III: Reaching Steady-state

As shown in Figure 38, it takes the new engine model around 90 cycles to reach steady state (vs. 9 cycles for Gen III a). The new engine model is more realistic.

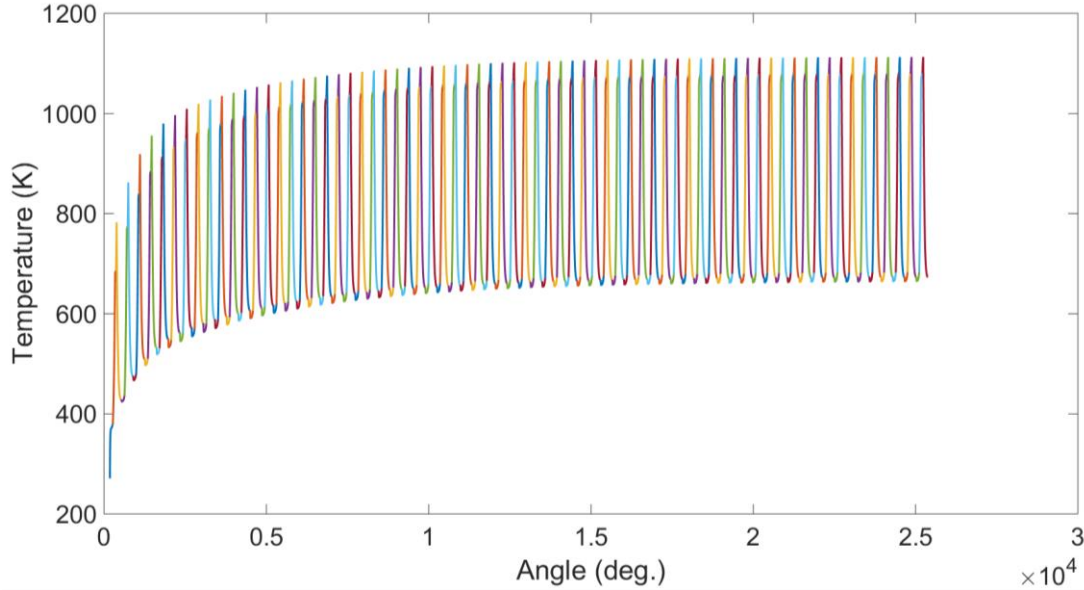


Figure 38: Reaching steady-state for Gen III b engine model

5.4 Cen III: Exploring the Engine's Parameter Space

In order to have a better understanding of the engine model's capabilities, it is important to explore its parameter space. Thus, a MATLAB script was implemented in order to identify designs that maximize power, efficiency, or BMEP (brake mean effective pressure) within specified limits on the parameter space.

BMEP is a parameter that characterizes the average pressure that affects a reciprocating piston [2]. While it is typically used for IC engines, this parameter can also be applied here to give a general comparison of this engine's BMEP with other IC engines and Stirling engines as well. The Equation for BMEP is [18]:

$$BMEP = \frac{P_{o/p} n_R}{V_d N} \quad (49)$$

where $P_{o/p}$ is the power output, $n_R = 1$ for two-stroke engine, V_d is the displaced volume, and N is the number of revolutions per second.

The initial parameters are presented in Table 6 and Table 7.

Table 6: Model parameters and the ranges over which they are varied

Parameters	Range of variation
Compression ratio	4 to 30
Cold reservoir initial pressure	0.5 MPa to 8 MPa
Cold reservoir volume	0.5 V _{max} to 50V _{max}
Hot reservoir volume	0.5 V _{max} to 50V _{max}

Table 7: Initial Conditions for Gen III b

Engine Speed (RPM)	1800
Dead Volume (cm³)	60
$T_{init, hot}$ (K)	1000
$T_{init, cold}$ (K)	300
$P_{init, hot}$ (MPa)	10

5.5 Results

The MATLAB design ‘optimization’ script investigated 4000 different designs in order to find the optimal results in terms of power output, efficiency, and BMEP. The results are presented in Table 8.

Table 8: Optimum Results (Gen III b)

	Optimal Power	Optimal Efficiency	Optimal BMEP
BMEP (kPa)	273	70.3	500.4
Efficiency (%)	28.5	51.5	20.4
Power (kW)	5.9	1.9	2.7

5.5.1 Optimum Power Output

It is important to see how the engine’s peak power output varies with other parameters like compression ratio, cold reservoir’s volume, and hot reservoir’s

volume. The test cases that correspond to maximum power outputs are presented in Figure 39 (designated by black squares). It is shown that the peak power output occurs at a compression ratio equal to 12. Also, it is important to note that this ‘family’ of power output peaks corresponds to when the hot reservoir’s volume is equal to the cold reservoir’s volume, and it also corresponds to when each reservoir’s volume is equal to 50 times the volume of the piston chamber (piston chamber volume at BDC).

Additionally, it is important to see the effect of the reservoirs’ pressure ratio

(*i. e.* $\frac{P_{hot}}{P_{cold}}$) on these power output peaks. This will be shown next.

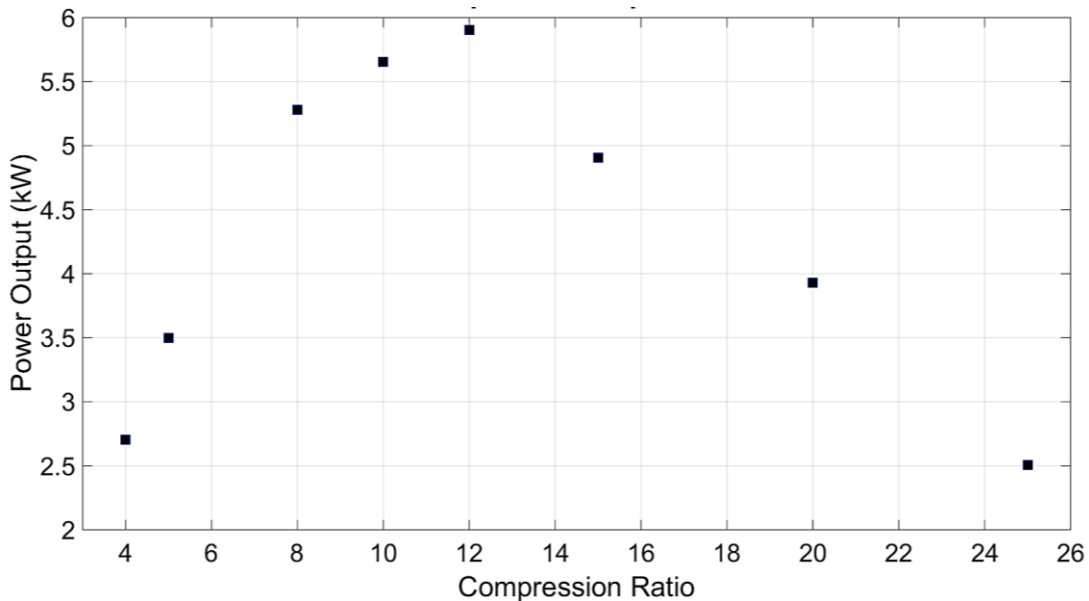


Figure 39: Power output peaks vs. compression ratio

5.5.2 Effect of Reservoirs’ Pressure on Optimal Results

Furthermore, it is important to see how the power output peaks, presented in Figure 39, vary with the reservoirs’ pressure ratio. In order to see that, these same power output peaks will be plotted in terms of reservoirs’ pressure ratio, as will be shown in Figure 40.

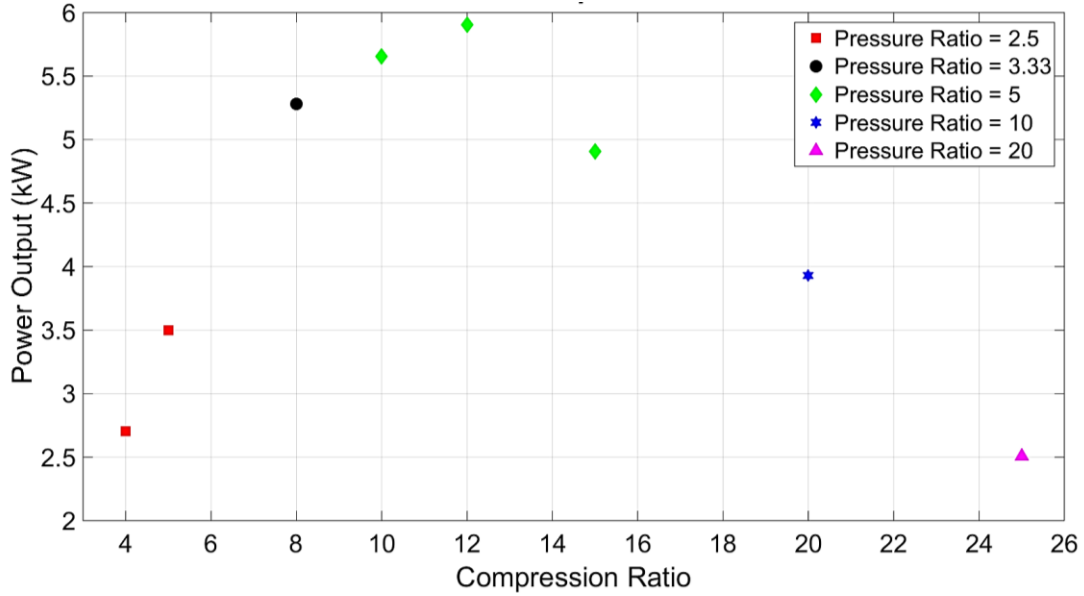


Figure 40: Effect of reservoirs' pressure ratio

The figure above shows that the reservoirs pressure ratio impacts the engine's performance. In other words, the plot shows that as the compression ratio increases, the pressure ratio required to achieve an optimum power output must also increase.

5.5.3 Optimum BMEP

Figure 41 shows the variation of BMEP as a function of compression ratio.

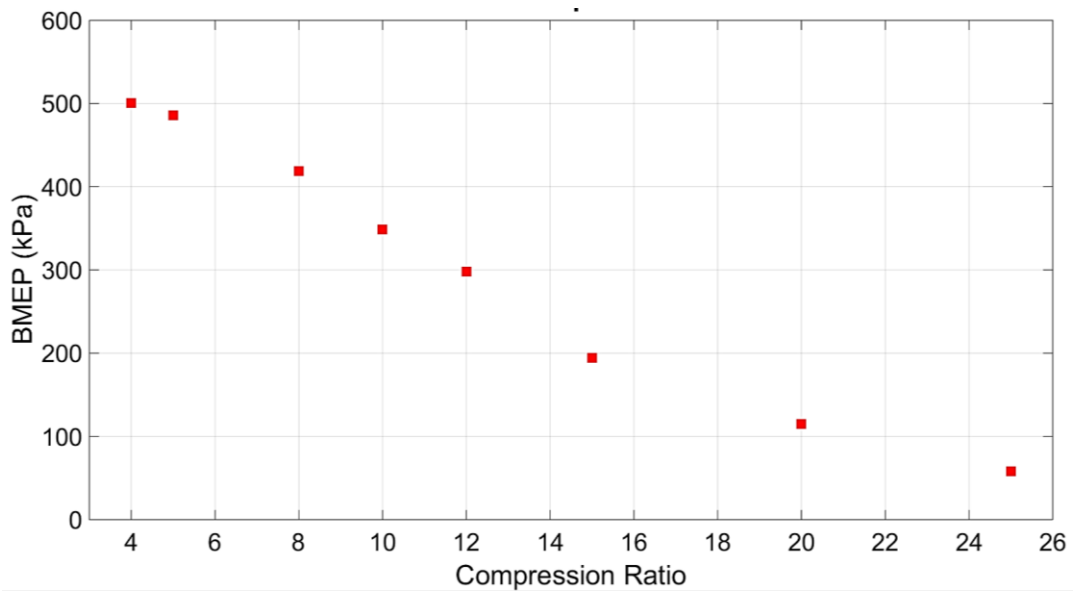


Figure 41: BMEP vs. compression ratio (Gen III b)

As shown in Figure 41, BMEP is highest at a low compression ratio ($rc = 4$). Eq. 49 shows that BMEP is inversely proportional to the displaced volume. So, it is expected for BMEP to be higher at a low compression ratio.

5.5.4 Optimum Efficiency

As shown in Figure 42, efficiency is highest when the compression ratio is equal to 15. At higher compression ratios, the efficiency starts to drop.

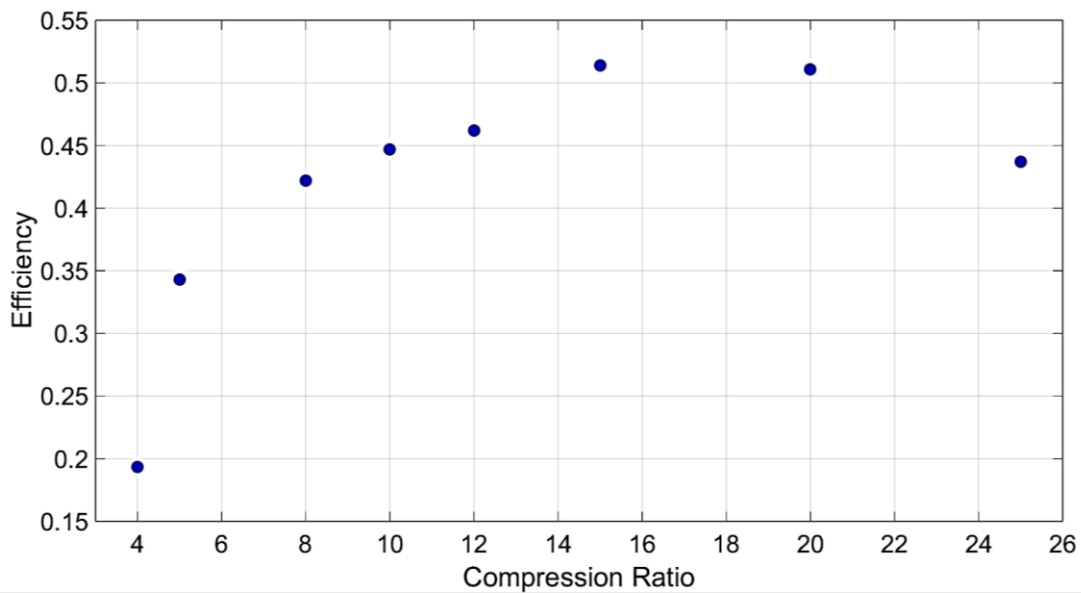


Figure 42: Efficiency peaks vs. compression ratio

5.6 Current Model: Shortcomings

While the new computational model has a time-dependent heat transfer model, it is not very realistic because it assumes that the tubes bank is isothermal. Incropera [16], also warns that calculating the heat transfer this way can overestimate the actual heat transfer rates. So, it is important to implement a more realistic heat transfer model that takes into account the surface temperature variation of the heating/cooling tubes. This will be done next.

Chapter 6: Soony Gen III Performance – Another Heat

Exchanger Model

6.1 Overview

The problem with the previous heat exchanger models is that they did not account for the fact that the temperatures of the source and sink streams will change as they pass through the heat exchanger. This chapter will investigate the engine's performance with a better heat transfer model that incorporates this effect, as shown in Figure 43.

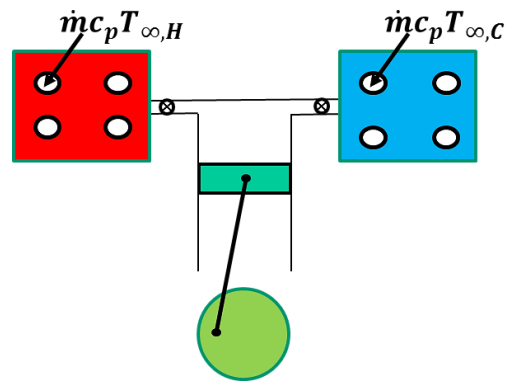


Figure 43: Schematic of Gen III b engine model

In this model, the source or sink streams run through pipes inside the hot and cold reservoirs, as shown in the Figure 44. Heat from the source stream heats the tube walls which, in turn, heats the engine's working fluid in the hot reservoir. The situation is reversed in the cold reservoir where heat is transferred from the working fluid to the tube wall and then to the sink stream. In this conceptual model, the fluid running inside the pipes is air. Air enters the pipe at some initial temperature and exits at a different temperature due to the heat transfer process occurring between the flow and the tube wall. The flow through the tube is steady and there is one entrance and

one exit so $\dot{m}_i = \dot{m}_e$. Heat loss due to streamwise conduction in the tube wall is assumed to be negligible.

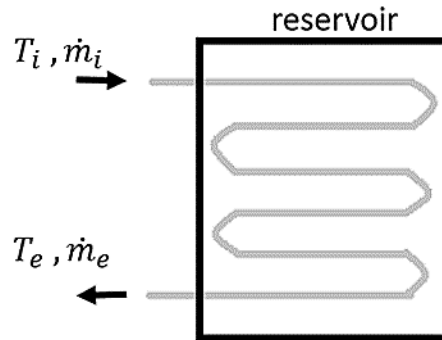


Figure 44: Conceptual heat transfer model

6.2 Thermodynamic Model

The heat transfer rate between the tube and its surroundings is approximated based on the mass flow rate entering through the pipe, the pipe's inlet temperature, the pipe's dimensions (diameter and length), and the surrounding temperature (T_∞), as shown in Figure 45.

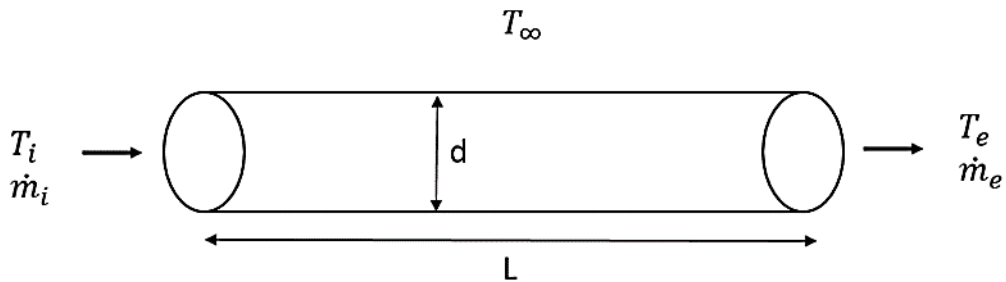


Figure 45: Schematic of the tube and the surrounding temperature

The heat transfer rate between the internal flow and the tube wall is determined as follows:

6.2.1 Step 1: Specific heat at constant pressure

The specific heat at constant pressure, c_p , of the air flowing inside the tube is

calculated using the following expression [19]:

$$c_p = 1.93 * 10^{-10} T^4 - 7.9 * 10^{-7} T^3 + 0.0011 T^2 - 0.45 T + 1.06 * 10^3 \quad (50)$$

6.2.2 Step 2: Calculate the dynamic viscosity

The dynamic viscosity is calculated as a function of temperature, using Sutherland's formula:

$$\mu = \mu_{ref} \left(\frac{T}{T_{ref}} \right)^{1.5} \left(\frac{T_{ref} + C}{T + C} \right) \quad (51)$$

Where, for air, $T_{ref} = 291.15 K$, $\mu_{ref} = 18.27 * 10^{-6} Pa.s$, and $C = 120 K$.

6.2.3 Step 3: Calculate the thermal conductivity

The variation of thermal conductivity with temperature is small but is accounted for by the following equation [17]:

$$k = a + bT \quad (52)$$

where a and b depend on the type of gas. For air, $a \approx 0.016$, and $b \approx 5.2 * 10^{-5}$.

6.2.4 Step 4: Calculate the Prandtl number

Prandtl number can be expressed as a function of the specific heat at constant pressure, dynamic viscosity, and thermal conductivity:

$$Pr = \frac{c_p \mu}{k} \quad (53)$$

6.2.5 Step 5: Calculate the Reynolds number

For a flow in a circular tube, the Reynolds can be expressed as a function of mass flow rate through the tube, the tube's inner diameter, and dynamic viscosity [16]:

$$Re_D = \frac{4\dot{m}}{\pi D \mu} \quad (54)$$

6.2.6 Step 6: Calculate the Nusselt number

The Nusselt number for internal heat transfer inside the tube can be approximated using the Dittus-Boelter equation [16]:

$$Nu_D = 0.023 Re_D^{\frac{4}{5}} Pr^{\frac{1}{3}} \quad (55)$$

6.2.7 Step 7: Calculate the convective heat transfer coefficient (inside the tube)

The heat transfer coefficient for convection inside the tube depends on the Nusselt number, thermal conductivity, and the tube's inner diameter as follows [16].

$$h_i = Nu_D \frac{k}{D} \quad (56)$$

6.2.8 Step 8: Compute the overall heat transfer coefficient

The ability of heat to be transferred from the inner wall of the tube to the internal flow also depends on the ability of heat to be transferred from the external flow/environment to the outer wall of the tube. This effect is captured using an overall heat transfer coefficient which depends on the convective heat transfer coefficients inside (h_i), and outside the pipe (h_o) [16]:

$$\bar{U} = (h_i^{-1} + h_o^{-1}) \quad (57)$$

6.2.9 Step 9: Outside heat transfer coefficient

The flow on the outside of the tubes ranges from zero velocity (free convection) when no working fluid enters or leaves the reservoirs) to a small but finite velocity (forced convection) when working fluid enters or leaves the reservoir. Therefore, the heat transfer coefficient can vary from approximately 50 and 290 W/m² K [17]. Since the

designs of the heat exchangers are completely unknown at this point, the outside heat transfer is approximated as $100 \text{ W/m}^2 \text{ K}$ throughout the cycle.

6.2.10 Step 10: Compute fluid exit temperature

After calculating the above equations, it is now possible to approximate the temperature of the air exiting the tube [16]. The exit temperature depends on the mass flow rate through the pipe, the temperature of the surroundings (i.e. the hot or cold reservoir temperature), the fluid's temperature at the tube's inlet, the overall convective heat transfer coefficient, the tube's surface temperature, and the specific heat at constant pressure. The expressions of the exit temperature for both the source and sink are presented next:

$$T_{eh} = T_{\infty} - (T_{hr} - T_i) \exp\left(\frac{-U * A}{\dot{m} * c_p}\right) \quad (58)$$

$$T_{ec} = T_{\infty} - (T_{cr} - T_i) \exp\left(\frac{-U * A}{\dot{m} * c_p}\right) \quad (59)$$

6.2.11 Step 11: Compute the heat transfer rate

The heat transfer rates in the hot and cold reservoirs are given by:

$$\dot{Q} = \dot{m} * c_p (T_e - T_i) \quad (60)$$

These expressions are used to compute \dot{Q}_H and \dot{Q}_C in the models for the hot and cold reservoirs (i.e. equations 16 and 17 in Chapter 3).

6.3 Exploring the Parameter Space

As before, the engine model is updated with the new hot and cold reservoir heat transfer rates and used to identify the designs and operating conditions associated with peak power, efficiency, or BMEP.

6.3.1 Inputs

The parameter space is explored by computing the performance of 3456 different combinations of operating parameters. The parameters considered and the ranges over which they are varied are presented in Table 9 and Table 10. The volumes of the hot and cold reservoirs are assumed to be equal because the previous heat transfer model optimization showed that the engine's peak performance occurs when the reservoirs' volumes are equal. The calculations took approximately 3 weeks.

MATLAB *ODE45* was used to accomplish this task.

Table 9: Model parameters and the ranges over which they are varied

Parameters	Range of variation
Compression ratio	3 to 40
Cold reservoir initial pressure	0.2 to 9 Mpa
Cold reservoir volume	$5 V_{cyl, max}$ to $50 V_{cyl, max}$
Hot fluid's inlet temperature through pipe ($T_{in, hot}$)	800 to 1200 K.
Hot air mass flow rate through the pipe (\dot{m}_{hot})	0.2 to 0.8 kg/sec
Cold air mass flow rate through the pipe (\dot{m}_{cold})	$= \dot{m}_{hot}$

Additionally, the main constant parameters are:

Table 10: Constant parameters

Cylinder's dead volume (V_{min})	6e-05 m ³
Hot reservoir's initial pressure	10 MPa
Engine's speed	1800 rpm
Working fluid	Air
Cold air inlet temperature through the pipe	300 K

6.4 Results

Table 11 shows the optimum results achieved by this engine model in terms of power output, efficiency, and BMEP.

Table 11: Optimum results for a source mass flow rate equal to 0.5 kg/sec (Gen III c)

	Optimal Power	Optimal Efficiency	Optimal BMEP
BMEP (kPa)	200	38.5	388.6
Efficiency (%)	36.2	60.1	31
Power (kW)	6.83	2	2.67

6.4.1 Power Output Peaks vs. Compression Ratio

Figure 46 shows the 'family' of power output peaks as a function of compression ratio (for a source stream equal to 0.5 kg/sec). It is shown that the peak power output occurs at a compression ratio equal to 20. Also, it is important to note that this

‘family’ of power output peaks corresponds to when each reservoir’s volume is equal to 50 times the volume of the piston chamber (piston chamber volume at BDC).

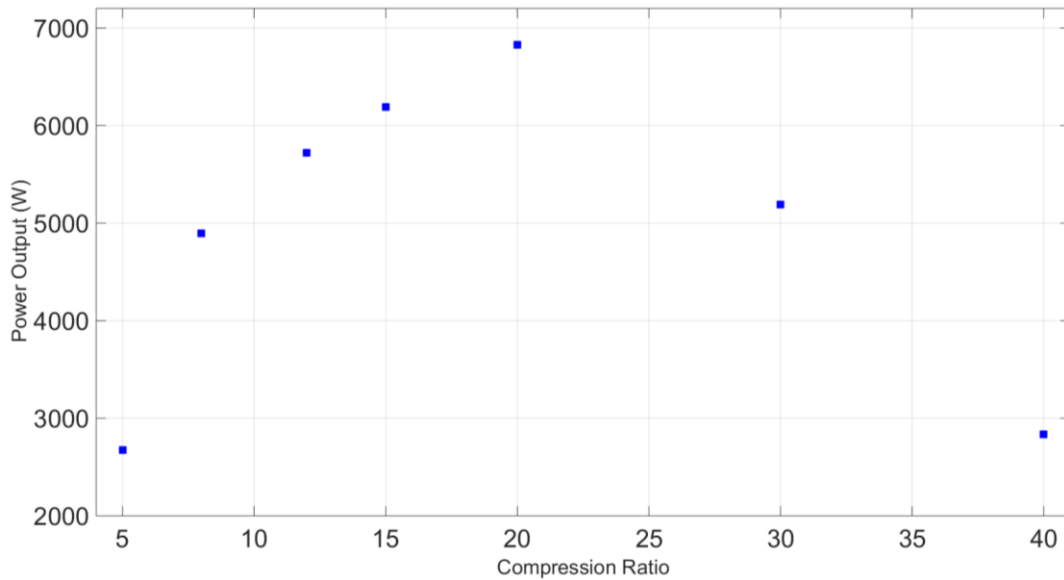


Figure 46: Power output vs. compression ratio (Sink mass flow rate = 2 x source mass flow rate)

Furthermore, it is important to investigate the effect of the source/sink mass flow rate on the engine’s performance. This will be done next.

6.4.2 Effect of source/sink mass flow rates

The ‘family’ of power output peaks shown in Figure 46 corresponds to a source mass flow rate value that is equal to 0.5 kg/sec. However, it is important to investigate the engine’s performance over a range of source/sink mass flow rates (at a certain compression ratio). Figure 47 shows that, for a compression ratio equal to 12, the power output of the engine model reaches an asymptote at a source mass flow rate that is approximately equal to 0.8 kg/sec.

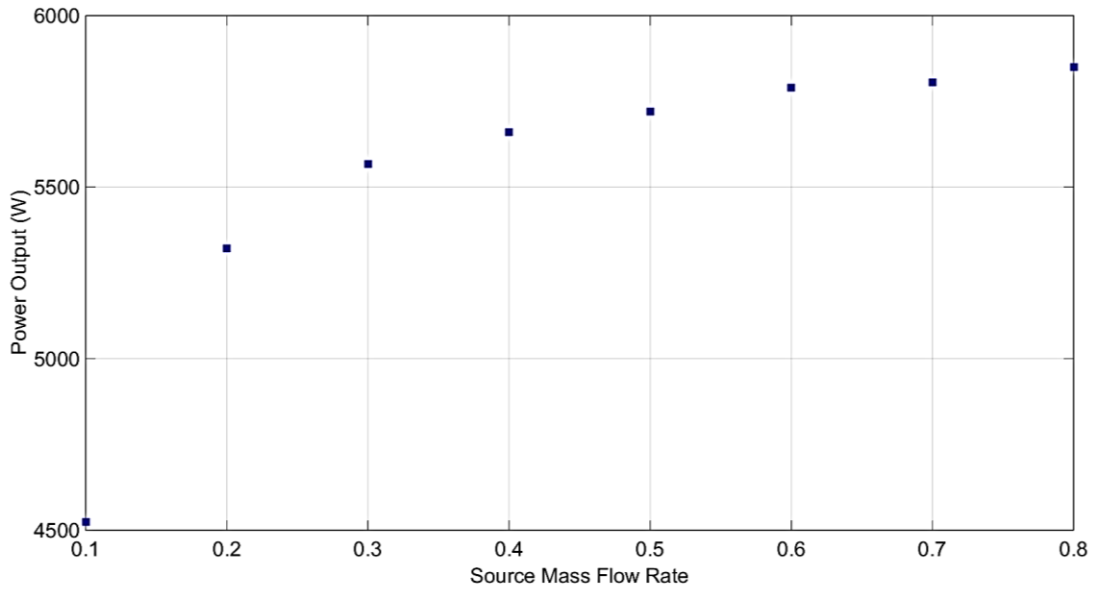


Figure 47: Effect of source/sink mass flow rates on the engine's performance (Sink mass flow rate = 2 x source mass flow rate)

6.4.3 BMEP vs. Compression Ratio

As shown in Figure 48, BMEP is highest at a low compression ratio ($rc = 8$). BMEP is inversely proportional to the displaced volume. So, it is expected for BMEP to be higher at a low compression ratio. As shown in the figure below, the peak BMEP achieved by this engine is 388.6 kPa, which is far lower than most Stirlings.

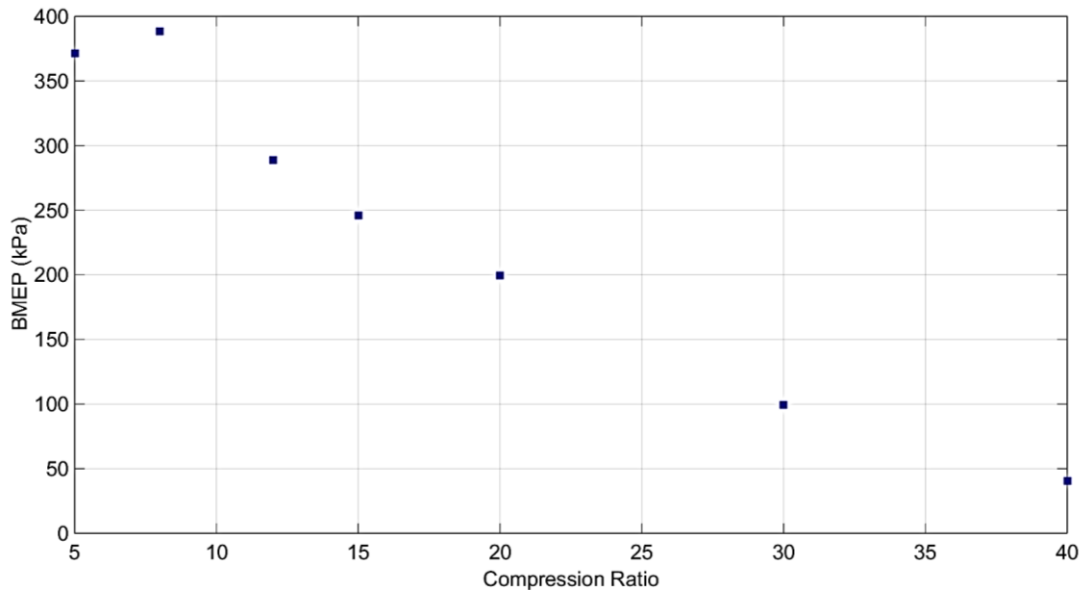


Figure 48: BMEP vs. compression ratio (Sink mass flow rate = 2 x source mass flow rate)

6.4.4 Efficiency vs. Compression Ratio

As shown in Figure 49, efficiency is highest when the compression ratio is equal to 30 (efficiency = 60.1%). At higher compression ratios, the efficiency starts to drop.

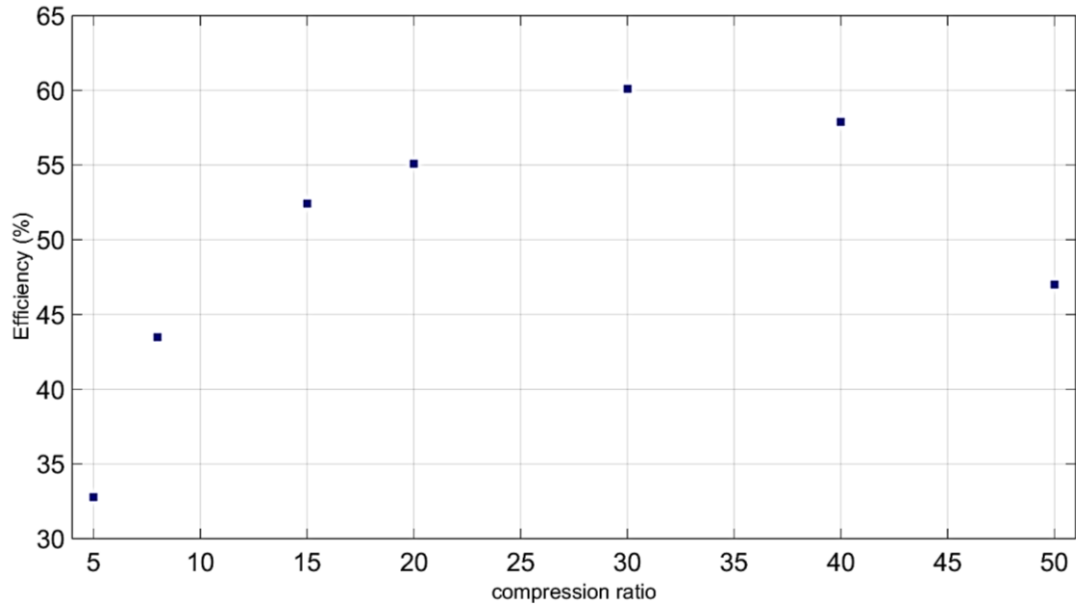


Figure 49: Peak efficiency values vs. compression ratio

Figure 50 shows the ratio of heat rates that correspond to each case plotted above.

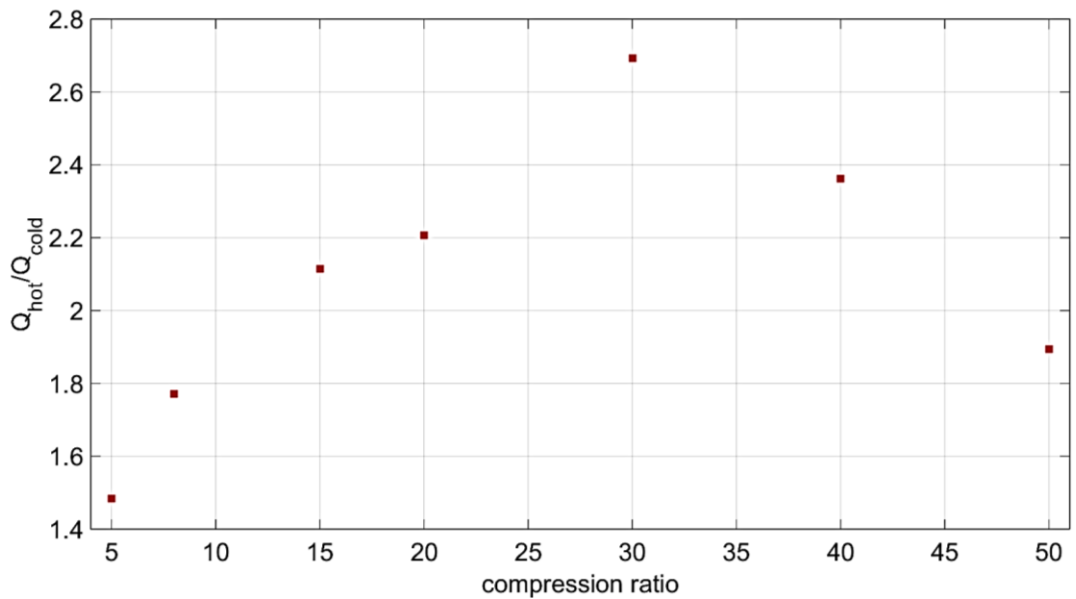


Figure 50: Ratio of heat rates vs. compression ratio

As shown in the figures above, the efficiency peaks are directly proportional to the ratio of heat transfer rates, into the hot reservoir and out of the cold reservoir.

6.4.5 Effect of changing the reservoirs volumes

Figure 46 has shown the ‘family’ of peak power output values as a function of compression ratio. It is important to note that all these peak values correspond to when each reservoir’s volume is equal to 50 times the displaced volume of the working cylinder.

However, it is also important to investigate how each of these peak power output values will vary with varying the reservoirs volume. The results are shown in Figure 51. As it would be expected, decreasing the size of the reservoirs will also decrease the performance of the engine.

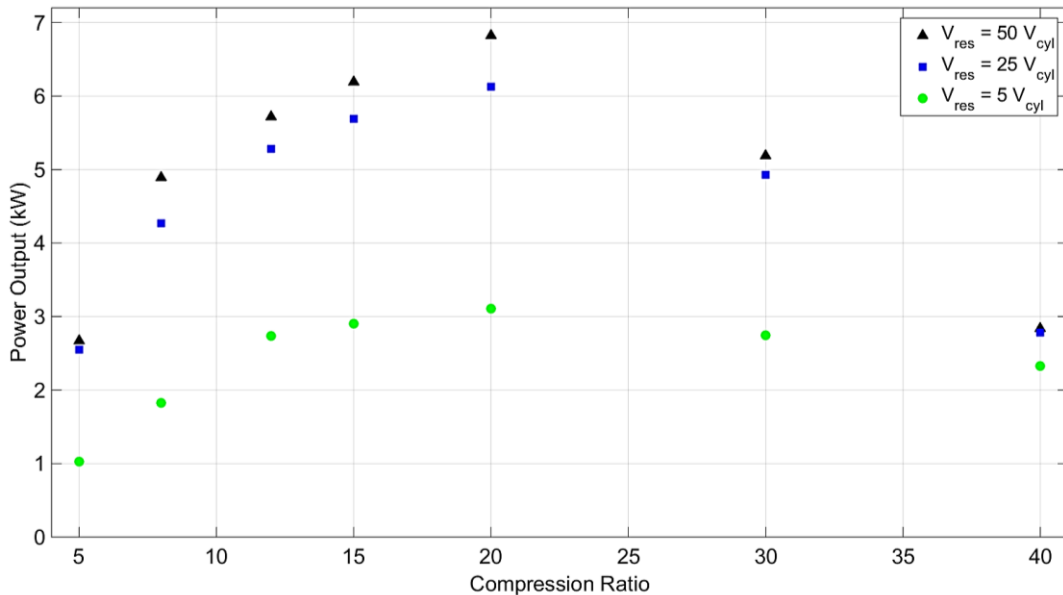


Figure 51: Effect of varying the reservoirs volume

Chapter 7: Conclusion

7.1 Summary of Findings

The main objective of this thesis is to investigate the performance of a new type of externally heated air engine design developed by Soony Systems Inc. as part of a combined heating and cooling system for private residences. A thermodynamic model of the engine was developed and used to predict the performance of approximately 3,000 different engine designs. Designs that maximized power output, overall efficiency, or brake mean effective pressure (BMEP) have been identified. Although not a part of the original project, the heat exchangers responsible for maintaining the hot and cold reservoir temperatures were modeled in three different ways.

The results show that the Soony engine has the potential to achieve higher thermodynamic efficiencies than Stirling engines because its cycle more closely approximates a Carnot cycle than a Stirling engine. However, this comes at the cost of significantly lower BMEP (brake mean effective pressure) indicating that the Soony model doesn't use its working volume as efficiently as a Stirling.

7.2 Main Contributions

1. Created a quasi-static model for the original 'Gen II' Soony design.
2. Showed that the Gen II design was not viable but that it could be 'fixed' by removing the diaphragm.

3. Created a thermodynamic model for the Gen III engine where the heating/cooling rates in the hot/cold reservoirs respectively were assumed to be known constants.
4. Created a second thermodynamic model for the Gen III engine with more realistic time-dependent models for the heat transfer processes occurring in the hot and cold reservoirs. However, the temperatures of the heat exchanger tubes heating the reservoirs were assumed to be known constants.
5. Used the second model of the Gen III engine to investigate around 4,000 different engine designs and identified the configurations associated with peak power output, efficiency, and BMEP.
6. Created a third thermodynamic model for the engine with an even more realistic time-dependent heat transfer model where the heat exchanger tubes are no longer isothermal.
7. Used the third model of the Gen III engine to investigate 3,000 different designs and identified the designs that maximize power output, efficiency, and BMEP.

7.3 Future Work

While this work was able to investigate the parameter space of the engine through a series of computational models, the following improvements can be made:

1. Investigate the engine performance at different speeds.
2. Incorporate the variation of c_p with temperature.
3. Incorporate the engine model into a larger thermodynamic model of a residential CHP system.

4. Investigate the variation of the engine performance (Efficiency, power, and BMEP) with compression ratio.
5. Improve the third heating model by incorporating a time-dependent heat transfer convective coefficient for the outer-tube heat transfer.
6. Design a physical hot/cold reservoirs.
7. Investigate different fluids as source/sink streams, and at different mass flow rates.
8. Investigate the performance of the engine model with isochoric heating and cooling processes, in order to see how the cycle would compare to an ideal Stirling cycle.

Appendices

A. Gen III a - Dynamic Model

MATLAB Function (Step1):

```
function f = step1(t,y)
%% This function correspond to the first half of the upstroke (step 1)
f=zeros(12,1);
global Vmin;%min volume
global rc;%compression ratio
global R;%ratio of connecting rod length to crank radius
global w;%rpm (rad/sec)
global R_gas;%gas constant
global Cp;%specific heat at constant pressure
global Cv;%specific heat at constant volume
global A_cr;%cold reservoir area
global gamma;
global n;% number of upper slits
global Qdot_h;
global Qdot_c;
global Cd;% Coefficient of Discharge

%% First Case (Pcold >= Pcyl)

if( (y(8)>=y(5)) && (y(5)<y(11)) )
m=w*t+pi;
f(1,1)=Vmin*(rc-1)*0.5*(w*sin(m)+(w*sin(m)*cos(m)...
/(sqrt((R^2)-((sin(m))^2 ))));%dV

if((y(8)>y(5)))
P_s=0.528*y(8);
if (y(5)<P_s)%choked
flow=Cd*A_cr*sqrt( gamma*(y(8)*y(8)/(R_gas*y(7)))* ....
( 2/(gamma+1) )^( ( gamma+1 )/(gamma-1) ) );%choked
else%unchoked
c=( ( ( y(5)/y(8))^ ( 2/gamma) ) - ( ( y(5)/y(8))...
^(gamma+1)/gamma));
flow=Cd*A_cr*sqrt((2*y(8)*y(8)/(R_gas* y(7) ))*...
(gamma/(gamma-1))*c);%unchoked
end
else
flow=0;
end
```

```

% Working Cylinder
f(2,1)=-n*flow;% mass rate into cylinder
f(3,1)=abs((y(5))*f(1,1));% work on cylinder
f(4,1)=(1/(y(2)*(Cp-R_gas)))*(f(3,1)+f(2,1)*...
    (Cp*y(7)-Cp*y(4)+R_gas*y(4)));% dT of cylinder
f(5,1)=(f(2,1)*R_gas*y(4)+y(2)*R_gas*f(4,1)-y(5)*f(1,1))/y(1);% dP cylinder

% Cold Reservoir
f(6,1)=-n*flow;% flow of cold reservoir
f(7,1)=(f(6,1)*R_gas*y(7)+Qdot_c)/(y(6)*(Cp-R_gas));% dT of cold reservoir
f(8,1)=y(8)*((f(6,1)/y(6))+(f(7,1)/y(7)));% dP of cold reservoir

% Hot Reservoir
f(9,1)=0;% flow in/out hot reservoir
f(10,1)=Qdot_h/(y(9)*Cv);% dT of hot reservoir
f(11,1)=y(11)*f(10,1)/y(10);% dP of hot reservoir

% Cylinder specific entropy
f(12,1)=(Cp/y(4))*f(4,1)-(R_gas/y(5))*f(5,1);
end

%% Second Case (Pcold < Pcyl)
if( (y(5)>y(8)) && (y(5)<y(11)) )

m=w*t+pi;
f(1,1)=Vmin*(rc-1)*0.5*(w*sin(m)+(w*sin(m)*cos(m)...
    /(sqrt((R^2)-((sin(m))^2 ))));% dV

P_s=0.528*y(5);
if (y(8)<P_s)%choked
    flow=Cd*A_cr*sqrt( gamma*(y(5)*y(5)/(R_gas*y(4)))...
        * ( 2/(gamma+1))^( ( gamma+1)/(gamma-1)));% choked
else%unchoked
    c=(( ( y(8)/y(5))^2/gamma) - (( y(8)/y(5))^((gamma+1)/gamma)));
    flow=Cd*A_cr*sqrt((2*y(5)*y(5)/(R_gas* y(4)))...
        *(gamma/(gamma-1))*c);% unchoked
end

% Working Cylinder
f(2,1)=-n*flow;% mass rate into cylinder
f(3,1)=abs((y(5))*f(1,1));% work on cylinder
f(4,1)=(1/(y(2)*(Cp-R_gas)))*(f(3,1)+f(2,1)*R_gas*y(4));% dT of cylinder
f(5,1)=(f(2,1)*R_gas*y(4)+y(2)*R_gas*f(4,1)-y(5)*f(1,1))/y(1);% dP cylinder

```

```

%Cold Reservoir
f(6,1)=n*flow;% flow of cold reservoir
f(7,1)=(f(6,1)*(R_gas*y(7)+Cp*y(4)-Cp*y(7))+Qdot_c)...
/(y(6)*(Cp-R_gas));% dT of cold reservoir
f(8,1)=y(8)*((f(6,1)/y(6))+(f(7,1)/y(7)));% dP of cold reservoir

%Hot Reservoir
f(9,1)=0;% flow in/out hot reservoir
f(10,1)=Qdot_h/(y(9)*Cv);% dT of hot reservoir
f(11,1)=y(11)*(f(10,1)/y(10));% dP of hot reservoir

%Cylinder specific entropy
f(12,1)=(Cp/y(4))*f(4,1) -(R_gas/y(5))*f(5,1);

end

```

MATLAB Function (Step2):

```

function f = step1b(t,y)
%% This function correspond to the second half of the upstroke (step 2)
f=zeros(12,1);
global Vmin;% min volume
global rc;% compression ratio
global R;% ratio of connecting rod length to crank radius
global w;% rpm (rad/sec)
global R_gas;% gas constant
global Cp;% specific heat at constant pressure
global Cv;% specific heat at constant volume
global A_h;% hot reservoir area
global gamma;
global n;% number of upper slits
global Qdot_h;
global Qdot_c;
global Cd;% Coefficient of Discharge
m=w*t+pi;
f(1,1)=Vmin*(rc-1)*0.5*(w*sin(m)+(w*sin(m)*cos(m)...
/(sqrt((R^2)-((sin(m))^2 ))));% dV

if (y(5)>y(11))

P_s=0.528*y(5);
if (y(11)<P_s)% choked
flow=Cd*A_h*sqrt( gamma*(y(5)*y(5)/(R_gas*y(4)))*...

```



```

        ( 2/(gamma+1))^( ( gamma+1 )/(gamma-1));%choked
else%unchoked
    c=( ( y(11)/y(5))^ ( 2/gamma)) - ...
        ( ( y(11)/y(5))^( (gamma+1)/gamma));
    flow=Cd*A_h*sqrt((2*y(5)*y(5)/(R_gas* y(4)))*...
        (gamma /(gamma-1))*c);%unchoked
end
else
    flow=0;
end

% Working Cylinder
f(2,1)=-n*flow;% mass rate into cylinder
f(3,1)=abs((y(5))*f(1,1));% work on cylinder
f(4,1)=(1/(y(2)*(Cp-R_gas)))*(f(3,1)+f(2,1)*R_gas*y(4));%dT of cylinder
f(5,1)=(f(2,1)*R_gas*y(4)+y(2)*R_gas*f(4,1)-y(5)*f(1,1))/y(1);%dP cylinder

% Cold Reservoir
f(6,1)=0;% flow of cold reservoir
f(7,1)=Qdot_c/(y(6)*Cv);%dT of cold reservoir
f(8,1)=y(8)*(f(7,1)/y(7));%dP of cold reservoir

% Hot Reservoir
f(9,1)=n*flow;% flow in/out hot reservoir
f(10,1)=(f(9,1)*(R_gas*y(10)+Cp*y(4)-Cp*y(10))+Qdot_h)...
    /(y(9)*(Cp-R_gas));%dT of hot reservoir
f(11,1)=y(11)*((f(9,1)/y(9))+f(10,1)/y(10));%dP of hot reservoir

% Cylinder specific entropy
f(12,1)=(Cp/y(4))*f(4,1) -(R_gas/y(5))*f(5,1);

```

MATLAB Function (Step 3 and 4):

```

function f = step2(t,y)
%% This function correspond to the downstroke (step 3 and 4)
f=zeros(12,1);
global Vmin;% min volume
global rc;% compression ratio
global R;% ratio of connecting rod length to crank radius
global w;% rpm (rad/sec)
global R_gas;% gas constant
global Cp;% specific heat at constant pressure
global Cv;% specific heat at constant volume
global A_h;% cold reservoir area

```

```

global gamma;
global n; %number of upper slits
global Qdot_h;
global Qdot_c;
global Mhot1;
global Cd;% Coefficient of Discharge
m=w*t+pi;
f(1,1)=Vmin*(rc-1)*0.5*(w*sin(m)+(w*sin(m)*cos(m)...
/(sqrt((R^2)-((sin(m))^2 ))));%dV
if(y(11)>y(5)&&(y(9)>Mhot1))
P_s=0.528*y(11);
if (y(5)<P_s)%choked
flow=Cd*A_h*sqrt( gamma*(y(11)*y(11)/(R_gas*y(10)))*...
( 2/(gamma+1) )^( ( gamma+1 )/(gamma-1) ) );
else%unchoked
c=( ( y(5)/y(11))^ ( 2/gamma) ) - ...
( ( y(5)/y(11))^ ( gamma+1/gamma) ));
flow=Cd*A_h*sqrt((2*y(11)*y(11)/(R_gas* y(10)))*...
*(gamma/(gamma-1) )*c);%unchoked
end
else
flow=0;
end

% Working Cylinder
f(2,1)=n*flow;%mass rate into cylinder
f(3,1)=-abs((y(5))*f(1,1));% work on cylinder
f(4,1)=(1/(y(2)*(Cp-R_gas)))*(f(3,1)+f(2,1)...
*(Cp*y(10)-Cp*y(4)+R_gas*y(4)));%dT of cylinder
f(5,1)=(f(2,1)*R_gas*y(4)+y(2)*R_gas...
*f(4,1)-y(5)*f(1,1))/y(1);%dP of cylinder

%Cold Reservoir
f(6,1)=0;%flow of cold reservoir
f(7,1)=Qdot_c/(y(6)*Cv);%dT of cold reservoir
f(8,1)=y(8)*((f(7,1)/y(7)));%dP of cold reservoir

%Hot Reservoir
f(9,1)=-n*flow;%flow out of hot reservoir
f(10,1)=(f(9,1)*R_gas*y(10)+Qdot_h)/(y(9)*(Cp-R_gas));%dT of hot reservoir
f(11,1)=y(11)* ( f(9,1)/y(9))+f(10,1)/y(10) );%dP of hot reservoir

%Cylinder specific entropy
f(12,1)=(Cp/y(4))*f(4,1) -(R_gas/y(5))*f(5,1);

```

MATLAB Main Script:

```
% Wiam Attar
% This engine model incorporates a coefficient of discharge
% It also assumes constant heat addition and removal

clc
clear ALL;
format long
%% _____Global
Variables_____
global Vmin;%min volume (m^3)
global Vmax;%maximum working volume (m^3)
global rc;%compression ratio
global R;%ratio of connecting rod length to crank radius
global a;%Crank radius
global l;%Connecting rod length
global w;%rpm (rad/sec)
global R_gas;%gas constant
global gamma;%ratio of specific heats
global Cp;%specific heat at constant pressure
global Cv;%specific heat at constant volume
global A_cr;%cold reservoir area
global A_h;%hot reservoir area
global n;%number of upper slits
global Qdot_h;% Rate of Heat added to the hot reservoir (J/s)
global Qdot_c;% Rate of Heat removed from the cold reservoir (J/s)
global Mhot1;% Initial Mass in Hot Reservoir
global Kb;% Boltzmann Constant (J/K)
global h;%Planck's Constant (J.s)
global Na;%Avogadro's Number (particles/mole)
global Mcr1;%initial mass in cold reservoir (kg)
global e;% 2.718281828459046
global kk;%constant 1.38044e-16 ( Boltzmann )
global M;% Molar Mass g/mole
global w_el;% Electronic degeneracy
global sigma_r;% Rotational Temperature (K)
global D0;% Dissociation Energy (erg)
global sigma_v;% Vibrational Temperature (K)
global mp;%mass of one molecule (kg/molecule)
global Cd;% Coefficient of Discharge

%%
_____Inputs_____
% Coefficient of Discharge
```

```

Cd=0.61;

% Constant Heat Rates In/Out (J/s)
Qdot_h=7000;
Qdot_c=-4100;

% Minimum Volume (TDC Volume)
Vmin=70e-06;%m^3

% Compression Ratio
rc=7;

% RPM
w=1800*2*pi/60;%rad/sec

% Number of slits is the same for cold and hot reservoirs connection
n=30;

% Area of each hot reservoir's slit
A_h=(2e-05);

% Area of each cold reservoir's slit
A_cr=(8e-04)/30;

% Gas Properties (Air)
R_gas=287;
gamma=1.4;
Cp=1005;
Cv=718;
mp=4.65e-26;% mass of one molecule (kg/molecule)
M=28;% Molar Mass
w_el=1;% Electronic degeneracy
sigma_r=2.89;% Rotational Temperature (K)
D0=9.76*1.602e-12;% Dissociation Energy (erg)
sigma_v=3390;% Vibrational Temperature (K)

% Geometric Dimension
a=0.2;% crank radius
l=0.25;% connecting rod length

% Constants
Kb=1.38064852e-23;% Boltzman Constant (J/K)
h=6.626070040e-34;% Planck's Constant (J.s)
Na=6.0221409e+23;% Avogadros
e=2.7182818;
kk=1.38044e-16;% Boltzmann

```

```

% BDC Volume (i.e. maximum Volume)
Vmax=rc*Vmin;

% Cold Reservoir Initial Conditions
Tcr1=300;% initial temperature of cold reservoir
Pcr1=1.5e+06;%initial pressure of cold reservoir
Vcr=1000e-06;% volume of cold reservoir
Mcr1=Pcr1*Vcr/(R_gas*Tcr1);%initial mass in cold reservoir

% Working Cylinder Initial Conditions
Tcyl1=273.15;% starting temperature at BDC
Pcyl1=0.2e+06;% starting pressure at BDC
Vcyl1=Vmax;% Cylinder's volume at BDC
Mcyl1=Pcyl1*Vcyl1/(R_gas*Tcyl1);%initial mass in working cylinder at BDC

% Hot Reservoir Initial Conditions
Thot1=1200;% initial hot reservoir temperature
Phot1=9e+06;% initial hot reservoir pressure
Vhot=1000e-06;% Volume in hot reservoir
Mhot1=Phot1*Vhot/(R_gas*Thot1);%initial mass in hot reservoir

R=l/a;%ratio of connecting rod length to crank radius

%Calculating Entropy
% Working Cylinder
V=8.314*Tcyl1/Pcyl1;
q_trans=(1.88e+26)*V.*(M*Tcyl1).^1.5);
q_rot=Tcyl1/(2*sigma_r);
q_vib_elect=w_el.*(exp((D0)/((1.38044e-16)*Tcyl1)))/...
(1-exp(-sigma_v./Tcyl1));
q_tot=q_trans.*q_rot.*q_vib_elect;
A_NKT=-log(q_tot*(e)./Na);
U_NKT=(5/2)+ ( ((sigma_v./Tcyl1).*exp(-sigma_v./Tcyl1))/...
(1-exp(-sigma_v./Tcyl1)) ) -(D0./(Tcyl1*(kk)));
S_NK_1=U_NKT-A_NKT;
S_J_mole_K=S_NK_1*Na*Kb; %J/mole.K
S_specific_J_Kg_K=S_J_mole_K*1000/M; %J/Kg.K
Entropy_init=(S_specific_J_Kg_K.*Mcyl1)/Mcyl1; %J/K-kg

%% Additional Integration Variables (In order to run multiple cycles)
time0=0;% initial start time of the cycle
L=0; %Initial Net Work Ouput Value at the start
k=2;% Additional Variable that will help calculate the start ...
...time of every cycle__t=(theta-pi)/w
p=1;% Additional Variable that will help calculate the time...

```

...at TDC $\theta = (\theta - \pi) / \omega$ where $t = \pi / \omega, 3\pi / \omega, 5\pi / \omega, \text{etc...}$

%%

Step1

Cycles_number=14;

for H=1:Cycles_number

% The time when cold reservoir Interaction with the working cylinder stops

avg=0.5*(time0+(p*pi/w)); %the interaction with the cold reservoir ...

...stops midway through the upstroke

options = odeset('AbsTol',1e-19,'RelTol',1e-19);

[t1,Y]=ode45('step1',[time0 avg],[Vmax M cyl1 L T cyl1 P cyl1 M cr1 T cr1 ...

P cr1 M hot1 T hot1 P hot1 Entropy_init],options);

xx=(t1*w+pi)*180/pi;% x-axis (for plotting purposes)

% In order to make the angle run from 180 to 540, we need to deduct the

% sum of the angles that accumulated in previous cycles, during which the

% engine was approaching its steady-state behavior

angl_deduction=(Cycles_number-1)*360;

if (H==Cycles_number)% Activate this to see only last cycle

figure(1)

plot((xx-angl_deduction),Y(:,1),'-', 'LineWidth',2)

xlim([170 550])

grid on

xlabel('Crank Angle (deg.)','FontSize', 25)

ylabel('Piston Chamber Volume (m^3)','FontSize', 25)

set(gca,'FontSize',25)

hold on

figure(2)

plot((xx-angl_deduction),Y(:,2),'-', 'LineWidth',2)

xlim([170 550])

grid on

xlabel('Crank Angle (deg.)','FontSize', 25)

ylabel('M_C_y_l_i_n_d_e_r (kg)','FontSize', 25)

set(gca,'FontSize',25)

hold on

figure(3)

plot((xx-angl_deduction),-Y(:,3),'-', 'LineWidth',2)

xlim([170 550])

```

grid on
xlabel('Crank Angle (deg.)','FontSize', 25)
ylabel('Work Output (Joule)','FontSize', 25)
set(gca,'FontSize',25)
hold on

figure(4)
plot((xx-angl_deduction),Y(:,4),'-', 'LineWidth',2)
xlim([170 550])
grid on
xlabel('Crank Angle (deg.)','FontSize', 25)
ylabel('T_C_y_l_i_n_d_e_r (K)','FontSize', 25)
set(gca,'FontSize',25)
hold on

figure(5)
plot((xx-angl_deduction),Y(:,5),'-', 'LineWidth',2)
xlim([170 550])
grid on
xlabel('Crank Angle (deg.)','FontSize', 25)
ylabel('P_C_y_l_i_n_d_e_r (Pa)','FontSize', 25)
set(gca,'FontSize',25)
hold on

figure(6)
plot((xx-angl_deduction),Y(:,6),'-', 'LineWidth',2)
xlim([170 550])
grid on
xlabel('Crank Angle (deg.)','FontSize', 25)
ylabel('M_c_o_l_d (kg)','FontSize', 25)
set(gca,'FontSize',25)
hold on

figure(7)
plot((xx-angl_deduction),Y(:,7),'-', 'LineWidth',2)
xlim([170 550])
grid on
xlabel('Crank Angle (deg.)','FontSize', 25)
ylabel('T_c_o_l_d (K)','FontSize', 25)
set(gca,'FontSize',25)
hold on

figure(8)
plot((xx-angl_deduction),Y(:,8),'-', 'LineWidth',2)
xlim([170 550])
grid on

```

```

xlabel('Crank Angle (deg.)','FontSize', 25)
ylabel('P_c_o_l_d (Pa)','FontSize', 25)
set(gca,'FontSize',25)
hold on

```

```

figure(9)
plot((xx-angl_deduction),Y(:,9),'-', 'LineWidth',2)
xlim([170 550])
grid on
xlabel('Crank Angle (deg.)','FontSize', 25)
ylabel('M_h_o_t (kg)','FontSize', 25)
set(gca,'FontSize',25)
hold on

```

```

figure(10)
plot((xx-angl_deduction),Y(:,10),'-', 'LineWidth',2)
xlim([170 550])
grid on
xlabel('Crank Angle (deg.)','FontSize', 25)
ylabel('T_h_o_t (K)','FontSize', 25)
set(gca,'FontSize',25)
hold on

```

```

figure(11)
plot((xx-angl_deduction),Y(:,11),'-', 'LineWidth',2)
xlim([170 550])
grid on
xlabel('Crank Angle (deg.)','FontSize', 25)
ylabel('P_h_o_t (pa)','FontSize', 25)
set(gca,'FontSize',25)
hold on

```

```

figure(16)
plot(Y(:,1)/Y(:,2),Y(:,5),'b-', 'LineWidth',1)
grid on
xlabel('v (m^{3}/kg)','FontSize', 25)
ylabel('P_c_y_l (Pa)','FontSize', 25)
set(gca,'FontSize',25)
hold on

```

```

figure(17)
plot(Y(:,12),Y(:,4),'b-', 'LineWidth',2)
grid on
xlabel('s (J/kg-K)','FontSize', 25)
ylabel('T_c_y_l (K)','FontSize', 25)

```



```

set(gca,'FontSize',25)
hold on

% Entropy Calculation proof
for i=2:length(Y(:,4))
    dT(i-1)=Y(i,4)-Y(i-1,4);
    dP(i-1)=Y(i,5)-Y(i-1,5);
    ds(i-1)=(Cp./Y(i,4)).*dT(i-1)-(R_gas./Y(i,5)).*dP(i-1);
end
ds_new=zeros(1,length(xx));

for i=2:length(xx)
    ds_new(i)=ds(i-1);
end
figure(18)
subplot(2,3,2)
plot((xx-angl_deduction),ds_new,'-', 'LineWidth',2)
xlim([170 550])
hold on
grid on
xlabel('Crank Angle (deg.)','FontSize', 25)
ylabel('ds (J/kg-K)','FontSize', 25)
set(gca,'FontSize',25)
ylim([-0.1 0.05])

subplot(2,3,5)
plot((xx-angl_deduction),Y(:,12),'-', 'LineWidth',2)
xlim([170 550])
grid on
hold on
xlabel('Crank Angle (deg.)','FontSize', 25)
ylabel('s (J/kg-K)','FontSize', 25)
set(gca,'FontSize',25)

figure(19)
subplot(3,7,[10 12])
plot((xx-angl_deduction),Y(:,5),'b-', 'LineWidth',2)
xlim([170 550])
grid on
ylabel('P_C_y_l_i_n_d_e_r (Pa)','FontSize', 25)
set(gca,'FontSize',25)
hold on

subplot(3,7,[17 19])

```

```

plot((xx-angl_deduction),Y(:,8),'b-', 'LineWidth',2)
xlim([170 550])
grid on
xlabel('Crank Angle (deg.)','FontSize', 25)
ylabel('P_c_o_l_d (Pa)','FontSize', 25)
set(gca,'FontSize',25)
hold on

```

```

subplot(3,7,[3 5])
plot((xx-angl_deduction),Y(:,11),'b-', 'LineWidth',2)
xlim([170 550])
grid on
ylabel('P_h_o_t (pa)','FontSize', 25)
set(gca,'FontSize',25)
hold on

```

```

figure(20)
subplot(3,7,[10 12])
plot((xx-angl_deduction),Y(:,4),'b-', 'LineWidth',2)
xlim([170 550])
grid on
ylabel('T_C_y_l_i_n_d_e_r (K)','FontSize', 25)
set(gca,'FontSize',25)
hold on

```

```

subplot(3,7,[17 19])
plot((xx-angl_deduction),Y(:,7),'b-', 'LineWidth',2)
xlim([170 550])
grid on
xlabel('Crank Angle (deg.)','FontSize', 25)
ylabel('T_c_o_l_d (K)','FontSize', 25)
set(gca,'FontSize',25)
hold on

```

```

subplot(3,7,[3 5])
plot((xx-angl_deduction),Y(:,10),'b-', 'LineWidth',2)
xlim([170 550])
grid on
ylabel('T_h_o_t (K)','FontSize', 25)
set(gca,'FontSize',25)
hold on

```

```

figure(21)
subplot(3,7,[10 12])
plot((xx-angl_deduction),Y(:,2),'b-', 'LineWidth',2)

```

```

xlim([170 550])
grid on
ylabel('M_C_y_l_i_n_d_e_r (kg)','FontSize', 25)
set(gca,'FontSize',25)
hold on

subplot(3,7,[17 19])
plot((xx-angl_deduction),Y(:,6),'b-','LineWidth',2)
xlim([170 550])
grid on
xlabel('Crank Angle (deg.)','FontSize', 25)
ylabel('M_c_o_l_d (kg)','FontSize', 25)
set(gca,'FontSize',25)
hold on

subplot(3,7,[3 5])
plot((xx-angl_deduction),Y(:,9),'b-','LineWidth',2)
xlim([170 550])
grid on
ylabel('M_h_o_t (kg)','FontSize', 25)
set(gca,'FontSize',25)
hold on

end
%% _____Step
2_____

options = odeset('AbsTol',1e-19,'RelTol',1e-19);
[t2,Z]=ode45('step1b',[avg p*pi/w],[Y(end,1) Y(end,2) Y(end,3) Y(end,4) ...
    Y(end,5) Y(end,6) Y(end,7) Y(end,8) Y(end,9) Y(end,10) Y(end,11) ...
    Y(end,12)],options);

rr=(t2*w+pi)*180/pi;

if (H==Cycles_number)

figure(1)
plot((rr-angl_deduction),Z(:,1),'-','LineWidth',2)
hold on

figure(2)
plot((rr-angl_deduction),Z(:,2),'-','LineWidth',2)
hold on

figure(3)
plot((rr-angl_deduction),-Z(:,3),'-','LineWidth',2)

```

```

hold on

figure(4)
plot((rr-angl_deduction),Z(:,4),'-', 'LineWidth',2)
hold on

figure(5)
plot((rr-angl_deduction),Z(:,5),'-', 'LineWidth',2)
hold on

figure(6)
plot((rr-angl_deduction),Z(:,6),'-', 'LineWidth',2)
hold on

figure(7)
plot((rr-angl_deduction),Z(:,7),'-', 'LineWidth',2)
hold on

figure(8)
plot((rr-angl_deduction),Z(:,8),'-', 'LineWidth',2)
hold on

figure(9)
plot((rr-angl_deduction),Z(:,9),'-', 'LineWidth',2)
hold on

figure(10)
plot((rr-angl_deduction),Z(:,10),'-', 'LineWidth',2)
hold on

figure(11)
plot((rr-angl_deduction),Z(:,11),'-', 'LineWidth',2)
hold on

figure(16)
plot(Z(:,1)./Z(:,2),Z(:,5),'b-', 'LineWidth',1)
hold on

figure(17)
plot(Z(:,12),Z(:,4),'b-', 'LineWidth',2)
hold on

% Entropy proof
for i=2:length(Z(:,4))
    dT(i-1)=Z(i,4)-Z(i-1,4);

```

```

    dP(i-1)=Z(i,5)-Z(i-1,5);
    ds(i-1)=(Cp./Z(i,4)).*dT(i-1)-(R_gas./Z(i,5)).*dP(i-1);
end
ds_new=zeros(1,length(rr));

for i=2:length(rr)
    ds_new(i)=ds(i-1);
end
figure(18)
subplot(2,3,2)
plot((rr-angl_deduction),ds_new,'-', 'LineWidth',2)
hold on
grid on
grid minor

subplot(2,3,5)
plot((rr-angl_deduction),Z(:,12),'-', 'LineWidth',2)
grid on
grid minor
hold on

figure(19)
subplot(3,7,[10 12])
plot((rr-angl_deduction),Z(:,5),'b-', 'LineWidth',2)
hold on

subplot(3,7,[17 19])
plot((rr-angl_deduction),Z(:,8),'b-', 'LineWidth',2)
hold on

subplot(3,7,[3 5])
plot((rr-angl_deduction),Z(:,11),'b-', 'LineWidth',2)
hold on

figure(20)
subplot(3,7,[10 12])
plot((rr-angl_deduction),Z(:,4),'b-', 'LineWidth',2)
hold on

subplot(3,7,[17 19])
plot((rr-angl_deduction),Z(:,7),'b-', 'LineWidth',2)
hold on

subplot(3,7,[3 5])
plot((rr-angl_deduction),Z(:,10),'b-', 'LineWidth',2)

```

```

hold on

figure(21)
subplot(3,7,[10 12])
plot((rr-angl_deduction),Z(:,2),'b-','LineWidth',2)
hold on

subplot(3,7,[17 19])
plot((rr-angl_deduction),Z(:,6),'b-','LineWidth',2)
hold on

subplot(3,7,[3 5])
plot((rr-angl_deduction),Z(:,9),'b-','LineWidth',2)
hold on
end

%% _____ Step 3 and
4_____

options = odeset('AbsTol',1e-19,'RelTol',1e-19);

[t3,X]=ode45('step2',[p*pi/w k*pi/w],[Z(end,1) Z(end,2) Z(end,3)...
    Z(end,4) Z(end,5) Z(end,6) Z(end,7) Z(end,8) Z(end,9) Z(end,10)...
    Z(end,11) Z(end,12)],options);

yy=(t3*w+pi)*180/pi;

if (H==Cycles_number)

figure(1)
plot((yy-angl_deduction),X(:,1),'--','LineWidth',2)
hold on
legend('BDC to 270^{o}','270^{o} to TDC','TDC to BDC')
figure(2)
plot((yy-angl_deduction),X(:,2),'--','LineWidth',2)
hold on
legend('BDC to 270^{o}','270^{o} to TDC','TDC to BDC')
figure(3)
plot((yy-angl_deduction),-X(:,3),'--','LineWidth',2)
hold on
legend('BDC to 270^{o}','270^{o} to TDC','TDC to BDC')
figure(4)
plot((yy-angl_deduction),X(:,4),'--','LineWidth',2)
hold on
legend('BDC to 270^{o}','270^{o} to TDC','TDC to BDC')

```

```

figure(5)
plot((yy-angl_deduction),X(:,5),'--','LineWidth',2)
hold on
legend('BDC to 270^{o}','270^{o} to TDC','TDC to BDC')
figure(6)
plot((yy-angl_deduction),X(:,6),'--','LineWidth',2)
hold on
legend('BDC to 270^{o}','270^{o} to TDC','TDC to BDC')
figure(7)
plot((yy-angl_deduction),X(:,7),'--','LineWidth',2)
hold on
legend('BDC to 270^{o}','270^{o} to TDC','TDC to BDC')
figure(8)
plot((yy-angl_deduction),X(:,8),'--','LineWidth',2)
hold on
legend('BDC to 270^{o}','270^{o} to TDC','TDC to BDC')
figure(9)
plot((yy-angl_deduction),X(:,9),'--','LineWidth',2)
hold on
legend('BDC to 270^{o}','270^{o} to TDC','TDC to BDC')
figure(10)
plot((yy-angl_deduction),X(:,10),'--','LineWidth',2)
hold on
legend('BDC to 270^{o}','270^{o} to TDC','TDC to BDC')
figure(11)
plot((yy-angl_deduction),X(:,11),'--','LineWidth',2)
hold on
legend('BDC to 270^{o}','270^{o} to TDC','TDC to BDC')

figure(16)
plot(X(:,1)/X(:,2),X(:,5),'b-','LineWidth',1)
hold on
figure(17)
plot(X(:,12),X(:,4),'b-','LineWidth',2)
hold on

% Entropy proof
for i=2:length(X(:,4))
    dT(i-1)=X(i,4)-X(i-1,4);
    dP(i-1)=X(i,5)-X(i-1,5);
    ds(i-1)=(Cp./X(i,4)).*dT(i-1)-(R_gas./X(i,5)).*dP(i-1);
end
ds_new=zeros(1,length(yy));

for i=2:length(yy)

```

```

    ds_new(i)=ds(i-1);
end
figure(18)
subplot(2,3,2)
plot((yy-angl_deduction),ds_new,'-', 'LineWidth',2)
hold on
grid on
grid minor

subplot(2,3,5)
plot((yy-angl_deduction),X(:,12),'-', 'LineWidth',2)
grid on
grid minor
hold on

figure(19)
subplot(3,7,[10 12])
plot((yy-angl_deduction),X(:,5),'b-', 'LineWidth',2)
hold on

subplot(3,7,[17 19])
plot((yy-angl_deduction),X(:,8),'b-', 'LineWidth',2)
hold on

subplot(3,7,[3 5])
plot((yy-angl_deduction),X(:,11),'b-', 'LineWidth',2)
hold on

figure(20)
subplot(3,7,[10 12])
plot((yy-angl_deduction),X(:,4),'b-', 'LineWidth',2)
hold on

subplot(3,7,[17 19])
plot((yy-angl_deduction),X(:,7),'b-', 'LineWidth',2)
hold on

subplot(3,7,[3 5])
plot((yy-angl_deduction),X(:,10),'b-', 'LineWidth',2)
hold on

figure(21)
subplot(3,7,[10 12])
plot((yy-angl_deduction),X(:,2),'b-', 'LineWidth',2)

```



```

hold on

subplot(3,7,[17 19])
plot((yy-angl_deduction),X(:,6),'b-', 'LineWidth',2)
hold on

subplot(3,7,[3 5])
plot((yy-angl_deduction),X(:,9),'b-', 'LineWidth',2)
hold on

end
% Updating initial conditions to restart the for-loop:
time0=(k*pi)/w;
Vmax=X(end,1);
Mcy11=X(end,2);
L=0;
Tcy11=X(end,4);
Pcy11=X(end,5);
Mcr1=X(end,6);
Tcr1=X(end,7);
Pcr1=X(end,8);
Mhot1=X(end,9);
Thot1=X(end,10);
Phot1=X(end,11);
Entropy_init=X(end,12);
% Updating time variables
p=p+2;
k=k+2;

end
%% end of script

```

B. Gen III b - Dynamic Model

MATLAB Function (Step 1):

```

function f = step1(t,y)
%% This corresponds to the first half of the upstroke (step 1)
f=zeros(14,1);
global Vmin;% min volume
global rc;% compression ratio
global R;% ratio of connecting rod length to crank radius
global w;% rpm (rad/sec)

```

```

global R_gas;% gas constant
global Cp;% specific heat at constant pressure
global Cv;% specific heat at constant volume
global A_cr;% cold reservoir area
global gamma;
global n; % number of upper slits
global T_s_hot;
global T_s_cold;
global h_conv;
global ha;
global ca;
global CD; % Coefficient of Discharge

%% If Pcold >= Pcyl

if( (y(8)>=y(5)) && (y(5)<y(11)) )
m=w*t+pi;
f(1,1)=Vmin*(rc-1)*0.5*(w*sin(m)+(w*sin(m)*cos(m)/...
(sqrt((R^2)-((sin(m))^2 ))));% dV

if((y(8)>y(5)))
P_s=0.528*y(8);
if (y(5)<P_s)%choked
flow=CD*A_cr*sqrt( gamma*(y(8)*y(8)/(R_gas*y(7)))*...
( 2/(gamma+1))^( ( gamma+1 )/(gamma-1)));%choked
else%unchoked
c=((( y(5)/y(8))^ ( 2/gamma ) ) ...
- ( ( y(5)/y(8))^((gamma+1)/gamma ) ) );
flow=CD*A_cr*sqrt((2*y(8)*y(8)/(R_gas* y(7)))*...
(gamma)/(gamma-1))*c;%unchoked
end
else
flow=0;
end

%% Qdot
Qdot_h=h_conv*ha*(T_s_hot-y(10));% W
Qdot_c=h_conv*ca*(T_s_cold-y(7));

% Working Cylinder
f(2,1)=n*flow;% mass rate into cylinder
f(3,1)=abs((y(5))*f(1,1));% work on cylinder
f(4,1)=(1/(y(2)*(Cp-R_gas)))*(f(3,1) +f(2,1)*...
(Cp*y(7)-Cp*y(4)+R_gas*y(4)));%dT of cylinder
f(5,1)=(f(2,1)*R_gas*y(4)+y(2)*R_gas*f(4,1)-y(5)*f(1,1))/y(1);%dP cylinder

```

```

% Cold Reservoir
f(6,1)=-n*flow;% flow of cold reservoir
f(7,1)=(f(6,1)*R_gas*y(7)+Qdot_c)/(y(6)*(Cp-R_gas));% dT of cold reservoir
f(8,1)=y(8)*((f(6,1)/y(6))+(f(7,1)/y(7)));% dP of cold reservoir

% Hot Reservoir
f(9,1)=0;% flow in/out hot reservoir
f(10,1)=Qdot_h/(y(9)*Cv);% dT of hot reservoir
f(11,1)=y(11)*(f(10,1)/y(10));% dP of hot reservoir
f(12,1)=Qdot_h;
f(13,1)=Qdot_c;

% Cylinder specific entropy
f(14,1)=(Cp/y(4))*f(4,1) -(R_gas/y(5))*f(5,1);

end

%% If P_cyl > P_cold
if( (y(5)>y(8)) && (y(5)<y(11)) )

m=w*t+pi;
f(1,1)=Vmin*(rc-1)*0.5*(w*sin(m)+(w*sin(m)*cos(m)...
/(sqrt((R^2)-((sin(m))^2 ))));% dV

P_s=0.528*y(5);
if (y(8)<P_s)% choked
    flow=CD*A_cr*sqrt( gamma*(y(5)*y(5)/(R_gas*y(4)))*...
    ( 2/(gamma+1))^ ( ( gamma+1)/(gamma-1)));% choked
else% unchoked
    c=((( y(8)/y(5) )^( 2/gamma ))-(y(8)/y(5))^((gamma+1)/gamma));
    flow=CD*A_cr*sqrt((2*y(5)*y(5)/(R_gas* y(4)))...
    *(gamma /(gamma-1))*c);% unchoked
end

%% Qdot
Qdot_h=h_conv*ha*(T_s_hot-y(10));% W
Qdot_c=h_conv*ca*(T_s_cold-y(7));

% Working Cylinder
f(2,1)=-n*flow;% mass rate into cylinder
f(3,1)=abs((y(5))*f(1,1));% work on cylinder
f(4,1)=(1/(y(2)*(Cp-R_gas)))*(f(3,1)+f(2,1)*R_gas*y(4));% dT of cylinder
f(5,1)=(f(2,1)*R_gas*y(4)+y(2)*R_gas*f(4,1)-y(5)*f(1,1))/y(1);% dP cylinder

```

```

%Cold Reservoir
f(6,1)=n*flow;% flow of cold reservoir
f(7,1)=(f(6,1)*(R_gas*y(7)+Cp*y(4)-Cp*y(7))+Qdot_c)...
/(y(6)*(Cp-R_gas));% dT cold reservoir
f(8,1)=y(8)*((f(6,1)/y(6))+(f(7,1)/y(7)));% dP of cold reservoir

%Hot Reservoir
f(9,1)=0;% flow in/out hot reservoir
f(10,1)=Qdot_h/(y(9)*Cv);% dT of hot reservoir
f(11,1)=y(11)*(f(10,1)/y(10));% dP of hot reservoir
f(12,1)=Qdot_h;
f(13,1)=Qdot_c;
%Cylinder specific entropy
f(14,1)=(Cp/y(4))*f(4,1) -(R_gas/y(5))*f(5,1);

end

```

MATLAB Function (Step 2)

```

function f = step2(t,y)
%% This corresponds to the second half of the upstroke (step 2)

f=zeros(14,1);
global Vmin;% min volume
global rc;% compression ratio
global R;% ratio of connecting rod length to crank radius
global w;% rpm (rad/sec)
global R_gas;% gas constant
global Cp;% specific heat at constant pressure
global Cv;% specific heat at constant volume
global A_h;% hot reservoir area
global gamma;
global n;% number of upper slits
global T_s_hot;
global T_s_cold;
global h_conv;
global h_conv2;
global ha;
global ca;
global CD;% Coefficient of Discharge

m=w*t+pi;
f(1,1)=Vmin*(rc-1)*0.5*(w*sin(m)+(w*sin(m))*cos(m)...

```

```

/(sqrt((R^2)-((sin(m))^2 ))));%dV

if (y(5)>y(11))

P_s=0.528*y(5);
if (y(11)<P_s)%choked
    flow=CD*A_h*sqrt( gamma*(y(5)*y(5)/(R_gas*y(4)))*...
        ( 2/(gamma+1))^(( gamma+1 )/(gamma-1)));%choked
else%unchoked
    c=(( ( y(11)/y(5))^ ( 2/gamma))-((y(11)/y(5))^((gamma+1)/gamma)));
    flow=CD*A_h*sqrt((2*y(5)*y(5)/(R_gas* y(4)))*...
        (gamma /(gamma-1))*c);%unchoked
end
else
    flow=0;
end

%% Qdot
Qdot_h=h_conv*ha*(T_s_hot-y(10));%W
Qdot_c=h_conv2*ca*(T_s_cold-y(7));

% Working Cylinder
f(2,1)=-n*flow;%mass rate into cylinder
f(3,1)=abs((y(5))*f(1,1));%work on cylinder
f(4,1)=(1/(y(2)*(Cp-R_gas)))*(f(3,1)+f(2,1)*R_gas*y(4));%dT of cylinder
f(5,1)=(f(2,1)*R_gas*y(4)+y(2)*R_gas*f(4,1)-y(5)*f(1,1))/y(1);%dP cylinder

% Cold Reservoir
f(6,1)=0;%flow of cold reservoir
f(7,1)=Qdot_c/(y(6)*Cv);%dT of cold reservoir
f(8,1)=y(8)*(f(7,1)/y(7));%dP of cold reservoir

% Hot Reservoir
f(9,1)=n*flow;%flow in/out hot reservoir
f(10,1)=(f(9,1)*(R_gas*y(10)+Cp*y(4)-Cp*y(10))+Qdot_h)/...
    (y(9)*(Cp-R_gas));%dT of hot reservoir
f(11,1)=y(11)*((f(9,1)/y(9))+f(10,1)/y(10));%dP of hot reservoir
f(12,1)=Qdot_h;
f(13,1)=Qdot_c;

% Cylinder specific entropy
f(14,1)=(Cp/y(4))*f(4,1) -(R_gas/y(5))*f(5,1);

```

MATLAB Function (Step 3 and 4)

```

function f = step3(t,y)
%% This corresponds to the downstroke (step 3 and 4)
f=zeros(14,1);
global Vmin;% min volume
global rc;% compression ratio
global R;% ratio of connecting rod length to crank radius
global w;% rpm (rad/sec)
global R_gas;% gas constant
global Cp;% specific heat at constant pressure
global Cv;% specific heat at constant volume
global A_h;% cold reservoir area
global gamma;
global n; % number of upper slits
global Mhot1;
global T_s_hot;% wall surface temperature
global T_s_cold;% wall surface temperature
global h_conv;% Convective heat transfer coefficient (forced convection)
global h_conv2;% Convective heat transfer coefficient (free convection)
global ha;
global ca;
global CD; % Coefficient of Discharge

m=w*t+pi;
f(1,1)=Vmin*(rc-1)*0.5*(w*sin(m)+(w*sin(m)*cos(m)/(sqrt((R^2)-...
((sin(m))^2 ))));% dV
if(y(11)>y(5)&&(y(9)>Mhot1))
P_s=0.528*y(11);
if (y(5)<P_s)%choked
flow=CD*A_h*sqrt( gamma*(y(11)*y(11)/(R_gas*y(10)))*...
( 2/(gamma+1))^ ( gamma+1 )/(gamma-1));%choked
else%unchoked
c=(( ( y(5)/y(11))^ ( 2/gamma))-(( y(5)/y(11))^((gamma+1)/gamma)));
flow=CD*A_h*sqrt((2*y(11)*y(11)/(R_gas* y(10) ))*...
(gamma /(gamma-1))*c);%unchoked
end
else
flow=0;
end

%% Qdot
Qdot_h=h_conv*ha*(T_s_hot-y(10));% W
Qdot_c=h_conv2*ca*(T_s_cold-y(7));

```

```

% Working Cylinder
f(2,1)=n*flow;% mass rate into cylinder
f(3,1)=-abs((y(5))*f(1,1));% work on cylinder
f(4,1)=(1/(y(2)*(Cp-R_gas)))*(f(3,1)+f(2,1)*...
    (Cp*y(10)-Cp*y(4)+R_gas*y(4)));% dT of cylinder
f(5,1)=(f(2,1)*R_gas*y(4)+y(2)*R_gas*f(4,1)-y(5)*f(1,1))/y(1);% dP cylinder

% Cold Reservoir
f(6,1)=0;% flow of cold reservoir
f(7,1)=Qdot_c/(y(6)*Cv);% dT of cold reservoir
f(8,1)=y(8)*((f(7,1)/y(7)));% dP of cold reservoir

% Hot Reservoir
f(9,1)=-n*flow;% flow out of hot reservoir
f(10,1)=(f(9,1)*R_gas*y(10)+Qdot_h)/(y(9)*(Cp-R_gas));% dT of hot reservoir
f(11,1)=y(11)*((f(9,1)/y(9))+f(10,1)/y(10));% dP of hot reservoir
f(12,1)=Qdot_h;
f(13,1)=Qdot_c;

% Cylinder specific entropy
f(14,1)=(Cp/y(4))*f(4,1)-(R_gas/y(5))*f(5,1);

```

MATLAB Main Script:

```

% Wiam Attar
clc
clear all;
format long
%%

```

Variables

```

-
global Vmin;% min volume (m^3)
global Vmax;% maximum working volume (m^3)
global rc;% compression ratio
global R;% ratio of connecting rod length to crank radius
global a;% Crank radius
global l;% Connecting rod length
global w;% rpm (rad/sec)
global R_gas;% gas constant
global gamma;% ratio of specific heats
global Cp;% specific heat at constant pressure
global Cv;% specific heat at constant volume
global A_cr;% cold reservoir area

```

```

global A_h;%hot reservoir area
global n; %number of upper slits
global Mhot1;% Initial Mass in Hot Reservoir
global Kb;% Boltzmann Constant (J/K)
global h;%Planck's Constant (J.s)
global Na;%Avogadro's Number (particles/mole)
global Mcr1;%initial mass in cold reservoir (kg)
global e;% 2.718281828459046
global kk;%constant 1.38044e-16
global M;% Molar Mass g/mole
global w_el;% Electronic degeneracy
global sigma_r; %Rotational Temperature (K)
global D0; %Dissociation Energy (erg)
global sigma_v; %Vibrational Temperature (K)
global mp;%mass of one molecule (kg/molecule)
global T_s_hot;
global T_s_cold;
global h_conv;% Forced convection coeff
global h_conv2;% Free convection coeff
global CD; %Coefficient of Discharge
global ha;
global ca;

```

```
%%
```

Inputs

```

rc=7;
Pcr1=1.5e+06;
Vmin=70e-06;%m^3
Vmax=rc*Vmin;
Vcr=1000e-06;
Vhot=Vcr;
CD=0.61;% Coefficient of Discharge (1 or 0.61)

% Air Gas Properties
R_gas=287;
gamma=1.4;
Cp=1005;
Cv=718;
mp=4.65e-26;%mass of one molecule (kg/molecule)
M=28;% Molar Mass
w_el=1;
sigma_r=2.89;
D0=9.76*1.602e-12;
sigma_v=3390;

```



```

%% -----
Tcr1=300;% initial temperature of cold reservoir
Phot1=9e+06;% initial hot reservoir pressure
Thot1=1200;% initial hot reservoir temperature
Pcyl1=0.2e+06;% starting pressure at BDC
Tcyl1=273.15;% starting temperature at BDC
T_s_hot=1300;
T_s_cold=260;
h_conv=230;

cd=0.02;% cold pipe diameter
sep_c=1.1*cd-cd;% distance between pipes
for nc=5:5:1000
    Total_Area_c=((nc*cd)+(nc+1)*(sep_c))^2;
    fluid_Area_c=Total_Area_c-((nc^2)*(pi*(cd/2)^2));
    Total_res_depth_c=Vcr/fluid_Area_c;
    if (Total_res_depth_c<0.5)
        break
    end
end
cl=Total_res_depth_c*nc^2;

hd=0.02;
sep_h=1.1*hd-hd;
for nh=5:5:1000
    Total_Area_h=((nh*hd)+(nh+1)*(sep_h))^2;
    fluid_Area_h=Total_Area_h-((nh^2)*(pi*(hd/2)^2));
    Total_res_depth_h=Vhot/fluid_Area_h;
    if (Total_res_depth_h<0.5)
        break
    end
end
hl=Total_res_depth_h*nh^2;
w=1800*2*pi/60;% rad/sec
h_conv2=30;
ha=pi*hd*hl;
ca=pi*cd*cl;

% Number of slits is the same for cold and hot reservoirs connection
n=30;
% Area of each hot reservoir's slit
A_h=(2e-05);
% Area of each cold reservoir's slit
A_cr=(8e-04)/30;

```

```

% Geometric Dimension
a=0.2;%crank radius
l=0.25;%connecting rod length
% Constants
Kb=1.38064852e-23;%Boltzman Constant (J/K)
h=6.626070040e-34;%Planck's Constant (J.s)
Na=6.0221409e+23;%Avogadros
e=2.7182818;
kk=1.38044e-16;

% Cold Reservoir Initial Conditions
Mcr1=Pcr1*Vcr/(R_gas*Tcr1);%initial mass in cold reservoir
% Working Cylinder Initial Conditions
Vcyl1=Vmax;%Volume at BDC;
Mcy11=Pcyl1*Vcyl1/(R_gas*Tcyl1);%mass in working cylinder
% Hot Reservoir Initial Conditions
Mhot1=Phot1*Vhot/(R_gas*Thot1);%initial mass in hot reservoir
%calculating the ratio of connecting rod length to crank radius:
R=l/a;
% Additional Integration Variables
time0=0;%initial start time of the cycle
L=0; %Initial Net Work Ouput Value at the start
k=2;% Additional Variable that will help calculate the start time ...
...of every cycle__t=(theta-pi)/w
p=1;% Additional Variable that will help calculate the time at ...
...TDC __t=(theta-pi)/w__ where t=pi/w,3pi/w,5pi/w,etc...
%%

Abstol=1e-05;
RelTol=1e-05;

% Calculating Entropy IC
K_boltzmann=(1.38e-23);
ratio_ent=1./(Pcyl1./(K_boltzmann*Tcyl1));
m_ent=(0.79*28+0.21*32)*0.001/(6.022e+23);
N_ent=Pcyl1.*Vcyl1./(K_boltzmann*Tcyl1);%number of molecules
h_ent=6.626e-34;
log_ent=log(((2*pi*m_ent*K_boltzmann.*Tcyl1...
/(h_ent^2)).^(1.5)).*(ratio_ent));
Entropy1_in=N_ent.*K_boltzmann.*(3.5+ log_ent+log(Tcyl1/5.78)+...
(3390./Tcyl1).*((exp(-3390./Tcyl1))./(1-exp(-3390./Tcyl1)))...
-log(1-(exp(-3390./Tcyl1)))+log(1));
Entropy1_init=Entropy1_in/Mcy11;

```

```
%%
```

```
Step1
```

```
Length=70;% Number of cycles  
for H=1:Length
```

```
% The time when cold reservoir Interaction with the working cylinder stops  
avg=0.5*(time0+(p*pi/w)); %the interaction with the cold reservoir ...  
...stops midway through the upstroke
```

```
options = odeset('AbsTol',Abstol,'RelTol',RelTol);  
[t1,Y]=ode45('step1',[time0 avg],[Vmax M cyl1 L T cyl1 P cyl1 M cr1 T cr1 ...  
P cr1 M hot1 T hot1 P hot1 L L Entropy1_init],options);
```

```
xx=(t1*w+pi)*180/pi;
```

```
if H==Length-1
```

```
figure(19)  
plot((xx-((H-1)*360)),Y(:,2),'LineWidth',2)  
set(gca,'FontSize',25)  
title('Mass in Working Cylinder vs. Crank Angle');  
xlabel('Angle (deg.)')  
ylabel('Mass in Working Cylinder (kg)')  
hold on
```

```
figure(22)  
plot((xx-((H-1)*360)), -Y(:,3)*30,'LineWidth',2)  
set(gca,'FontSize',25)  
title('Power Ouput vs. Crank Angle');  
xlabel('Angle (deg.)')  
ylabel('Power Ouput (Watts)')  
hold on
```

```
figure(23)  
plot((xx-((H-1)*360)),Y(:,4),'LineWidth',2)  
% title('Temperature in Working Cylinder vs. Crank Angle');  
xlabel('Angle (deg.)')  
ylabel('Temperature (K)')  
set(gca,'FontSize',25)
```

```
hold on
```

```
figure(24)  
plot((xx-((H-1)*360)),Y(:,5),'LineWidth',2)  
set(gca,'FontSize',25)  
title('Pressure in Working Cylinder vs. Crank Angle');
```

```

xlabel('Angle (deg.)')
ylabel('Pressure (pa)')
hold on
figure(25)
plot((xx-((H-1)*360)),Y(:,6),'LineWidth',2)
set(gca,'FontSize',25)
title('Mass in Cold Reservoir vs. Crank Angle');
xlabel('Angle (deg.)')
ylabel('Mass (kg)')
hold on
figure(26)
plot((xx-((H-1)*360)),Y(:,7),'LineWidth',2)
set(gca,'FontSize',25)
title('Tempearature in Cold Reservoir vs. Crank Angle');
xlabel('Angle (deg.)')
ylabel('Temperature (K)')
hold on
figure(27)
plot((xx-((H-1)*360)),Y(:,8),'LineWidth',2)
set(gca,'FontSize',25)
title('Pressure in Cold Reservoir vs. Crank Angle');
xlabel('Angle (deg.)')
ylabel('Pressure (pa)')
hold on
figure(28)
plot((xx-((H-1)*360)),Y(:,9),'LineWidth',2)
set(gca,'FontSize',25)
title('Mass in Hot Reservoir vs. Crank Angle');
xlabel('Angle (deg.)')
ylabel('Mass (kg)')
hold on
figure(29)
plot((xx-((H-1)*360)),Y(:,10),'LineWidth',2)
set(gca,'FontSize',25)
title('Temperature in Hot Reservoir vs. Crank Angle');
xlabel('Angle (deg.)')
ylabel('Temperature (K)')
hold on
figure(30)
plot((xx-((H-1)*360)),Y(:,11),'LineWidth',2)
set(gca,'FontSize',25)
title('Pressure in Hot Reservoir vs. Crank Angle');
xlabel('Angle (deg.)')
ylabel('Pressure (pa)')
hold on
figure(31)

```

```

plot(Y(:,1)./Y(:,2),Y(:,5),'LineWidth',2)
set(gca,'FontSize',25)
title('Working Cylinder P-V Diagram');
xlabel('V (m3)')
ylabel('Pressure (pa)')
hold on

figure(32)
plot(Y(:,14),Y(:,4),'LineWidth',2)
hold on

figure(33)
plot((xx-((H-1)*360)),Y(:,12),'LineWidth',2)
set(gca,'FontSize',25)
title('Q in Hot Reservoir vs. Crank Angle');
hold on
figure(34)
plot((xx-((H-1)*360)),Y(:,13),'LineWidth',2)
set(gca,'FontSize',25)
title('Q in Cold Reservoir vs. Crank Angle');
hold on

end

%% _____ Step
2_____

options = odeset('AbsTol',Abstol,'RelTol',RelTol);
[t2,Z]=ode45('step2',[avg p*pi/w],[Y(end,1) Y(end,2) Y(end,3) Y(end,4) ...
    Y(end,5) Y(end,6) Y(end,7) Y(end,8) Y(end,9) Y(end,10) Y(end,11) ...
    Y(end,12) Y(end,13) Y(end,14)],options);

rr=(t2*w+pi)*180/pi;

if H==Length-1

mass2=Z(:,2);
figure(19)
plot((rr-((H-1)*360)),mass2,'LineWidth',2)
set(gca,'FontSize',25)
title('Mass in Working Cylinder vs. Crank Angle');
xlabel('Angle (deg.)')
ylabel('Mass in Working Cylinder (kg)')
hold on

figure(22)

```

```

plot((rr-((H-1)*360)),Z(:,3)*30,'LineWidth',2)
set(gca,'FontSize',25)
title('Power Ouput vs. Crank Angle');
xlabel('Angle (deg.)')
ylabel('Power Ouput (Watts)')
hold on

```

```

figure(23)
plot((rr-((H-1)*360)),Z(:,4),'LineWidth',2)
hold on

```

```

figure(24)
plot((rr-((H-1)*360)),Z(:,5),'LineWidth',2)
set(gca,'FontSize',25)
title('Pressure in Working Cylinder vs. Crank Angle');
xlabel('Angle (deg.)')
ylabel('Pressure (pa)')
hold on

```

```

figure(25)
plot((rr-((H-1)*360)),Z(:,6),'LineWidth',2)
set(gca,'FontSize',25)
title('Mass in Cold Reservoir vs. Crank Angle');
xlabel('Angle (deg.)')
ylabel('Mass (kg)')
hold on

```

```

figure(26)
plot((rr-((H-1)*360)),Z(:,7),'LineWidth',2)
set(gca,'FontSize',25)
title('Tempearature in Cold Reservoir vs. Crank Angle');
xlabel('Angle (deg.)')
ylabel('Temperature (K)')
hold on

```

```

figure(27)
plot((rr-((H-1)*360)),Z(:,8),'LineWidth',2)
set(gca,'FontSize',25)
title('Pressure in Cold Reservoir vs. Crank Angle');
xlabel('Angle (deg.)')
ylabel('Pressure (pa)')
hold on

```

```

figure(28)
plot((rr-((H-1)*360)),Z(:,9),'LineWidth',2)
set(gca,'FontSize',25)
title('Mass in Hot Reservoir vs. Crank Angle');
xlabel('Angle (deg.)')
ylabel('Mass (kg)')
hold on

```

```

figure(29)
plot((rr-((H-1)*360)),Z(:,10),'LineWidth',2)
set(gca,'FontSize',25)
title('Temperature in Hot Reservoir vs. Crank Angle');
xlabel('Angle (deg.)')
ylabel('Temperature (K)')
hold on
figure(30)
plot((rr-((H-1)*360)),Z(:,11),'LineWidth',2)
set(gca,'FontSize',25)
title('Pressure in Hot Reservoir vs. Crank Angle');
xlabel('Angle (deg.)')
ylabel('Pressure (pa)')
hold on

figure(31)
plot(Z(:,1)./Z(:,2),Z(:,5),'LineWidth',2)
set(gca,'FontSize',25)
title('Working Cylinder P-V Diagram');
xlabel('V (m^{3})')
ylabel('Pressure (pa)')
hold on

figure(32)
plot(Z(:,14),Z(:,4),'LineWidth',2)
hold on

figure(33)
plot((rr-((H-1)*360)),Z(:,12),'LineWidth',2)
hold on
figure(34)
plot((rr-((H-1)*360)),Z(:,13),'LineWidth',2)
hold on

end

%% _____ Step 3 and
4 _____

options = odeset('AbsTol',Abstol,'RelTol',RelTol);
[t3,X]=ode45('step3',[p*pi/w k*pi/w],[Z(end,1) Z(end,2) Z(end,3) ...
    Z(end,4) Z(end,5) Z(end,6) Z(end,7) Z(end,8) Z(end,9) Z(end,10)...
    Z(end,11) Z(end,12) Z(end,13) Z(end,14)],options);

yy=(t3*w+pi)*180/pi;

```

```

if H==Length-1

figure(19)
plot((yy-((H-1)*360)),X(:,2),'LineWidth',2)
set(gca,'FontSize',25)
title('M_C_y_1 vs. Crank Angle');
xlabel('Angle (deg.)')
ylabel('Mass in Working Cylinder (kg)')
xlim([min((xx-((H-1)*360))) max((yy-((H-1)*360)))]])
hold on

figure(22)
plot((yy-((H-1)*360)),-X(:,3)*30,'LineWidth',2)
set(gca,'FontSize',25)
title('Power Ouput vs. Crank Angle');
xlabel('Angle (deg.)')
ylabel('Power Ouput (Watts)')
xlim([min((xx-((H-1)*360))) max((yy-((H-1)*360)))]])
hold on

figure(23)
plot((yy-((H-1)*360)),X(:,4),'LineWidth',2)
xlim([min((xx-((H-1)*360))) max((yy-((H-1)*360)))]])
hold on

figure(24)
plot((yy-((H-1)*360)),X(:,5),'LineWidth',2)
set(gca,'FontSize',25)
title('Pressure in Working Cylinder vs. Crank Angle');
xlabel('Angle (deg.)')
ylabel('Pressure (pa)')
xlim([min((xx-((H-1)*360))) max((yy-((H-1)*360)))]])
hold on
figure(25)
plot((yy-((H-1)*360)),X(:,6),'LineWidth',2)
set(gca,'FontSize',25)
title('Mass in Cold Reservoir vs. Crank Angle');
xlabel('Angle (deg.)')
ylabel('Mass (kg)')
xlim([min((xx-((H-1)*360))) max((yy-((H-1)*360)))]])
hold on
figure(26)

```



```

plot((yy-((H-1)*360)),X(:,7),'LineWidth',2)
set(gca,'FontSize',25)
title('Temperature in Cold Reservoir vs. Crank Angle');
xlabel('Angle (deg.)')
ylabel('Temperature (K)')
xlim([min((xx-((H-1)*360))) max((yy-((H-1)*360)))]])
hold on
figure(27)
plot((yy-((H-1)*360)),X(:,8),'LineWidth',2)
set(gca,'FontSize',25)
title('Pressure in Cold Reservoir vs. Crank Angle');
xlabel('Angle (deg.)')
ylabel('Pressure (pa)')
xlim([min((xx-((H-1)*360))) max((yy-((H-1)*360)))]])
hold on
figure(28)
plot((yy-((H-1)*360)),X(:,9),'LineWidth',2)
set(gca,'FontSize',25)
title('Mass in Hot Reservoir vs. Crank Angle');
xlabel('Angle (deg.)')
ylabel('Mass (kg)')
xlim([min((xx-((H-1)*360))) max((yy-((H-1)*360)))]])
hold on
figure(29)
plot((yy-((H-1)*360)),X(:,10),'LineWidth',2)
set(gca,'FontSize',25)
title('Temperature in Hot Reservoir vs. Crank Angle');
xlabel('Angle (deg.)')
ylabel('Temperature (K)')
xlim([min((xx-((H-1)*360))) max((yy-((H-1)*360)))]])
hold on
figure(30)
plot((yy-((H-1)*360)),X(:,11),'LineWidth',2)
set(gca,'FontSize',25)
title('Pressure in Hot Reservoir vs. Crank Angle');
xlabel('Angle (deg.)')
ylabel('Pressure (pa)')
xlim([min((xx-((H-1)*360))) max((yy-((H-1)*360)))]])
hold on
figure(31)
plot(X(:,1)./X(:,2),X(:,5),'LineWidth',2)
set(gca,'FontSize',25)
title('Working Cylinder P-V Diagram');
xlabel('V (m3)')
ylabel('Pressure (pa)')
hold on

```

```

figure(32)
plot(X(:,14),X(:,4),'LineWidth',2)
hold on

figure(33)
plot((yy-((H-1)*360)),X(:,12),'LineWidth',2)
hold on
figure(34)
plot((yy-((H-1)*360)),X(:,13),'LineWidth',2)
hold on
end
% Updating initial conditions to restart the for-loop:
time0=(k*pi)/w;
Vmax=X(end,1);
Mcy11=X(end,2);
L=0;
Tcy11=X(end,4);
Pcy11=X(end,5);
Mcr1=X(end,6);
Tcr1=X(end,7);
Pcr1=X(end,8);
Mhot1=X(end,9);
Thot1=X(end,10);
Phot1=X(end,11);
Entropy1_init=X(end,14);
% Updating time variables
p=p+2;
k=k+2;

end

```

C. Gen III c - Dynamic Model

MATLAB Function (Step 1):

```

function f = step1(t,y)
%% This corresponds to the first half of the upstroke (step 1)
f=zeros(13,1);
global Vmin;% min volume
global rc;% compression ratio
global R;% ratio of connecting rod length to crank radius
global w;% rpm (rad/sec)
global R_gas;% gas constant
global Cp;% specific heat at constant pressure
global Cv;% specific heat at constant volume

```

```

global A_cr;%cold reservoir area
global gamma;
global n; %number of upper slits
global CD; %Coefficient of Discharge
global N_cold;
global N_hot;
global mdot_in_h;
global Tmi_h;
global mdot_in_c;
global Tmi_c;
global U_bar_h;
global Cp_code_h;
global U_bar_c;
global Cp_code_c;
global As_h;
global As_c;

%% If Pcold >= Pcy1

if( (y(8)>=y(5)) && (y(5)<y(11)) )
    %% -----
    Tm_o=y(10)-(y(10)-Tmi_h)*exp((-U_bar_h*As_h)/(mdot_in_h*Cp_code_h));
    Qdot_h=N_hot*mdot_in_h*Cp_code_h*(Tmi_h-Tm_o);

    Tm_o=y(7)-(y(7)-Tmi_c)*exp((-U_bar_c*As_c)/(mdot_in_c*Cp_code_c));
    Qdot_c=N_cold*mdot_in_c*Cp_code_c*(Tmi_c-Tm_o);
    %% -----

m=w*t+pi;
f(1,1)=Vmin*(rc-1)*0.5*(w*sin(m)+(w*sin(m)*cos(m)/(sqrt((R^2)...
    -((sin(m))^2 ))));%dV

if((y(8)>y(5)))
P_s=0.528*y(8);
    if (y(5)<P_s)%choked
        flow=CD*A_cr*sqrt( gamma*(y(8)*y(8)/(R_gas*y(7)))* ...
            ( 2/(gamma+1))^ ( ( gamma+1 )/(gamma-1 )));%choked
    else%unchoked
        c=((y(5)/y(8))^ (2/gamma))- ( ( y(5)/y(8))^ ( gamma+1)/gamma));
        flow=CD*A_cr*sqrt((2*y(8)*y(8)/(R_gas* y(7)))*...
            (gamma /(gamma-1))*c );%unchoked
    end
else
    flow=0;

```

```

end
% Working Cylinder
f(2,1)=n*flow;% mass rate into cylinder
f(3,1)=abs((y(5))*f(1,1));% work on cylinder
f(4,1)=(1/(y(2)*(Cp-R_gas)))*(f(3,1)+f(2,1)*...
    (Cp*y(7)-Cp*y(4)+R_gas*y(4)));% dT of cylinder
f(5,1)=(f(2,1)*R_gas*y(4)+y(2)*R_gas*f(4,1)-y(5)*f(1,1))/y(1);% dP cylinder

% Cold Reservoir
f(6,1)=-n*flow;% flow of cold reservoir
f(7,1)=(f(6,1)*R_gas*y(7)+Qdot_c)/(y(6)*(Cp-R_gas));% dT of cold reservoir
f(8,1)=y(8)*((f(6,1)/y(6)+(f(7,1)/y(7)));% dP of cold reservoir

% Hot Reservoir
f(9,1)=0;% flow in/out hot reservoir
f(10,1)=Qdot_h/(y(9)*Cv);% dT of hot reservoir
f(11,1)=y(11)*(f(10,1)/y(10));% dP of hot reservoir
f(12,1)=Qdot_h;
f(13,1)=Qdot_c;

end

%% If P_cyl > P_cold
if( (y(5)>y(8)) && (y(5)<y(11)) )

    %% -----
    Tm_o=y(10)-(y(10)-Tmi_h)*exp((-U_bar_h*As_h)/(mdot_in_h*Cp_code_h));
    Qdot_h=N_hot*mdot_in_h*Cp_code_h*(Tmi_h-Tm_o);

    Tm_o=y(7)-(y(7)-Tmi_c)*exp((-U_bar_c*As_c)/(mdot_in_c*Cp_code_c));
    Qdot_c=N_cold*mdot_in_c*Cp_code_c*(Tmi_c-Tm_o);
    %% -----
    m=w*t+pi;
    f(1,1)=Vmin*(rc-1)*0.5*(w*sin(m)+(w*sin(m)*cos(m)/...
        (sqrt((R^2)-((sin(m))^2 ))));% dV

    P_s=0.528*y(5);
    if (y(8)<P_s)% choked
        flow=CD*A_cr*sqrt( gamma*(y(5)*y(5)/(R_gas*y(4)))* ...
            ( 2/(gamma+1))^ ( ( gamma+1)/(gamma-1)));% choked
    else% unchoked
        c((( ( y(8)/y(5))^ ( 2/gamma))-((y(8)/y(5))^((gamma+1)/gamma )));
        flow=CD*A_cr*sqrt((2*y(5)*y(5)/...
            (R_gas* y(4)))*(gamma/(gamma-1))*c);% unchoked
    end
end

```

```

% Working Cylinder
f(2,1)=-n*flow;% mass rate into cylinder
f(3,1)=abs((y(5))*f(1,1));% work on cylinder
f(4,1)=(1/(y(2)*(Cp-R_gas)))*(f(3,1)+f(2,1)*R_gas*y(4));% dT of cylinder
f(5,1)=(f(2,1)*R_gas*y(4)+y(2)*R_gas*f(4,1)-y(5)*f(1,1))/y(1);% dP cylinder

% Cold Reservoir
f(6,1)=n*flow;% flow of cold reservoir
f(7,1)=(f(6,1)*(R_gas*y(7)+Cp*y(4)-Cp*y(7))+Qdot_c)...
/(y(6)*(Cp-R_gas));% dT of cold reservoir
f(8,1)=y(8)*((f(6,1)/y(6))+f(7,1)/y(7));% dP of cold reservoir

% Hot Reservoir
f(9,1)=0;% flow in/out hot reservoir
f(10,1)=Qdot_h/(y(9)*Cv);% dT of hot reservoir
f(11,1)=y(11)*(f(10,1)/y(10));% dP of hot reservoir
f(12,1)=Qdot_h;
f(13,1)=Qdot_c;

end

```

MATLAB Function (Step 2):

```

function f = step2(t,y)
%% This step corresponds to second half of the upstroke (step 2)
f=zeros(13,1);
global Vmin;% min volume
global rc;% compression ratio
global R;% ratio of connecting rod length to crank radius
global w;% rpm (rad/sec)
global R_gas;% gas constant
global Cp;% specific heat at constant pressure
global Cv;% specific heat at constant volume
global A_h;% hot reservoir area
global gamma;
global n;% number of upper slits
global CD;% Coefficient of Discharge
global mdot_in_h;
global Tmi_h;
global mdot_in_c;
global Tmi_c;
global N_cold;
global N_hot;
global U_bar_h;
global Cp_code_h;

```

```

global U_bar_c;
global Cp_code_c;
global As_h;
global As_c;
%% -----
Tm_o=y(10)-(y(10)-Tmi_h)*exp((-U_bar_h*As_h)/(mdot_in_h*Cp_code_h));
Qdot_h=N_hot*mdot_in_h*Cp_code_h*(Tmi_h-Tm_o);

Tm_o=y(7)-(y(7)-Tmi_c)*exp((-U_bar_c*As_c)/(mdot_in_c*Cp_code_c));
Qdot_c=N_cold*mdot_in_c*Cp_code_c*(Tmi_c-Tm_o);
%% -----

m=w*t+pi;
f(1,1)=Vmin*(rc-1)*0.5*(w*sin(m)+(w*sin(m)*cos(m)...
/(sqrt((R^2)-((sin(m))^2 ))));%dV

if (y(5)>y(11))

P_s=0.528*y(5);
if (y(11)<P_s)%choked
    flow=CD*A_h*sqrt( gamma*(y(5)*y(5)/(R_gas*y(4)))*...
        ( 2/(gamma+1))^ ( gamma+1 )/(gamma-1 ));%choked
else%unchoked
    c= ( ( y(11)/y(5))^ ( 2/gamma)) - ...
        ( ( y(11)/y(5))^ ( gamma+1)/gamma ));
    flow=CD*A_h*sqrt((2*y(5)*y(5)/...
        (R_gas* y(4)))*(gamma /(gamma-1))*c);%unchoked
end
else
    flow=0;
end

% Working Cylinder
f(2,1)=-n*flow;% mass rate into cylinder
f(3,1)=abs((y(5))*f(1,1));% work on cylinder
f(4,1)=(1/(y(2)*(Cp-R_gas)))*(f(3,1)+f(2,1)*R_gas*y(4));% dT of cylinder
f(5,1)=(f(2,1)*R_gas*y(4)+y(2)*R_gas*f(4,1)-y(5)*f(1,1))/y(1);% dP cylinder

% Cold Reservoir
f(6,1)=0;% flow of cold reservoir
f(7,1)=Qdot_c/(y(6)*Cv);% dT of cold reservoir
f(8,1)=y(8)*(f(7,1)/y(7));% dP of cold reservoir

% Hot Reservoir
f(9,1)=n*flow;% flow in/out hot reservoir

```

```

f(10,1)=(f(9,1)*(R_gas*y(10)+Cp*y(4)-Cp*y(10))+Qdot_h)/...
(y(9)*(Cp-R_gas));%dT of hot reservoir
f(11,1)=y(11)*((f(9,1)/y(9))+f(10,1)/y(10));%dP of hot reservoir
f(12,1)=Qdot_h;
f(13,1)=Qdot_c;

```

MATLAB Function (Step 3 and 4)

```

function f = step3(t,y)
%% This corresponds to the downstroke (step 3 and 4)
f=zeros(13,1);
global Vmin;%min volume
global rc;%compression ratio
global R;%ratio of connecting rod length to crank radius
global w;%rpm (rad/sec)
global R_gas;%gas constant
global Cp;%specific heat at constant pressure
global Cv;%specific heat at constant volume
global A_h;%cold reservoir area
global gamma;
global n;%number of upper slits
global Mhot1;
global CD;%Coefficient of Discharge
global N_cold;
global N_hot;
global mdot_in_h;
global Tmi_h;
global mdot_in_c;
global Tmi_c;
global U_bar_h;
global Cp_code_h;
global U_bar_c;
global Cp_code_c;
global As_h;
global As_c;
%% -----
Tm_o=y(10)-(y(10)-Tmi_h)*exp((-U_bar_h*As_h)/(mdot_in_h*Cp_code_h));
Qdot_h=N_hot*mdot_in_h*Cp_code_h*(Tmi_h-Tm_o);

Tm_o=y(7)-(y(7)-Tmi_c)*exp((-U_bar_c*As_c)/(mdot_in_c*Cp_code_c));
Qdot_c=N_cold*mdot_in_c*Cp_code_c*(Tmi_c-Tm_o);
%% -----
m=w*t+pi;
f(1,1)=Vmin*(rc-1)*0.5*(w*sin(m)+(w*sin(m)*cos(m))/...
(sqrt((R^2)-((sin(m))^2 ))));%dV

```

```

if(y(11)>y(5)&&(y(9)>Mhot1))
P_s=0.528*y(11);
if (y(5)<P_s)%choked
flow=CD*A_h*sqrt( gamma*(y(11)*y(11)/(R_gas*y(10)))*...
( 2/(gamma+1) )^( ( gamma+1 )/(gamma-1) ) );%choked
else%unchoked
c=(( y(5)/y(11) )^ ( 2/gamma ) ) -...
(( y(5)/y(11) )^( (gamma+1)/gamma ) );
flow=CD*A_h*sqrt((2*y(11)*y(11)/(R_gas* y(10) ))*...
(gamma/(gamma-1) )*c );%unchoked
end
else
flow=0;
end
% Working Cylinder
f(2,1)=n*flow;%mass rate into cylinder
f(3,1)=-abs((y(5))*f(1,1));% work on cylinder
f(4,1)=(1/(y(2)*(Cp-R_gas)))*(f(3,1)+f(2,1)*...
(Cp*y(10)-Cp*y(4)+R_gas*y(4)));%dT of cylinder
f(5,1)=(f(2,1)*R_gas*y(4)+y(2)*R_gas*f(4,1)-y(5)*f(1,1))/y(1);%dP cylinder

%Cold Reservoir
f(6,1)=0;% flow of cold reservoir
f(7,1)=Qdot_c/(y(6)*Cv);%dT of cold reservoir
f(8,1)=y(8)*((f(7,1)/y(7)));%dP of cold reservoir

%Hot Reservoir
f(9,1)=-n*flow;% flow out of hot reservoir
f(10,1)=(f(9,1)*R_gas*y(10)+Qdot_h)/(y(9)*(Cp-R_gas));%dT of hot reservoir
f(11,1)=y(11)* ( f(9,1)/y(9))+f(10,1)/y(10) );%dP of hot reservoir
f(12,1)=Qdot_h;
f(13,1)=Qdot_c;

```

MATLAB Function (To find fluid's inlet parameters as a function of temperature)

```
function [mu,k,Cp_code,Pr]=newFunc(T)
```

```

if (T<=300)
% Calculating dynamic viscosity
mu=(1.716e-05)*((T/273.15)^1.5)*((273.15+110.4)/(T+110.4));% % N.s/m^
% Calculating thermal conductivity
a=0.0017;

```



```

b=8.2e-05;
k=a+b*T ;%% W/m.K
%Calculating Prandtl number
Cp_code=1007;
Pr=Cp_code*mu/k;
end

if (T>300&&T<550)
% Calculating dynamic viscosity
mu=(1.716e-05)*((T/273.15)^1.5)*((273.15+110.4)/(T+110.4));%% N.s/m^
% Calculating thermal conductivity
a=0.00528;
b=7.13e-05;
k=a+b*T; %% W/m.K
%Calculating Prandtl number
Cp_code=1019.5;
Pr=Cp_code*mu/k;
end

if (T>=550&&T<=800)
% Calculating dynamic viscosity
mu=(1.716e-05)*((T/273.15)^1.5)*((273.15+110.4)/(T+110.4));%% N.s/m^
% Calculating thermal conductivity
a=0.016;
b=5.2e-05;
k=a+b*T ;%% W/m.K
%Calculating Prandtl number
Cp_code=1069.5;
Pr=Cp_code*mu/k;
end

if (T>800&&T<1100)
% Calculating dynamic viscosity
mu=(1.716e-05)*((T/273.15)^1.5)*((273.15+110.4)/(T+110.4));%% N.s/m^
% Calculating thermal conductivity
a=0.019395;
b=4.73e-05;
k=a+b*T; %% W/m.K
%Calculating Prandtl number
Cp_code=1125.5;
Pr=Cp_code*mu/k;
end

if (T>=1100)
% Calculating dynamic viscosity
mu=(1.716e-05)*((T/273.15)^1.5)*((273.15+110.4)/(T+110.4));%% N.s/m^

```

```

% Calculating thermal conductivity
a=0.0133;
b=5.25e-05;
k=a+b*T; %% W/m.K
%Calculating Prandtl number
Cp_code=1159;
Pr=Cp_code*mu/k;
end

end

```

MATLAB Main Script:

```

%% Wiam Attar
%% Gen III c engine model
clc
clear all;
format long
%%

```

Variables

```

-
global Vmin;% min volume (m^3)
global Vmax;% maximum working volume (m^3)
global rc;% compression ratio
global R;% ratio of connecting rod length to crank radius
global a;% Crank radius
global l;% Connecting rod length
global w;% rpm (rad/sec)
global R_gas;% gas constant
global gamma;% ratio of specific heats
global Cp;% specific heat at constant pressure
global Cv;% specific heat at constant volume
global A_cr;% cold reservoir area
global A_h;% hot reservoir area
global n;% number of upper slits
global Mhot1;% Initial Mass in Hot Reservoir
global Kb;% Boltzmann Constant (J/K)
global h;% Planck's Constant (J.s)
global Na;% Avogadro's Number (particles/mole)
global Mcr1;% initial mass in cold reservoir (kg)
global e;% 2.718281828459046
global kk;% constant 1.38044e-16
global M;% Molar Mass g/mole
global w_el;% Electronic degeneracy
global sigma_r;% Rotational Temperature (K)

```

```

global D0; %Dissociation Energy (erg)
global sigma_v; %Vibrational Temperature (K)
global mp;%mass of one molecule (kg/molecule)
global CD; %Coefficient of Discharge
global mdot_in_h;%internal mass flow rate into each tube heating the ...
...hot reservoir
global Tmi_h;%Inlet Temperature inside each hot tube heating the ...
...hot reservoir
global dia_h;%Diameter of each hot tube inside the hot reservoir
global length_h;%length of each hot tube running inside the hot reservoir
global Tm_bar_h;%Approximated Mean temperature inside each hot tube
global h_o_h;% Heat transfer coefficient between the hot tube surface ...
...and the hot reservoir
global mdot_in_c;%internal mass flow rate into each tube cooling the ...
...reservoir
global Tmi_c;%Inlet Temperature inside each cold tube cooling the reservoir
global dia_c;%Diameter of each cold tube inside the cold reservoir
global length_c;%length of each cold tube running inside the cold reservoir
global Tm_bar_c;%Approximated Mean temperature inside each cold tube
global h_o_c;% Heat transfer coefficient between the cold tube ...
...surface and the cold reservoir
global N_cold;% Number of cold tubes
global N_hot;% Number of hot tubes
global U_bar_h;% Overall heat transfer coeff (hot)
global Cp_code_h;% specific heat (hot res)
global U_bar_c;% Overall heat transfer coeff (cold)
global Cp_code_c;% Specific heat (cold res)
global As_h;
global As_c;

%=====
=====
%_____M_dot_in_tubes_____
_____
mdot_in_h=0.5/8;%Kg/sec total mass flow rate in all the tubes (hot res)

%_____RPM_____
_____
w=1800*2*pi/60;%rad/sec

%_____T_hot at tube
entrance_____
Tmi_h=1200;

%_____compression
ratio_____

```

```

rc=20;

%_____Initial Cold Reservoir
Pressure_____
Pcr1=1.0e+06;

%=====
=====
mdot_in_c=mdot_in_h;%Kg/sec % Mass flow rate in each tube

N_hot=8;
N_cold=2*N_hot;

Vmin=6e-05;%m^3
Vmax=rc*Vmin;
Vhot=0.06;
Vcr=Vhot;

h_o_c=109; % Convection coefficient (on the outside of the tubes)- hot res
h_o_h=109.6;% Convection coefficient (on the outside of the tubes)- cold res
Tmi_c=300;% Fluid inlet temp inside the cold tubes
dia_h=0.02;%diameter of hot tube
dia_c=0.02;% diameter of cold tube
Tm_bar_h=Tmi_h-8;% average temp inside hot tube (approx)
Tm_bar_c=Tmi_c+8;% average temp inside cold tube (approx)
length_h=0.9*Vhot/(N_hot*pi*((dia_h/2)^2)); %tube length - hot res
length_c=Vcr/(N_cold*pi*((dia_c/2)^2));% tube length - cold res

%% Finding the additional parameters of the flow

[mu,K_th,Cp_code,Pr]=newFunc(Tm_bar_h);
Re_h=(4*mdot_in_h)/(pi*dia_h*mu);% Reynolds number
Nu_h=0.023*(Re_h^(4/5))*(Pr^0.4);% Nusselt number
hi_h=Nu_h*(K_th/dia_h);% Convection coeff
U_bar_h=((h_o_h^-1)+(hi_h^-1))^-1;% Overall heat transfer coefficient
Cp_code_h=Cp_code;% specific heat at constant pressure
As_h=pi*dia_h*length_h;% surface area

[mu,K_th,Cp_code,Pr]=newFunc(Tm_bar_c);
Re_c=(4*mdot_in_c)/(pi*dia_c*mu);% Reynolds number
Nu_c=0.023*(Re_c^(4/5))*(Pr^0.4);% Nusselt number
hi_c=Nu_c*(K_th/dia_c);% Convection coeff
U_bar_c=((h_o_c^-1)+(hi_c^-1))^-1;% Overall heat transfer coefficient
Cp_code_c=Cp_code;% specific heat at constant pressure
As_c=pi*dia_c*length_c;% surface area

```

%%

Inputs

CD=0.61;% Coefficient of Discharge (1 or 0.61)
% Air Gas Properties
R_gas=287;
gamma=1.4;
Cp=1005;
Cv=718;
mp=4.65e-26;% mass of one molecule (kg/molecule)
M=28;% Molar Mass
w_el=1;
sigma_r=2.89;
D0=9.76*1.602e-12;
sigma_v=3390;

%% -----

Tcr1=300;% initial temperature of cold reservoir
Phot1=10e+06;% initial hot reservoir pressure
Pcyl1=100000;% starting pressure at BDC
Tcyl1=300;% starting temperature at BDC
Thot1=Tmi_h;% initial hot reservoir temperature

% Number of slits is the same for cold and hot reservoirs connection
n=1;
% Area of each hot reservoir's slit
A_h=1.2*30*(2e-05);
% Area of each cold reservoir's slit
A_cr=3*8e-04;

% Geometric Dimension
a=0.2;% crank radius
l=0.25;% connecting rod length
% Constants
Kb=1.38064852e-23;% Boltzman Constant (J/K)
h=6.626070040e-34;% Planck's Constant (J.s)
Na=6.0221409e+23;% Avogadro's
e=2.7182818;
kk=1.38044e-16;% Boltzman
% Cold Reservoir Initial Conditions
Mcr1=Pcr1*Vcr/(R_gas*Tcr1);% initial mass in cold reservoir
% Working Cylinder Initial Conditions
Vcyl1=Vmax;% Volume at BDC;

```

Mcy11=Pcyl1*Vcyl1/(R_gas*Tcyl1);%mass in working cylinder
% Hot Reservoir Initial Conditions
Mhot1=Phot1*Vhot/(R_gas*Thot1);%initial mass in hot reservoir
%calculating the ratio of connecting rod length to crank radius:
R=l/a;
% Additional Integration Variables
time0=0;%initial start time of the cycle
L=0; %Initial Net Work Ouput Value at the start
k=2;% Additional Variable that will help calculate the start time of...
...every cycle__t=(theta-pi)/w
p=1;% Additional Variable that will help calculate the time at...
...TDC __t=(theta-pi)/w__ where t=pi/w,3pi/w,5pi/w,etc...

CC=1000;

%%
_____Step1_____
_____
for H=1:CC

% The time when cold reservoir Interaction with the working cylinder stops
avg=0.5*(time0+(p*pi/w)); %the interaction with the cold reservoir ...
...stops midway through the upstroke

options = odeset('AbsTol',1e-05,'RelTol',1e-05);
[t1,Y]=ode45('step1',[time0 avg],[Vmax Mcy11 L Tcyl1 Pcyl1 Mcr1 Tcr1 ...
    Pcr1 Mhot1 Thot1 Phot1 L L],options);

xx=(t1*w+pi)*180/pi;
if H>(CC-4)
figure(1)
plot((xx),Y(:,1),'LineWidth',2)
set(gca,'FontSize',12)
title('Volume of Working Cylinder vs. Crank Angle','FontSize', 16);
xlabel('Angle (deg.)','FontSize', 12)
ylabel('Working Fluid Volume (m^3)','FontSize', 12)
hold on

figure(2)
plot((xx),Y(:,2),'LineWidth',2)
set(gca,'FontSize',12)
title('Mass in Working Cylinder vs. Crank Angle','FontSize', 16);
xlabel('Angle (deg.)','FontSize', 12)
ylabel('Mass in Working Cylinder (kg)','FontSize', 12)
hold on

```

```
figure(3)
plot((xx),-Y(:,3),'LineWidth',2)
set(gca,'FontSize',12)
title('Work on Working Cylinder vs. Crank Angle','FontSize', 16);
xlabel('Angle (deg.)','FontSize', 12)
ylabel('Work (Joule)','FontSize', 12)
hold on
```

```
figure(4)
plot((xx),Y(:,4),'LineWidth',2)
set(gca,'FontSize',12)
title('Temperature in Working Cylinder vs. Crank Angle','FontSize', 16);
xlabel('Angle (deg.)','FontSize', 12)
ylabel('Temperature (K)','FontSize', 12)
hold on
```

```
figure(5)
plot((xx),Y(:,5),'LineWidth',2)
set(gca,'FontSize',12)
title('Pressure in Working Cylinder vs. Crank Angle','FontSize', 16);
xlabel('Angle (deg.)','FontSize', 12)
ylabel('Pressure (pa)','FontSize', 12)
hold on
```

```
figure(6)
plot((xx),Y(:,6),'LineWidth',2)
set(gca,'FontSize',12)
title('Mass in Cold Reservoir vs. Crank Angle','FontSize', 16);
xlabel('Angle (deg.)','FontSize', 12)
ylabel('Mass (kg)','FontSize', 12)
hold on
```

```
figure(7)
plot((xx),Y(:,7),'LineWidth',2)
set(gca,'FontSize',12)
title('Temperature in Cold Reservoir vs. Crank Angle','FontSize', 16);
xlabel('Angle (deg.)','FontSize', 12)
ylabel('Temperature (K)','FontSize', 12)
hold on
```

```
figure(8)
plot((xx),Y(:,8),'LineWidth',2)
set(gca,'FontSize',12)
title('Pressure in Cold Reservoir vs. Crank Angle','FontSize', 16);
xlabel('Angle (deg.)','FontSize', 12)
ylabel('Pressure (pa)','FontSize', 12)
```

```

hold on

figure(9)
plot((xx),Y(:,9),'LineWidth',2)
set(gca,'FontSize',12)
title('Mass in Hot Reservoir vs. Crank Angle','FontSize', 16);
xlabel('Angle (deg.)','FontSize', 12)
ylabel('Mass (kg)','FontSize', 12)
hold on

figure(10)
plot((xx),Y(:,10),'LineWidth',2)
set(gca,'FontSize',12)
title('Temperature in Hot Reservoir vs. Crank Angle','FontSize', 16);
xlabel('Angle (deg.)','FontSize', 12)
ylabel('Temperature (K)','FontSize', 12)
hold on

figure(11)
plot((xx),Y(:,11),'LineWidth',2)
set(gca,'FontSize',12)
title('Pressure in Hot Reservoir vs. Crank Angle','FontSize', 16);
xlabel('Angle (deg.)','FontSize', 12)
ylabel('Pressure (pa)','FontSize', 12)
hold on

figure(12)
plot((xx),Y(:,12),'LineWidth',2)
set(gca,'FontSize',12)
title('Qin vs. Crank Angle','FontSize', 16);
xlabel('Angle (deg.)','FontSize', 12)
ylabel('Qin (J)','FontSize', 12)
hold on

figure(13)
plot((xx),Y(:,13),'LineWidth',2)
set(gca,'FontSize',12)
title('Qout vs. Crank Angle','FontSize', 16);
xlabel('Angle (deg.)','FontSize', 12)
ylabel('Qout (J)','FontSize', 12)
hold on
end
%% _____ Step
2 _____

options = odeset('AbsTol',1e-05,'RelTol',1e-05);

```



```
[t2,Z]=ode45('step2',[avg p*pi/w],[Y(end,1) Y(end,2) Y(end,3) Y(end,4)...
    Y(end,5) Y(end,6) Y(end,7) Y(end,8) Y(end,9) Y(end,10) Y(end,11)...
    Y(end,12) Y(end,13)],options);
```

```
rr=(t2*w+pi)*180/pi;
if H>(CC-4)
figure(1)
plot((rr),Z(:,1),'LineWidth',2)
set(gca,'FontSize',12)
title('Volume of Working Cylinder vs. Crank Angle','FontSize', 16);
xlabel('Angle (deg.)','FontSize', 12)
ylabel('Working Fluid Volume (m^3)','FontSize', 12)
hold on
```

```
figure(2)
plot((rr),Z(:,2),'LineWidth',2)
set(gca,'FontSize',12)
title('Mass in Working Cylinder vs. Crank Angle','FontSize', 16);
xlabel('Angle (deg.)','FontSize', 12)
ylabel('Mass in Working Cylinder (kg)','FontSize', 12)
hold on
```

```
figure(3)
plot((rr),-Z(:,3),'LineWidth',2)
set(gca,'FontSize',12)
title('Work on Working Cylinder vs. Crank Angle','FontSize', 16);
xlabel('Angle (deg.)','FontSize', 12)
ylabel('Work (Joule)','FontSize', 12)
hold on
```

```
figure(4)
plot((rr),Z(:,4),'LineWidth',2)
set(gca,'FontSize',12)
title('Temperature in Working Cylinder vs. Crank Angle','FontSize', 16);
xlabel('Angle (deg.)','FontSize', 12)
ylabel('Temperature (K)','FontSize', 12)
hold on
```

```
figure(5)
plot((rr),Z(:,5),'LineWidth',2)
set(gca,'FontSize',12)
title('Pressure in Working Cylinder vs. Crank Angle','FontSize', 16);
xlabel('Angle (deg.)','FontSize', 12)
ylabel('Pressure (pa)','FontSize', 12)
hold on
```

```
figure(6)
plot((rr),Z(:,6),'LineWidth',2)
set(gca,'FontSize',12)
title('Mass in Cold Reservoir vs. Crank Angle','FontSize', 16);
xlabel('Angle (deg.)','FontSize', 12)
ylabel('Mass (kg)','FontSize', 12)
hold on
```

```
figure(7)
plot((rr),Z(:,7),'LineWidth',2)
set(gca,'FontSize',12)
title('Temperature in Cold Reservoir vs. Crank Angle','FontSize', 16);
xlabel('Angle (deg.)','FontSize', 12)
ylabel('Temperature (K)','FontSize', 12)
hold on
```

```
figure(8)
plot((rr),Z(:,8),'LineWidth',2)
set(gca,'FontSize',12)
title('Pressure in Cold Reservoir vs. Crank Angle','FontSize', 16);
xlabel('Angle (deg.)','FontSize', 12)
ylabel('Pressure (pa)','FontSize', 12)
hold on
```

```
figure(9)
plot((rr),Z(:,9),'LineWidth',2)
set(gca,'FontSize',12)
title('Mass in Hot Reservoir vs. Crank Angle','FontSize', 16);
xlabel('Angle (deg.)','FontSize', 12)
ylabel('Mass (kg)','FontSize', 12)
hold on
```

```
figure(10)
plot((rr),Z(:,10),'LineWidth',2)
set(gca,'FontSize',12)
title('Temperature in Hot Reservoir vs. Crank Angle','FontSize', 16);
xlabel('Angle (deg.)','FontSize', 12)
ylabel('Temperature (K)','FontSize', 12)
hold on
```

```
figure(11)
plot((rr),Z(:,11),'LineWidth',2)
set(gca,'FontSize',12)
title('Pressure in Hot Reservoir vs. Crank Angle','FontSize', 16);
xlabel('Angle (deg.)','FontSize', 12)
ylabel('Pressure (pa)','FontSize', 12)
```

```

hold on

figure(12)
plot((rr),Z(:,12),'LineWidth',2)
set(gca,'FontSize',12)
title('Qin vs. Crank Angle','FontSize', 16);
xlabel('Angle (deg.)','FontSize', 12)
ylabel('Qin (J)','FontSize', 12)
hold on

figure(13)
plot((rr),Z(:,13),'LineWidth',2)
set(gca,'FontSize',12)
title('Qout vs. Crank Angle','FontSize', 16);
xlabel('Angle (deg.)','FontSize', 12)
ylabel('Qout (J)','FontSize', 12)
hold on

end
%% _____ Step 3 and
4 _____

options = odeset('AbsTol',1e-05,'RelTol',1e-05);
[t3,X]=ode45('step3',[p*pi/w k*pi/w],[Z(end,1) Z(end,2) Z(end,3) ...
    Z(end,4) Z(end,5) Z(end,6) Z(end,7) Z(end,8) Z(end,9) Z(end,10)...
    Z(end,11) Z(end,12) Z(end,13)],options);

yy=(t3*w+pi)*180/pi;

if H>(CC-4)
figure(1)
plot((yy),X(:,1),'LineWidth',2)
set(gca,'FontSize',12)
title('V_C_y_1 vs. Crank Angle','FontSize', 16);
xlabel('Angle (deg.)','FontSize', 12)
ylabel('Working Fluid Volume (m^3)','FontSize', 12)
hold on

figure(2)
plot((yy),X(:,2),'LineWidth',2)
set(gca,'FontSize',12)
title('M_C_y_1 vs. Crank Angle','FontSize', 16);
xlabel('Angle (deg.)','FontSize', 12)
ylabel('Mass in Working Cylinder (kg)','FontSize', 12)
hold on

```

```
figure(3)
plot((yy),-X(:,3),'LineWidth',2)
set(gca,'FontSize',12)
title('W_C_y_1 vs. Crank Angle','FontSize', 16);
xlabel('Angle (deg.)','FontSize', 12)
ylabel('Work (Joule)','FontSize', 12)
hold on
```

```
figure(4)
plot((yy),X(:,4),'LineWidth',2)
set(gca,'FontSize',12)
title('T_C_y_1 vs. Crank Angle','FontSize', 16);
xlabel('Angle (deg.)','FontSize', 12)
ylabel('Temperature (K)','FontSize', 12)
hold on
```

```
figure(5)
plot((yy),X(:,5),'LineWidth',2)
set(gca,'FontSize',12)
title('P_C_y_1 vs. Crank Angle','FontSize', 16);
xlabel('Angle (deg.)','FontSize', 12)
ylabel('Pressure (pa)','FontSize', 12)
hold on
```

```
figure(6)
plot((yy),X(:,6),'LineWidth',2)
set(gca,'FontSize',12)
title('M_C_o_1_d vs. Crank Angle','FontSize', 16);
xlabel('Angle (deg.)','FontSize', 12)
ylabel('Mass (kg)','FontSize', 12)
hold on
```

```
figure(7)
plot((yy),X(:,7),'LineWidth',2)
set(gca,'FontSize',12)
title('T_C_o_1_d vs. Crank Angle','FontSize', 16);
xlabel('Angle (deg.)','FontSize', 12)
ylabel('Temperature (K)','FontSize', 12)
hold on
```

```
figure(8)
plot((yy),X(:,8),'LineWidth',2)
set(gca,'FontSize',12)
title('P_C_o_1_d vs. Crank Angle','FontSize', 16);
xlabel('Angle (deg.)','FontSize', 12)
ylabel('Pressure (pa)','FontSize', 12)
```

```

hold on

figure(9)
plot((yy),X(:,9),'LineWidth',2)
set(gca,'FontSize',12)
title('M_H_o_t vs. Crank Angle','FontSize', 16);
xlabel('Angle (deg.)','FontSize', 12)
ylabel('Mass (kg)','FontSize', 12)
hold on

figure(10)
plot((yy),X(:,10),'LineWidth',2)
set(gca,'FontSize',12)
title('T_H_o_t vs. Crank Angle','FontSize', 16);
xlabel('Angle (deg.)','FontSize', 12)
ylabel('Temperature (K)','FontSize', 12)
hold on

figure(11)
plot((yy),X(:,11),'LineWidth',2)
set(gca,'FontSize',12)
title('P_H_o_t vs. Crank Angle','FontSize', 16);
xlabel('Angle (deg.)','FontSize', 12)
ylabel('Pressure (pa)','FontSize', 12)
hold on

figure(12)
plot((yy),X(:,12),'LineWidth',2)
set(gca,'FontSize',12)
title('Qin vs. Crank Angle','FontSize', 16);
xlabel('Angle (deg.)','FontSize', 12)
ylabel('Qin (J)','FontSize', 12)
hold on

figure(13)
plot((yy),X(:,13),'LineWidth',2)
set(gca,'FontSize',12)
title('Qout vs. Crank Angle','FontSize', 16);
xlabel('Angle (deg.)','FontSize', 12)
ylabel('Qout (J)','FontSize', 12)
hold on

end

```

```

% Updating initial conditions to restart the for-loop:
time0=(k*pi)/w;
Vmax=X(end,1);
Mcycl=X(end,2);
L=0;
Tcycl=X(end,4);
Pcycl=X(end,5);
Mcr1=X(end,6);
Tcr1=X(end,7);
Pcr1=X(end,8);
Mhot1=X(end,9);
Thot1=X(end,10);
Phot1=X(end,11);

% Updating time variables
p=p+2;
k=k+2;

% Number of cycle will show on the screen
Cycle_number=H
end

Work=-X(end,3)% per cycle
Qin=X(end,12)% per cycle
Qout=X(end,13)% per cycle
eff=Work/Qin% efficiency
%% end of script

```

Bibliography

- [1] T. Finkelstein and A. Organ, *Air Engines*. The American Society of Mechanical Engineers Press, 2001.
- [2] J. Majeski, "Stirling Engine Assessment," *EPRI, Energy Int. Inc. 127 Bellevue W. SE Suite 200 Bellevue, WA 98004*, vol. 1, no. 3, pp. 1–170, 2006.
- [3] G. Cayley, "Description of an Engine for affording Mechanical Power from Air expanded by Heat," *J. Philosophy, Chem. Arts*, vol. XVIII, 1807.
- [4] W. Poingdestre, "Description of Sir George Cayley's Hot-air Engine," vol. IX, no. 822, p. 352, 1850.
- [5] B. Johnston, "Adiabatic Expansion Heat engine And Method Of Operating," US 8,156,739 B2, 2012.
- [6] A. Matthew and J. Cowart, "THERMODYNAMIC MODELING OF 18TH CENTURY STEAM ENGINES," 2012.
- [7] C. R. Ferguson, *Internal Combustion Engines, Applied Thermosciences*. John Wiley & Sons, 1985.
- [8] M. A. Saad, *Compressible Fluid Flow*. Prentice-Hall, 1985.
- [9] *Risk Management Program Guidance for Offsite Consequence Analysis*. 1999.
- [10] "Measurement of fluid flow by means of pressure differential devices inserted in circular cross-section conduits running full - Part 2: Orifice plates (ISO 5167-2:2003)."
- [11] M. R. Chowdhury and V. G. Fester, "Modeling pressure losses for Newtonian and non-Newtonian laminar and turbulent flow in long square edged orifices," *Chem. Eng. Res. Des.*, vol. 90, no. 7, pp. 863–869, 2012.

- [12] A. J. W. Smith, *Pressure Losses in Ducted Flows*. Daniel Davey & CO., INC., 1971.
- [13] T. Oikonomou and G. Baris Bagci, “Clausius versus Sackur-Tetrode entropies,” *Stud. Hist. Philos. Sci. Part B - Stud. Hist. Philos. Mod. Phys.*, vol. 44, no. 2, pp. 63–68, 2013.
- [14] S. Sandler, *An Introduction to Applied Statistical Thermodynamics*. Wiley, 2011.
- [15] W. A. Khan, J. R. Culham, and M. M. Yovanovich, “Convection heat transfer from tube banks in crossflow: Analytical approach,” *Int. J. Heat Mass Transf.*, vol. 49, no. 25–26, pp. 4831–4838, 2006.
- [16] D. Incropera, *Fundamentals of heat and mass transfer*. Wiley & Sons, Inc., 1996.
- [17] L. Theodore, *Heat Transfer Applications for the Practicing Engineer*. 2011.
- [18] S. Menon and C. P. Cadou, “Scaling of Miniature Piston-Engine Performance, Part 1: Overall Engine Performance,” *J. Propuls. Power*, vol. 29, no. 4, pp. 774–787, 2013.
- [19] International Technological University, “Specific Heat of Air vs. Temperature.” [Online]. Available: <http://ninova.itu.edu.tr/tr/dersler/ucak-uzay-fakultesi/965/uck-421/ekKaynaklar?g96162>.